A Learning Control, Intervention Strategy for Location-Aware Adaptive Vehicle Dynamics Systems

Sukhwan Cho

Dissertation submitted to the faculty of the Virginia Polytechnic Institute and State University in partial fulfillment of the requirements for the degree of

Doctor of Philosophy

In

Mechanical Engineering

John B. Ferris, Committee Chair

Saied Taheri

Dennis Hong

Chris North

Alfred Wicks

June 08, 2015

Blacksburg, Virginia

Keywords: Predictive Control, Vehicle Stability Control, Real Time Simulation, Constrained Optimization, Learning Control

A Learning Control, Intervention Strategy for Location-Aware Adaptive Vehicle Dynamics Systems

Sukhwan Cho

Abstract

The focus of Location-Aware Adaptive Vehicle Dynamics System (LAAVDS) research is to develop a system to avoid situations in which the vehicle exceeds its handling capabilities. The proposed method is predictive, estimating the ability of the vehicle to successfully navigate upcoming terrain, and it is assumed that the future vehicle states and local driving environment is known. An Intervention Strategy must be developed such that the vehicle is navigated successfully along a road via modest changes to the driver′s commands and do so in a manner that is in harmony with the driver's intentions and not in a distracting or irritating manner. Clearly this research relies on the numerous new technologies being developed to capture and convey information about the local driving environment (e.g., bank angle, elevation changes, curvature, and friction coefficient) to the vehicle and driver.

My wife, Sanghee Huh, My endless love

My son, James Yuchan Cho, My another self

This dissertation is meaningless without them.

Their sacrifice, love and cheers made me to get through this Ph.D study in Blacksburg.

I dedicate this dissertation to them.

Acknowledgement

First of all, I would like to express my deepest appreciation to my advisor, Dr. John Ferris. He always made me to navigate to the right path. In spite of lack of my knowledge and depth, he never gave up to give me great advices continuously until the last moment. Without his support and help, this dissertation would not be completed.

I would greatly appreciate to my all committee members, Dr.Hong, Dr.North, Dr.Taheri, and Dr.Wicks who gave me a lot of advices and comments so that I can sail successfully during studying in Blacksburg.

I would greatly appreciate to all the VTPL members whom share their time to review my journal and conference papers. Whenever I got stuck in some problems, they encouraged me and became good friends that I could stand up again. Especially, I feel deep gratefulness to Yongsuk Kang. His sincere support was greatly helpful for me during my Ph.D study.

I would greatly appreciate to all the staff in Mechanical Engineering Department for their kind assistance during my Ph.D Study.

I am very grateful for the Volkswagen regarding their continuous support. Especially, I would like to appreciate to the Driver Assistant System team in Volkswagen for sharing their ideas and giving great advices.

I owe senior Korean friends one. Dr.Woon Kyoung Kim, Dr.Jiduck Choi, and Dr.Yongsuk Park, all of them always tried to give me sincere comments to get through Ph.D study. I also like to thank to my soul mate, Seungbeum Suh. He always took care of me and listened my voice whenever I had hard time in Blacksburg.

My father and father in the law have exerted strong influence on me that I made a decision to come to Virginia Tech for Ph.D study. Their greatly successful career in their life affects me very much to set up my ultimate goal in my whole life and navigate to the desired path. Without their tremendous support and mentoring for me, I would not be here. No words cannot describe how much I appreciate for their love, support, and mentoring.

My mother have dedicated her life for me and my family. Without her care and the deepest love toward me, I could not complete my Ph.D study successfully. She was truly my mother whom I love forever. My mother in the law has love me since I met her in 2006. She always tried to listen my voice and cure my soul whenever I had hard time. Any words in the world cannot describe their love for me. I would deeply appreciate for their support, sacrifice, and love.

I would also like to appreciate to my only brother and the sister in the law for cheers and mentoring during my life.

Table of Contents

List of Figures

1. Introduction

1.1 Motivation

Recently, the National Highway Transportation Safety Administration (NHTSA), released a report demonstrating the effectiveness of Electronic Stability Control (ESC) systems [1]. Specifically, NHTSA announced that ESC systems can reduce single vehicle crashes of passenger cars by 35%. .Single-vehicle SUV crashes can be reduced by 67%. Consequently, NHTSA's policy now requires ESC systems (from September 1, 2011) on passenger cars, multipurpose passenger vehicles, trucks, and buses with a gross vehicle weight rating of 4,536 Kg or less.

This statistical result justifies the necessity to develop various active vehicle control systems. Many groups are pursuing active safety systems for autonomous vehicles, including automotive companies and research institutions. This has been an active area of research for over 30 years and steady progress has resulted in many impressive contributions. Of course, when a human drives the vehicle, the computer is still of great assistance. For example, Anti-lock Braking Systems (ABS) and Electronic Stability Control (ESC) systems help maintain directional stability during braking and agile cornering.

As automotive technology has advanced, Driver Assistance Systems (DAS) have become increasingly used and as these various technologies are validated they become standard or even required. Initially, Anti-lock Braking Systems (ABS) were slowly introduced and after positive preliminary results they became more prevalent. Other DAS technologies include traction control and stability or vehicle dynamics control. These systems are very successful for the normal driver, by maintaining the vehicle's directional stability in extreme handling maneuvers.

Although DAS technologies (e.g., ESC, ABS, etc.) show splendid achievements, it also has some performance limitations. The main issue is that these systems are reactive; they only aid the driver once an extreme handling maneuver has been detected. These systems work very well at aiding the driver in controlling the vehicle during this maneuver, but provide no aid in avoiding these situations. Several Advanced Driver Assistance Systems (ADAS) are available today that predict the physics of the driving situation (automatic cruise control and braking systems). However, driving is a complex process; individual vehicles respond to their drivers, who make decisions based on their surroundings. This forms the motivation for exploring new active safety systems including the Location Aware Adaption of Vehicle Dynamic concept.

As noted by Matthews, one seminal question that faces the vehicle's driver (either human or computer) is predicting the capability of the vehicle as it encounters upcoming terrain [2]. The focus of Location-Aware Adaptive Vehicle Dynamics System (LAAVDS) research is to develop a system to avoid situations in which the vehicle exceeds its handling capabilities. The proposed method is predictive, estimating the ability of the vehicle to successfully navigate upcoming terrain, and it is assumed that the future vehicle states and local driving environment is known. An Intervention Strategy must be developed such that the vehicle is navigated successfully along a road via modest changes to the driver's commands and do so in a manner that is in harmony with the driver's intentions and not in a distracting or irritating manner. Clearly this research relies on the numerous new technologies being developed to capture and convey information about the local driving environment (e.g., bank angle, elevation changes, curvature, and friction coefficient) to the vehicle and driver.

Therefore the main purpose of this study is to develop the vehicle dynamic and control logic from the information provided by network infrastructure like Global Positioning System (GPS) or Satellite Information System. A firm theoretical background on the state of the art of ADAS is a significant prerequisite for developing this suggested system. Thus the rest of this chapter suggests a current ADAS system. Next the objectives, contributions of this study, and outline of this document will be provided.

1.2 Big Picture of the LAAVDS and Comparing with Current Stability Control System

Currently, there are various stability control system. The initial product is an Antilock Braking System (ABS).

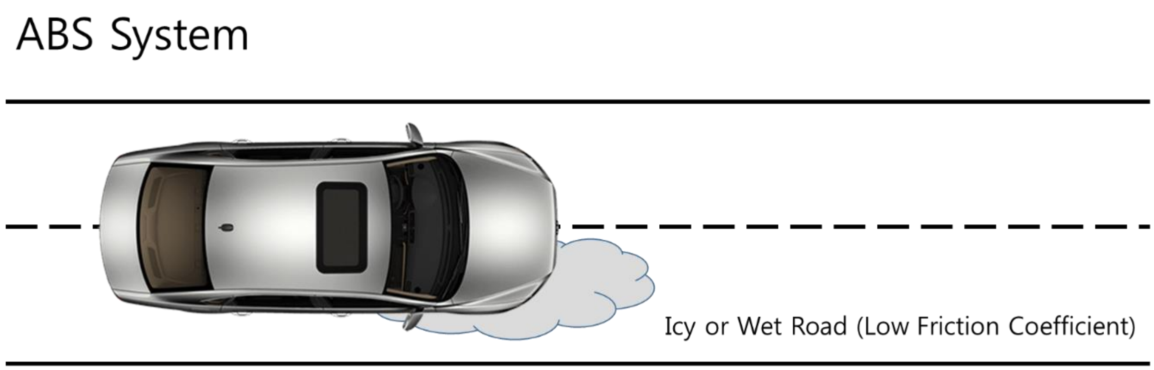

Figure 1.1. The Function of the ABS

As it can be seen from the Figure 1.1, there could be wheel lock situation when the driver modulates the brake pedal on the icy road or wet road which has low friction coefficient. For this event, the front right side tire may undergo the wheel lock mode. Then the Electronic Control Unit (ECU) monitors this and releases the brake pressure a little more to raise up the wheel rotational speed. This is the brief concept of the ABS System.

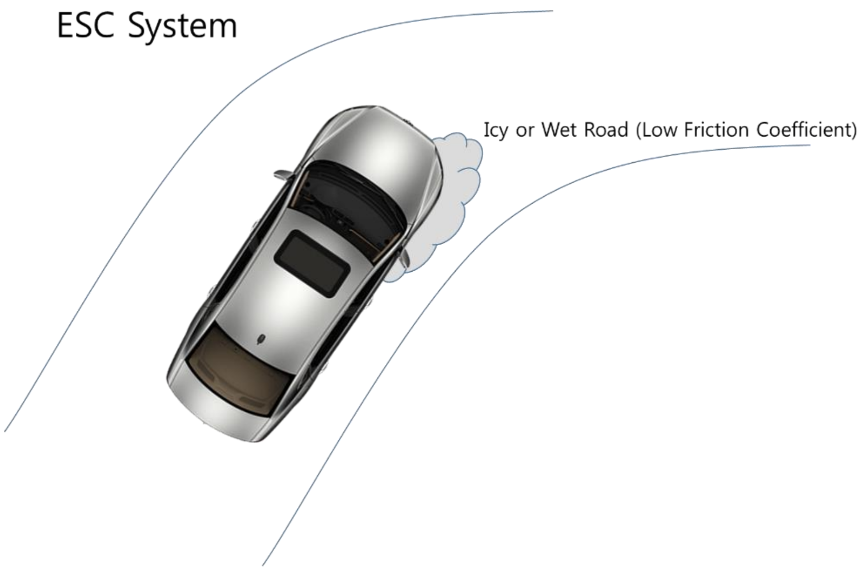

Figure 1.2. The Function of the ESC

In addition to the ABS, ESC is an advanced system than the ABS. This system continuously monitors the steering and vehicle's direction. When the system detects the probable loss of steering, the system begin to intervene the vehicle' motion to correct the vehicle's yaw motion.

Previous two technologies, ABS and ESC, control the vehicle motions when the vehicle faces and falls into the undesired and dangerous situations. Though they can correct the vehicle's stability for many cases after controlling the vehicle's brake pressure, steering angle, or torque distribution, sometimes these systems does not work properly if it is too late to take some vehicle control actions.

The start point of LAAVDS is here. The system is desired to control vehicle motions in advance to avoid such kind of undesirable and dangerous situations.

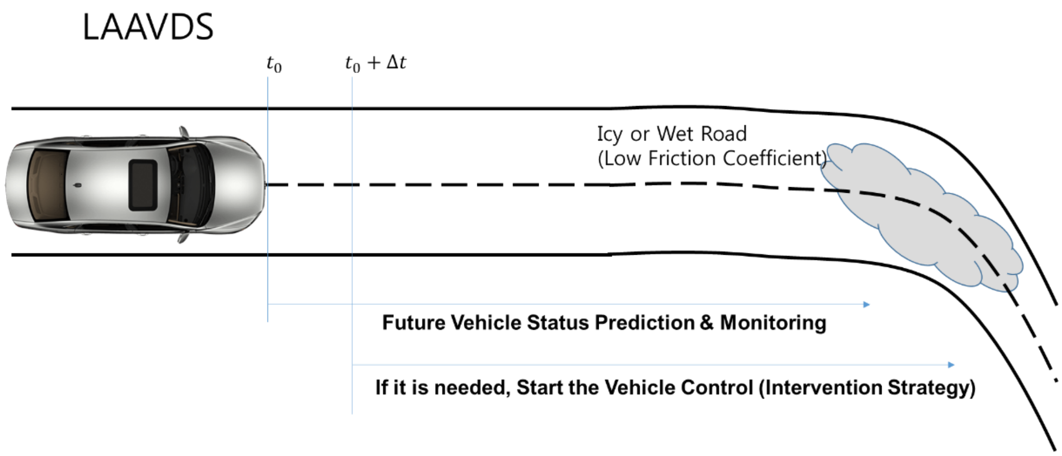

Figure 1.3. The Concept of the LAAVDS

As it can be seen from the Figure 1.3., the vehicle does a future prediction every fixed time step for next a few seconds and monitors the vehicle stability in advance. If the current vehicle driving condition is adverse for future road profile, then the system considers to intervene the vehicle's motion silently before facing the dangerous situation where the vehicle will lose its handling capability. By taking this action in advance, the chance to enable the ABS or ESC system will be reduced since the vehicle can secure the stability before facing that road profile.

Therefore, the biggest distinctive point to compare with current ABS or ESC system, the LAAVDS does a prediction for estimating the future vehicle states and take an active vehicle control action in advance before facing the dangerous situation while ESC or ABS system enable their functions when the vehicle falls into the undesirable condition.

1.3 Thesis Statement

The thesis of this work is that, given knowledge of the driving environment (road condition, banking, elevation changes), future driver intentions, and an accurate vehicle model; an effective Intervention Strategy (IS) can be developed such that the required changes to the driver commands (throttle, brake, and steering) can be estimated such that the vehicle maintains its handling capability.

1.4 Contributions

The following are the original contributions to the state-of-the-art that are developed in this work:

1. Predictive Throttle and Brake Modulation Technique by Iterative Learning Control Application

   The efficient throttle and brake modulation technique is developed to estimate the required change in throttle and brake in advance to keep the PM below threshold value and maintain the handling capability. First of all, the linear predictive inverse engine model and brake model are developed by system identification. Second, simplified drivetrain model is developed to convert the desired change in longitudinal force at the tire contact patch to the desired change in engine torque. Next switching model between throttle and brake is developed to determine the timing when to manipulate the brake rather than throttle. Last predictive model which has both a nonlinear correction model and a linear prediction model forming an Iterative Learning Control system is developed. The model is validated via simulation results.

2. Yaw Motion Neutralization Technique

   The Performance Margin level is maintained below a specified threshold by modulating the throttle and brake commands in a manner that is yaw-neutral. That is, the LAAVDS as currently envisioned does not induce a perturbation to the vehicle's yaw motion. In this way the LAAVDS control is decoupled to a great degree from yaw management systems such as Electronic Stability Control (ESC). For achieving this goal, steering correction model is developed as a first step. The reference model is derived from simple bicycle model. Then the sliding mode controller is developed to reject the perturbation and disturbance. This model is validated via simulation results. Eventually, it will be integrated and implemented into LAAVDS at the end.

3. Intervention Strategy

   Ultimately, it is desirable to develop the Intervention Strategy to control the vehicle motion by manipulating the throttle, brake, and steering for achieving the goal of LAAVDS. All the previous works, predictive throttle and brake modulation technique and linearized chassis model, are integrated and implemented into the constraints of the optimization. The constrained optimization is considered to derive the optimal change in throttle and brake during the vehicle control. The adaptive control law is developed which can update its control law continuously based on the error from the iterative learning control. Finally, the evolutionary optimization method is developed for the Intervention Strategy.

1.5 Dissertation Outline

The work is organized as follows:

Chapter 2: Recent technology in ADAS is introduced. Next previous work by the Vehicle Terrain Performance Laboratory (VTPL) is reviewed including the concept overview of LAAVDS, the definition of the Performance Margin (PM), and the linearized chassis model. Then completed works by other researches in terms of engine torque control, brake control, active steering control, differential braking control, constrained optimization design process, and iterative learning control framework are described.

Chapter 3: A Predictive Model for Throttle and Brake Modulation by Iterative Learning Control is developed. First the engine control technique to generate the desired longitudinal force at the tire contact patch is developed. Next the brake control technique is introduced which can cover the limited performance of manipulating the throttle input. Simulation results demonstrate this concept.

Chapter 4: A novel technique for electronic stability control by steering angle correction is developed. Reference model control scheme is used for developing the steering angle correction. First the reference model is developed from the simple bicycle model. Then the sliding mode controller is designed to eliminate the vehicle's perturbation motion by controlling the steering angle. Simulation results demonstrate this concept.

Chapter 5: The Intervention Strategy is developed. To enhance the comfortableness to the driver, the weighting method for time series elements and penalty function for using a brake are considered while developing the objective function. All the previous developments, a linear predictive powertrain model, a linear drivetrain model, and a linear chassis model by Bandy [4], are integrated and implemented into the constraints for the optimization.

1.6 Publications

Journals

1. Cho, S., Bandy, R., Ferris, J., Schlinkheider, J. et al., "Location-Aware Adaptive Vehicle Dynamics System: Brake Modulation," SAE Int. J. Passeng. Cars - Mech. Syst. 7(2):2014.

2. Cho, S., Bandy, R., Ferris, J., Schlinkheider, J. et al., "Location-Aware Adaptive Vehicle Dynamics System: Throttle Modulation," SAE Int. J. Passeng. Cars - Mech. Syst. 7(1):2014.

3. Bandy, R., Cho, S., Matthews, C., Celli, J. et al., "Location-Aware Adaptive Vehicle Dynamics System: Concept Development," SAE Int. J. Passeng. Cars - Mech. Syst. 7(1):2014.

4. Matthews, C., Cho, S., Ferris, J., Schlinkheider, J. et al., "Using Performance Margin and Dynamic Simulation for Location Aware Adaptation of Vehicle Dynamics," SAE Int. J. Passeng. Cars - Mech. Syst. 6(1):225-230, 2013, doi:10.4271/2013-01-0703.

5. Cho, S., Ferris, J., Schlinkheider, J. et al., "Convergence Analysis of Throttle Response in Iterative Learning Control." ASME Journal of Dynamic Systems Measurement and Control **(Will be submitted)**

6. Cho, S., Kang, Y., Ferris, J., Schlinkheider, J. et al., “Model based Predictive Control with the Application of Iterative Learning Control.” IEEE Intelligent Transportation System **(Will be submitted)**

7. Kang, Y., Cho, S., Ferris, J., Schlinkheider, J. et al., ., “A Real Time Driving Simulator.” IEEE Vehicular Technology **(Will be submitted)**

Conferences

1. Bandy, R. A., Cho, S., Ferris, J., Schlinkheider, J., et al, “Location-Aware Adaptive Vehicle Dynamics System: Linear Chassis Predictions.” ASME DSCC 2014 Automotive and Transportation System invited session (Submitted and tentatively accepted)

2. Review of Literature

2.1 Introduction

This chapter provides recent technology in terms of ADAS first. Then previous achievements by members of the Vehicle Terrain Performance Laboratory (VTPL) are introduced. The concept of an LAAVDS is described to provide a context for the novel contributions of this work. Then the Performance Margin (PM) is introduced as the control index of LAAVD. Next previous studies in terms of throttle and brake control are suggested. Then previous studies with respect to the active steering control and differential braking control are introduced. Last the iterative learning control are discussed.

2.2 Recent Trend of Advanced Driver Assistant Systems (ADAS)

Today, research is taking ADAS into new realms. The most prevalent research in the automotive industry is provided below.

Vehicle to Vehicle Communication **–** Ford, BMW, and Volvo among others are all working on systems that allow vehicles to share information between vehicles and provide drivers with more information to improve their driving abilities [5] [6] [7]. These warnings include traction control activation, traffic, emergency vehicles presence, children, pedestrians, cyclists, and other drivers. Some of these technologies use Wi-Fi, and others use cellular data, but the concept is similar. Some automakers have agreed that the best system would work across all manufacturers. LAAVDS could leverage this technology be transmitting road conditions to/from other near-by vehicles, and by supplying a database of information about road conditions.

Collision Avoidance Systems– Different organizations are addressing this with many different solutions. The central idea is to identify an impending collision and avoid it [8]. On the most basic level, systems use technologies to identify that an obstacle is stopped in the vehicle's path and then perform an emergency stop. Some systems can do other maneuvers such a lane change, and other obstacle avoidance. These systems employ a combination of sensor technologies to identify potential collisions. LAAVDS would work in concert with collision avoidance systems. While the LAAVDS monitored the upcoming road for hazardous conditions and pending extreme handling maneuvers, the Collision Avoidance Systems would be monitoring the road for obstacles. The LAAVDS would hand over control to the Collision Avoidance System when potential obstacles are detected.

Lane Keeping Assistant Systems – Similar to collision avoidance systems, there are many different organizations pursuing a way to keep the vehicle within the lane it is currently in [9]. Drivers can fail to stay within their lane for reasons such as distraction or even drowsiness, so these systems are designed to enable the car to aid the driver in staying in their lane. Basically, it is available to make this system by adding a vision sensor and Motor Driven Power Steering (MDPS). LAAVDS would use the lane keeping systems data stream by using the lane positioning information to predict the pending path that the driver will take. This will aid the LAAVD system in predicting the curvature of the vehicle's path and the resulting lateral forces that will be required to navigate upcoming curves.

Driver Monitoring Systems – These systems are designed with the same idea in mind, reducing accidents, but attempting to solve the problem from another direction [10]. These systems focus solely on the driver. By using cameras and sensors these systems can tell whether the driver is looking at the road, dozing off, or caught up in a telephone conversation. If a distracted driver is detected, systems use methods such as vibrations in the steering wheel or audible alerts to re-focus the driver on the road. LAAVDS can use the same driver warning systems as an initial step in the intervention strategy. When the LAAVD first detects an upcoming extreme handling scenario, the driver can be warned before throttle and braking modulation is employed.

2.3 Previous Studies in VTPL

2.3.1. Concept Overview of LAAVDS

It is important to take a look at the brief concept overview of LAAVDS. Bandy, R. in VTPL makes a good contribution for the overview of LAAVDS [4].

2.3.1.1. Background of Concept for LAAVDS

LAAVDS requires some assumptions and prerequisite information before developing. This is significant to consider the scope of the proposed LAAVDS research within the broader spectrum of vehicle safety and driver assistant systems. First of all, the feasibility of this proposed research is dependent on the ability to predict future vehicle states and the availability of information about the local driving environment like bank angle, elevation changes, curvature, and friction coefficient. Clearly then, LAAVDS depends on various cutting edge technologies being developed, researches by Zanten and Dietsche in Bandy's work [4], to deliver such information to the driver. Current various ADAS and LAAVDS can be arranged on a plot in Figure 2.1 which has the passive to active spectrum on the vertical axis and the safety to convenience or comfort spectrum on the horizontal axis. The Active Safety quadrant includes collision avoidance and automatic emergency braking. These two systems require an active vehicle control to maintain the vehicle's safety when the driver is not available to do so. In contrast, the lane departure warning, parking assistance, and blind spot monitoring in driver support quadrant do not perform an active vehicle control. Rather those systems provide the information around the vehicle so that the driver can make a decision to take an action for safety.

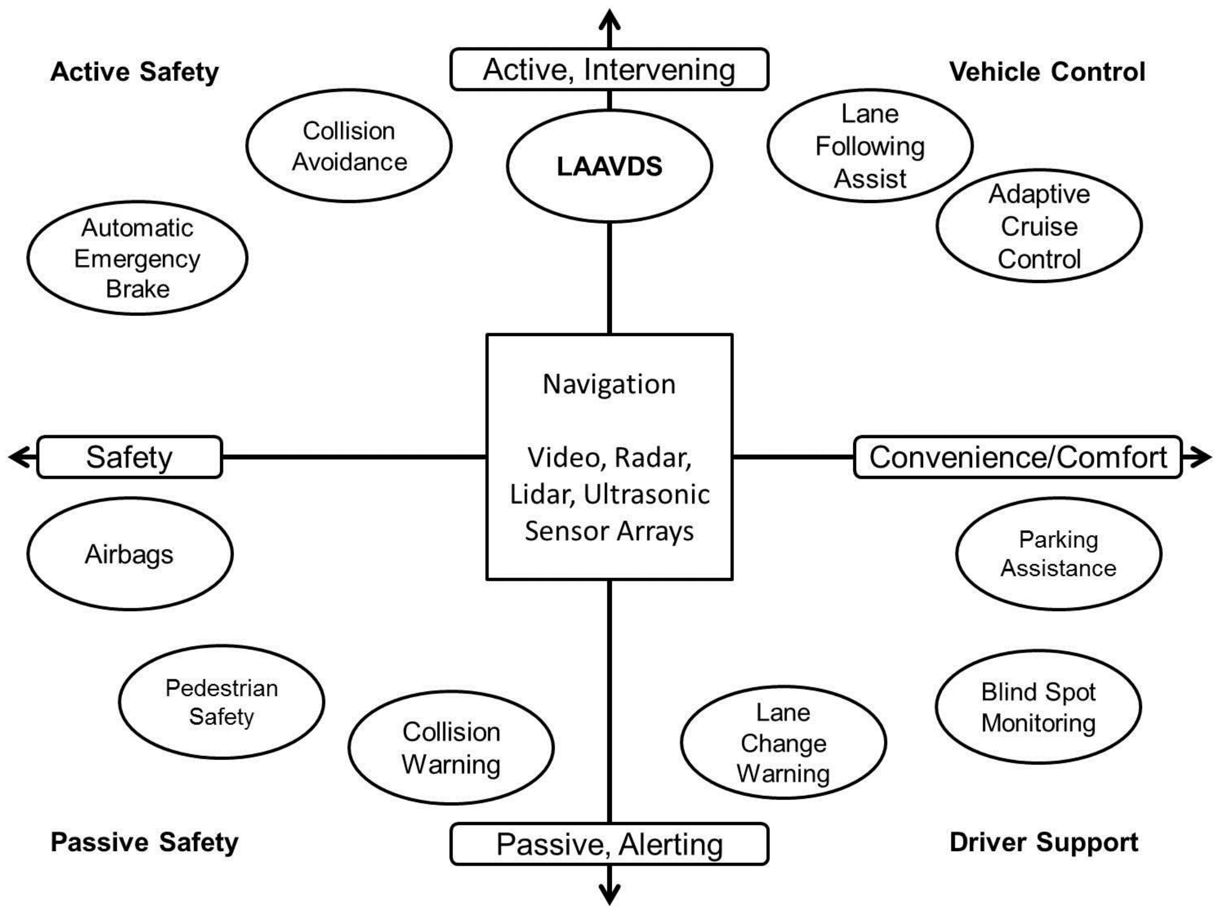

Figure 2.1. Map of Driver Assistance Systems

The LAAVDS can be lie on the middle of vehicle control and active safety since this system requires an active vehicle control (e.g., throttle, brake, and steering control) and intends to enhance the vehicle's safety actively at the same time. While the present scope of LAAVDS is to develop the one active safety system, it is being developed to implement into the autonomous vehicle eventually. To accommodate this, the standard SAE notation is used throughout the development of this system [11].

2.3.1.2. Definition of Performance Margin

Since LAAVDS pursues an active intervening rather than a passive reaction, the firm and robust intervention strategy is indispensable for this project. The detailed information for implementing it in simulation is introduced at next following section. For triggering the intervention strategy, it is required to develop the control index first. Matthew in VTPL makes a contribution for this area and that is Performance Margin (PM) [2]. PM is a metric quantifying the relative ability of the vehicle to successfully navigate the upcoming road conditions. It is defined as the ratio of the required tractive effort to navigate a turn under given conditions and the available tractive effort (for the front and rear respectively). The fraction of the available traction that is required for the vehicle to navigate a turn (given its speed and states) can be calculated. Specifically, the PM is the ratio of the required resultant tractive force to the maximum available tractive force and is written in Equation (2.1).

$$PM = \frac{\sqrt{F_x^2 + F_y^2}}{\mu F_z} \tag{2.1}$$

This metric should be continuously estimated for upcoming driving conditions to identify when it exceeds a user defined threshold, thus initiating the intervention strategy. Then the goal of intervention strategy is to bring the PM back within an acceptable range (below threshold value) by making modest modulations to the throttle and brake commands. The following constraints are placed on the Intervention Strategy design problem:

1. $PM_{front} < PM_{threshold}, \ \forall t < T$
2. $PM_{rear} < PM_{threshold}, \ \forall t < T$

Where T is the window of near-future times being predicted (e.g., 10 seconds)

2.3.1.3. Overview of Intervention Strategy and Implementation in Simulation

Bandy proposes the concept for implementing the intervention strategy in simulation environment [4]. The time step, for running an intervention strategy, is a tunable condition and can be adjusted based on specification requirement. At each time step, one time simulation is conducted on a full, non-linear vehicle model. This simulation is based on the current vehicle state, the driver commands (throttle, brake, steering), and the upcoming terrain information. The full, non-linear simulation is conducted for predefined time horizon, T, into near future. From this one time simulation, the vehicle response at the tire contact patch for this time horizon are estimated and then the PM is calculated from tire forces and friction coefficient according to Equation (2.1). This full, non-linear simulation is shown in the upper box in Figure 2.2.

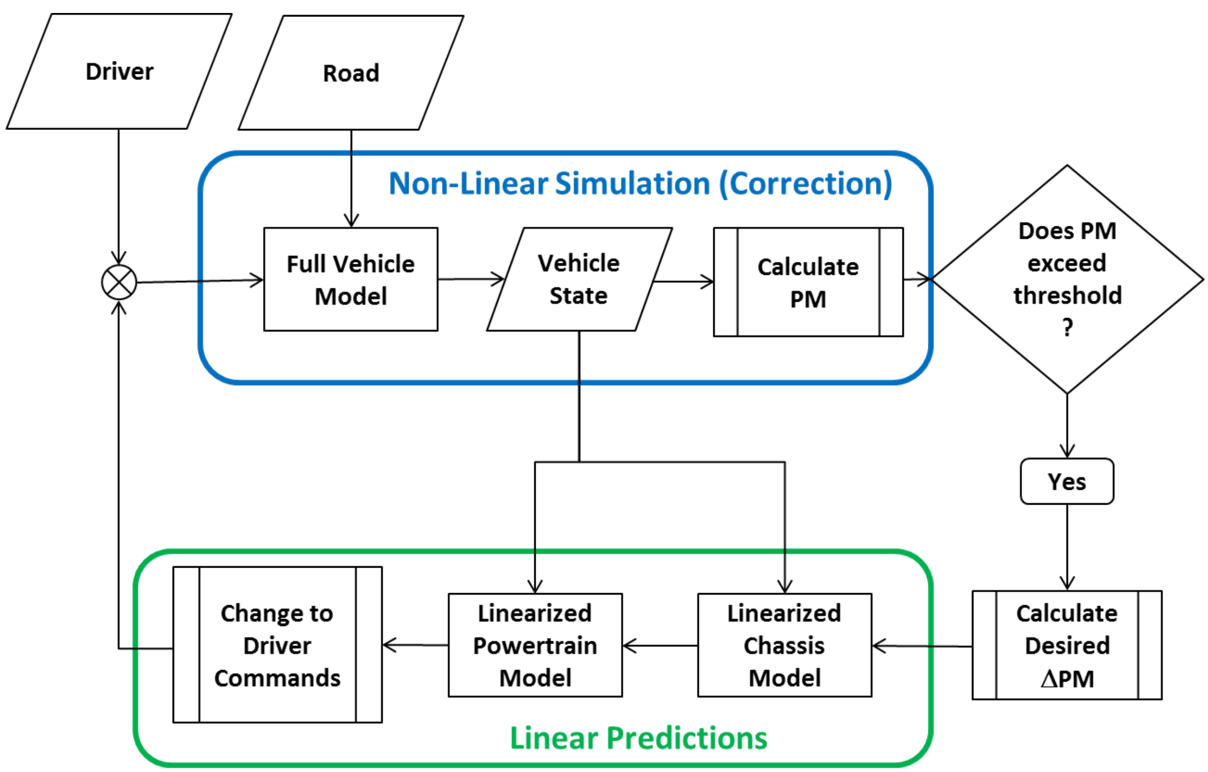

Figure 2.2. Overview of Intervention Strategy Implementation in Simulation

The vehicle states considered during simulation include the vehicle speed, longitudinal and lateral accelerations, yaw rates, suspension displacements and velocities. Road surface characteristics used in the full, non-linear simulation include elevation changes, bank angle, rutting, crowning, and the friction coefficient. The vehicle responses retrieved from the full, non-linear model are the forces and moments at each tire contact patch and a prediction of these states at each subsequent time step.

If there is an event that the PM exceeds the pre-defined threshold within the simulation time horizon, then a linear prediction of necessary changes to the longitudinal forces at the tire contact patch and corresponding required change in throttle and brake commands is calculated. This process is suggested in the lower box in Figure 2.2. In this way, a linear predictor and non-linear corrector is used to implement the intervention strategy for each time step.

2.4 Modulation Technology for Longitudinal Force at the Tire Contact Patch

For achieving the performance goal of the intervention strategy, it is of importance to secure the robust control method to modulate the longitudinal force at the tire contact patch. One of methods to modulate them is manipulating the throttle and brake. A significant amount of recent engine and brake torque control research has been geared towards nonlinear and optimization based control strategies for achieving performance goals. In this section, previous studies by other researchers are investigated.

2.4.1. Engine Torque Control Techniques

A numerous researches in engine torque control have been performed during last 3 decades. Yoon offers an approach for a nonlinear dynamic model of engines for designing powertrain controller [12]. Though this approach can provide accurate estimation of throttle manipulation, its modeling is complex and difficult. It is also inefficient to perform the computation because it requires a lot of calculations based on nonlinear model. Kang concentrates on sliding mode control to modulate the throttle valve for traction control [13]. Chamaillard makes an approach to control the engine torque by designing a robust controller which can be used on uncertain and non-linear systems [14]. He performs the system linearization and identification, an operating model design by minimization of a weighted frequencies criteria, PI and LQ controller design with robust property verification. Though this work suggest a good approach to define the engine by system identification, its model is still complex and include lots of sub components of the engine. Vermillion uses a model predictive engine torque control for delivering desired engine torque precisely [15]. His work presents the design and simulation results for an engine torque control strategy that uses online model predictive control (MPC) for delivering desired engine torque. Ioannou suggests the vehicle speed control by controlling the throttle input with sliding mode control [16]. Though its ultimate goal is to control the vehicle speed for the purpose of Adaptive Cruise Control (ACC), its work provides a good understanding how to manipulate the throttle input for controlling the engine torque to generate the desired vehicle speed. Gerdes also makes a great approach for handling the throttle input by the adaptive control scheme [17]. Rajamani provides the detailed information for designing the engine model in his book [58]. He suggests the method to design both gasoline engine and diesel engine. Regarding gasoline engine, two different approaches are provided. The first approach is a modeling by using parametric equations. This method considers the combustion as well as rotational dynamics of the engine. This covers the broad range of engine components dynamics and thus can describe the engine's performance not only steady state status but also transient state. Another method is to use an engine map. When the engine map is used to design an engine, two approaches can be considered. The one is a second order model and another one is a first order model. Regarding a second order model, the only difference to compare with the engine model that uses parametric equations is that some functions are experimentally derived. A first order engine model can be used if the intake manifold filling dynamics are ignored. However, it cannot describe the transient engine dynamics.

Though all of these works derive greatly successful results, they are based on real time and complex engine model or control law. These complex models require a lot of computing power. In this reason, it is reasonable to use these models when they are ran in simulation level. Since LAAVDS is required to be implemented into the real vehicle eventually, the proposed system in this dissertation focuses more on predictive control with simplified engine model. Therefore, more simple and efficient way to design the engine and control its torque is introduced in Chapter 3.

2.4.2. Brake Pressure Control Techniques

Likewise engine torque control, there are a lot of research in vehicle's brake control area. Yi offers an approach for nonlinear brake control by developing a nonlinear computer model and a linear model of the hydraulic brake actuator system [18]. It shows successful results for achieving the purpose of collision avoidance. However, there is lots of effort to represent all detailed information in terms of brake sub system. Liang concentrates on vehicle's longitudinal brake control by developing a modified sliding control with variable control parameter [19]. In similar manner like Yi's approach, it contains too many sub system to represent the brake model. Trachtler proposes the steering and suspension system as well as brake intervention scheme for optimized and integrated vehicle control [20]. This works suggests a great understanding for intervention strategy and integrated control for LAAVD system. Ioannou suggests the vehicle speed control by controlling the brake input as well as the throttle input with sliding mode control [16]. This approach provides a great understanding in terms of how to design the nonlinear controller for handling the throttle and brake input. Gerdes makes an approach for the adaptive controller for handling the throttle and brake input [17]. From this work, it suggests a great method how to switch the control between throttle and brake. Though these works derive greatly successful results and provides lots of ideas for improving the LAAVDS, they have one common problem. That's complexity and difficulty for modeling in terms of controller or plant.

Therefore, likewise the engine torque control, simplified brake model for intervention strategy is developed to overcome this kind of problems in Chapter 3.

2.5 Control for Vehicle's Yaw Motion Neutralization

It is desirable for LAAVDS to be a minimally intrusive. On the line of this goal, throttle and brake modulation is carried out if the PM exceeds its threshold. That is, the intervention strategy definitely brings back the PM below threshold but it does not achieve this goal by simply reducing the vehicle speed. Thus the system will reduce the PM just below threshold. Then it is expected that there can be a perturbation motion for the vehicle if there is a sharp corner for upcoming terrain. Yaw motion neutralization technique focuses on eliminating such kind of perturbation and disturbance. Its function seems like similar to current ESC system. However, it is considered not to make any confliction between ESC and LAAVDS.

For achieving this goal, it is important to understand about the current ESC system. A lot of research has been achieved in this area and it can be dived by two categories. One is a steering correction and another is differential braking technique.

Therefore, the study about this area is inevitable. Plenty of studies are achieved for this area and they are covered in next following section

2.5.1. Active Steering Control

One of technique to achieve the goal of yaw motion neutralization is an active steering control method. A lot of researches have been done for this area. Ackermann uses an active steering control to attenuate the yaw disturbances on the vehicle by robust unilateral decoupling of yaw and lateral mode [21]. It also aims at rollover avoidance of road vehicles. Since the LAAVDS focuses on rejecting the disturbances and enhancing the stability at the same time, it suggests a great understanding in terms of active steering control scheme. Zheng suggests a basic concept by an active steering control with front wheel steering [22]. In this work, the decoupling of the vehicle's lateral motion, yaw motion, and yaw damping are achieved simultaneously by feedback of both yaw rate and front steering angle with the scheduled gains. A bicycle model is used for steering dynamics and gives a great help to design and improve the LAAVDS steering dynamic model. Baslamisli develops a gain scheduled active steering control design method to preserve vehicle stability in extreme handling situations [23]. Its strategy to control the steering angle to prevent the vehicle from losing the stability in extreme condition gives an inspiration how to design our own steering control system. Falcone provides a model predictive control (MPC) approach for controlling an active front steering system in an autonomous vehicle [24]. Though LAAVDS does not focus on full autonomous vehicle, this work is greatly helpful to understand how LAAVDS can be updated later when it is implemented into autonomous system. Keviczky also suggests a MPC approach to active steering [25]. The purpose of its controller is to stabilize a vehicle along a desired path while rejecting wind gusts and fulfilling its physical constraints. This work focuses on vehicle's stability by MPC method while Falcone's work more concentrates on following the trajectory on slippery road. Since proposed yaw motion neutralization technique in the LAAVDS focuses on eliminating the perturbation and disturbances, this work is greatly helpful for solving the design problem in terms of yaw motion neutralization technique.

2.5.2. Differential Braking Control

Another technique to achieve the goal of yaw motion neutralization is a differential brake control method. Yi investigates the differential braking strategies for vehicle stability control [26]. In this work, a three degree of freedom (3 DOF) yaw plane vehicle model is used for controller. The brake control inputs are derived from the sliding control law based on a 3 DOF yaw plane vehicle model with differential braking. Its performance is also compared with the direct yaw moment controller. This works is greatly helpful to understand about the basic differential braking control with sliding mode technique.

Zhao provides an approach in terms of vehicle's lateral control and yaw stability control through differential braking [27]. In this work, a linearized vehicle model is used rather complicated one for the purpose of explanation of idea of differential braking and controller design. A fuzzy logic controller for lateral control and yaw stability control is developed in this work.

Cho investigates the unified chassis control scheme for optimized vehicle stability [28]. This work provides the information in terms of various and integrated vehicle control as well as ESC by differential braking. It gives a great impression how to integrate all the vehicle control system.

Zhang suggests a vehicle stability control strategy based on active torque distribution and differential braking [29]. This work presents a vehicle yaw stability control strategy to prevent from spinning and drifting out. The yaw stability control system is integrated with active torque distribution as well as differential braking. It provides good information for the switching timing between active torque distribution and differential braking. In this work, it is mentioned that the active torque distribution control method does not work properly if the friction coefficient of road is small or if the vehicle speed is too high.

2.6. Iterative Learning Control

Iterative learning control, or ILC, is one of the techniques for improving the transient response and tracking performance of plant, equipment, or systems that exhibit the same trajectory motion or operation. One of the widely known examples in terms of the ILC is a robot arm manipulation that executes the same operations repeatedly. There are many other problems which can be considered part of the framework of repetitive operations. Every repetition for this kind of manipulation can exhibit the same transient response and may not reach to the control goal. The purpose of the ILC is to reduce this kind of transient error based on the previous error whenever the same operation is repeated. Eventually, the norm of the transient error can be reduced and reaches zero as the same operations are iterated. Arimoto initially suggested the concept of the ILC [30]. After his launching the concept of the ILC, many researchers tried to prove the concept of the ILC with respect to the stability, convergence, robustness, and so on. The next following section introduces the previous researchers' achievements in this ILC area.

2.6.1. Convergence and its rate, Robustness

A numerous research papers try to demonstrate the convergence of ILC algorithms and analyze the robustness. Convergence is considered in every paper. However, some researchers explicitly consider these issues. Huang provides the information in terms of the phenomena of initial convergence followed by divergence and methods are suggested to avoid the problem [31]. Hideg discusses the fact that the actual norm can distort the stability of the ILC algorithm [32]. It should be clear, however, that the ability of the system to converge to the desired trajectory is a separate question from the speed with which the system can converge to the desired trajectory.

The robustness of the algorithm is defined herein as the speed with which the ILC converges to the desired trajectory. Amann's work suggests how to estimate the system's convergence speed by estimating the system's minimum singular value [3]. Moore provides the insight for the adaptive ILC scheme which enables the system can converge to the desired trajectory more quickly than the conventional ILC [33] by updating the control law for every iteration. Heinzinger calculates the error limits not only for the initial condition mismatch but also for the effects of state and output noise [34]. Saab discusses the robustness and convergence with respect to the 'D-type' ILC algorithm [35].

2.6.2. Vehicle Application of the ILC

The original ILC research focused on the robotics area. However, this technique being applied to various fields, among them are vehicle applications. Li provides the study and design of the longitudinal learning control system of the automobile [36]. For underwater vehicles, Venugopal applies the ILC for an autonomous underwater vehicle [37], in which they pursued an integrated neural network controller and learning algorithm for online learning control.

3. Throttle and Brake Predictive Modulation Model

The work developed in section 3.1 and 3.2 has been published in the proceedings of the SAE International Journal of Passenger Cars-Mechanical Systems, as "Location-Aware Adaptive Vehicle Dynamics System: Throttle Modulation" and ""Location-Aware Adaptive Vehicle Dynamics System: Brake Modulation", paper number 2014-01-0105 and 2014-01-0079 respectively

Real-time implementation requires the development of computationally efficient predictive vehicle models which is the focus of this work. This work develops one means to alter the future vehicle states: modulating the driver's throttle commands. First, changes to the longitudinal force are translated to changes in engine torque based on the current operating state (torque and speed) of the engine. Next, the required changes to the throttle to affect these desired changes to engine torque are estimated by developing a linearized, inverse engine model based on the steady-state conditions. These predicted changes to the throttle command are used in the correction stage of the algorithm in which a full non-linear vehicle model yields the resulting longitudinal force response to the predicted change in throttle. Finally, the predictor-corrector control loop is closed by comparing the desired longitudinal force to the resulting force. The performance of the throttle modulation method is exhibited through simulation results on two test cases. Results show that the proposed approach yields a significant overall performance improvement.

3.1. Model based Predictive Throttle Control

One critical component of this Intervention Strategy is the development of a predictive powertrain (engine and drivetrain) model. The issue being addressed is that using a full non-linear model to estimate future vehicle states is critical, but not realizable in real time. Therefore, a computationally efficient, but less accurate powertrain model must be developed to make timely predictions of future vehicle states. This prediction is then used in a predictor-corrector algorithm within the Intervention Strategy. The linear model is used to make fast predictions in real time and the full non-linear model is used to make corrections to these predictions. Although the full nonlinear model is not required to run in real time, it still must run quickly enough to make corrections to the linear predictive model several times a second.

The objective of this section is to develop the prediction model which can estimate the required change in throttle input to deliver the desired engine torque and resulting desired longitudinal force. First, the limitations on the performance of the engine are investigated. Second, the linearized inverse engine model is introduced. Third, the relationship between the engine torque and the longitudinal force is developed. Finally, a predictive model for estimating the future states of longitudinal force and throttle input is developed. The integration of these contributions is demonstrated through a case study wherein a desired change in longitudinal force is prescribed and the throttle change required to achieve this change in force is predicted. The accuracy and limitations of the method are discussed followed by concluding remarks.

3.1.1. Background

The feasibility of the proposed method is dependent on the ability to predict vehicle states and the availability of information about the local driving environment (location, friction, banking, etc.). The information available to the vehicle and the driver continues to grow and there is a great amount of research currently being done in both fields. An overview of the practicality of implementing a Global Positioning System (GPS)-based control system into ground vehicles is discussed by Beiker et al. [38]. Furthermore, Ahn proposes both longitudinal and lateral dynamics based algorithms to estimate friction using measurements from sensors that are available on typical commercial vehicles [39]. Lee develops a method to estimate the maximum tire-road friction coefficient by designing tractive force estimator, a brake gain estimator, and a normal force observer [40]. Pasterkamp suggests a method to estimate the friction by using a tire as a sensor [41]. Erdogan advises a sensor and estimation system to measure the friction coefficient between tire and road [42]. Hsu provides a method to estimate the tire slip angle and friction limits by using steering torque [43]. Based on these successful studies, it is assumed in this work that information about the current vehicle state and local driving environment are available.

The linear prediction-nonlinear correction process outlined by Bandy, et al. is fundamental to this work [4]. The system flowchart is reproduced here as Figure 3.1. A link between the desired change in longitudinal force, calculated from a desired change in Performance Margin, and the necessary throttle commands is developed here. This is represented as the "Linearized Powertrain Model" in the Linear Predictions box in Figure 3.1.

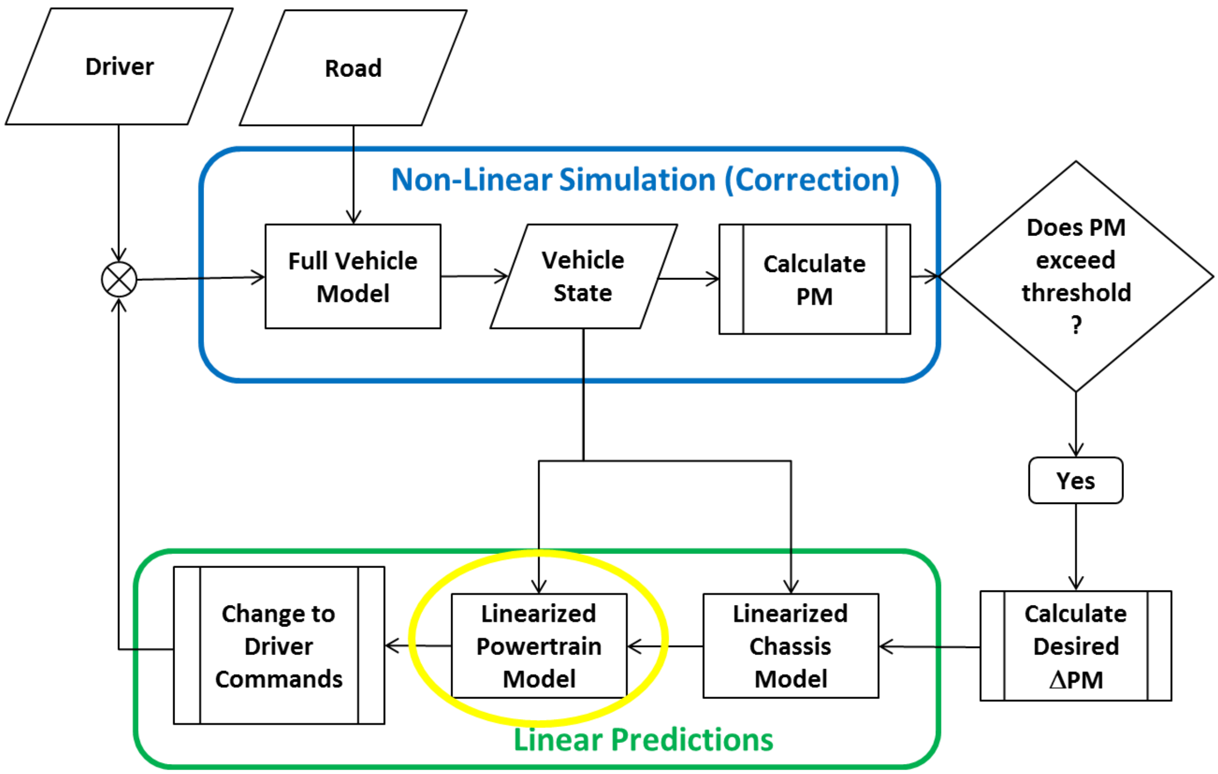

Figure 3.1 Overview of Intervention Strategy Implementation in Simulation

The success of this throttle manipulation method relies on the accurate and computationally efficient inverse engine model. Since the causality of the system dictates that the changes in throttle must cause a change in torque, the inverse model is defined herein as one in which a desired change is torque produces an estimated change in throttle. A significant amount of recent engine torque control research has been geared towards nonlinear and optimization based control strategies for achieving performance goals for various engine types. Yoon, Kang, Vermillion, Ioannou, and Gerdes use a nonlinear dynamic model of engines to control the engine torque [44] [45] [46] [47] [48]. The successful results of this research can be implemented in the nonlinear correction stage of the predictor-corrector process, highlighted in the upper box in Figure 3.1. However, the predictive capabilities of these results are limited by the processing capability of a typical Electronic Control Unit (ECU) in the host vehicle. A linearized and computationally efficient predictive model in which the throttle commands can be derived from desired engine torques to solve this efficiency issue.

3.1.2 Linear Predictive Engine Model

When there is a change in throttle angle position, there is a time delay of engine torque response; Figure 3.2 shows typical simulation results for this time delay. In the two leftmost graphs, the throttle command is a single sinusoid with a period of 200 milliseconds. The torque response is skewed and delayed approximately 50 milliseconds due to the inertia in the system. On the right side of the figure, the period of the sinusoid is extended to 4 seconds and the 50 millisecond delay is negligible. Therefore the first approach in developing an engine model is to limit the bandwidth of throttle control to elicit steady-state torque responses.

Note that throughout this development the changes in the longitudinal forces at the left and right front tire contact patches are identical so that no additional yaw moment is induced. Future work should incorporate yaw control into the overall Intervention Strategy. Also in the current development it is assumed that no gear shifting occurs during the throttle modulation, thus avoiding these impulsive changes to the longitudinal force.

n

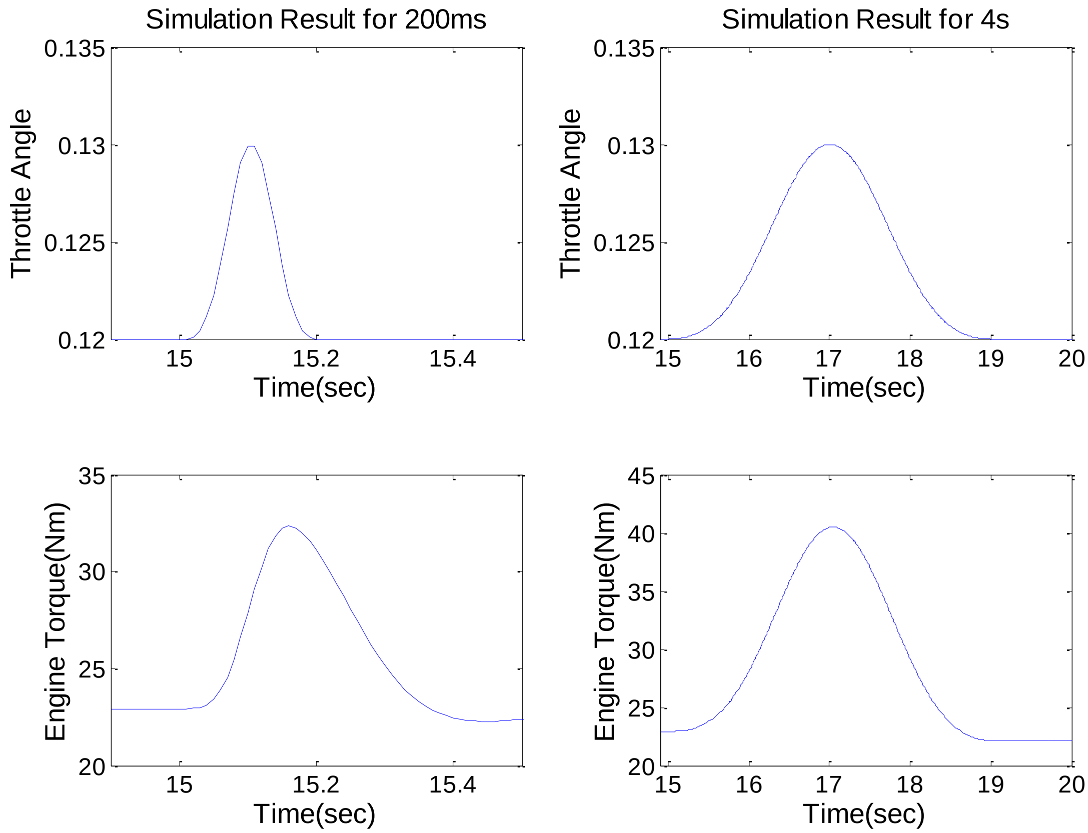

Figure 3.2. Time delay for resulting change in engine torque response from change in throttle input

The Frequency Response Function (FRF) of the engine torque due to throttle commands for a specific example is shown in Figure 3.3. In this case, the system exhibits a proportional gain response up to approximately 0.7 Hz. The torque response is not controllable at frequencies higher than 1.5 Hz. That is, any request to change the engine torque beyond this frequency cannot be achieved by manipulating the throttle. Intermediate frequencies will be dominated by the dynamics of the powertrain system which are avoided in this work.

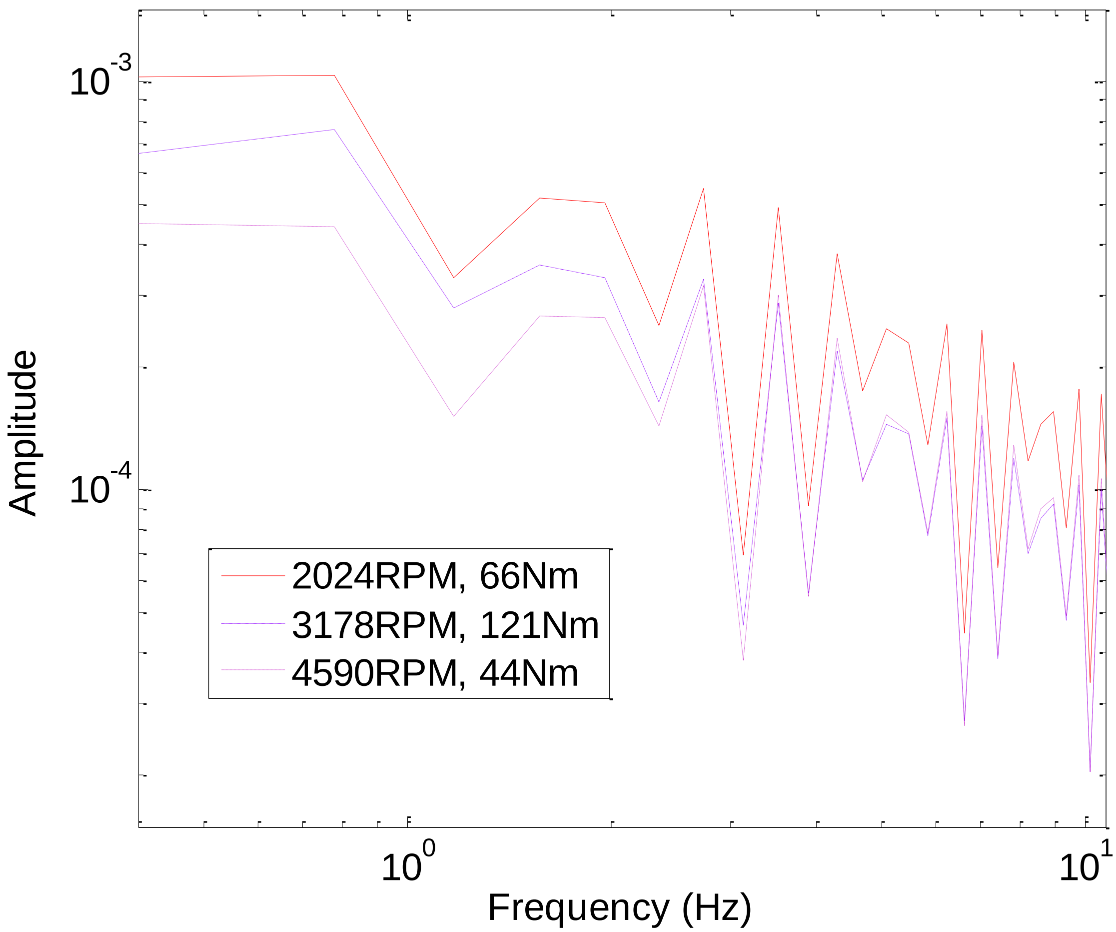

Figure 3.3. Result with respect to the magnitude of FRF for change in throttle input and resulting engine torque output

It is assumed that the engine state, when operating under steady-state conditions, can be adequately described by its speed and torque (η_{ss}, τ_{ss}). The FRF for a wide range of engine states all demonstrate similar tendencies in their response. Specifically, if there is a small change to the throttle, ΔTh, there is a proportional response in the resulting change in torque, $\Delta\tau$, assuming that the change in throttle occurs at a frequency less than 0.7 Hz. At these frequencies, only the gain changes as the state changes. Although the causality is such that the change in throttle causes the change in torque, the inverse relationship is desirable in developing the Intervention Strategy. From this observation, the inverse FRF is defined as a function of frequency, f, and parameterized by the engine speed and torque (η_{ss}, τ_{ss}), as shown in Equation (3.1).

$$H_{inv-eng}(f;\eta_{ss},\tau_{ss}) = \frac{\Delta Th(f;\eta_{ss},\tau_{ss})}{\Delta\tau(f;\eta_{ss},\tau_{ss})} \tag{3.1}$$

For example, consider the case in which there is negligible change in the phase as the state changes and the magnitude of the response is only a function of the engine state, not the frequency. In this case, it may appropriate to approximate the FRF by the transfer function in Equation (3.2).

$$G_{inv-eng}(s) = K_p(\eta_{ss},\tau_{ss}) \cdot \frac{(1+T_z \cdot s)}{s \cdot (1+T_p \cdot s)} \tag{3.2}$$

A system identification process proceeds by simulating the system at steady-state conditions over a wide range of engine states. In this particular example, the engine states are distributed from 870 to 6000 rpm and from -10 to 400 Nm, thus forming a calibration map. At each of these calibration points, the frequency response for the change in throttle and change in torque are calculated and the time constants, T_z and T_p, are determined by the cutoff frequencies in the bode plot. The proportional gain, K_p, is defined as a function of the engine state and can be approximated by a bivariate polynomial of the form represented in Equation (3.3).

$$\widehat{K}_p(\eta_{ss},\tau_{ss}) = \beta_0 + \beta_1\eta_{ss} + \beta_2\tau_{ss} + \beta_3\eta_{ss}^2 + \beta_4\tau_{ss}^2 + \beta_5\eta_{ss}^3 + \beta_6\tau_{ss}^3 + \beta_7\eta_{ss}^{-1} + \beta_8\tau_{ss}^{-1} + \beta_9\eta_{ss}^{-2} + \beta_{10}\tau_{ss}^{-2} \tag{3.3}$$

The polynomial coefficients, β_i, are found using a generalized inverse approach such that the squared error in the estimate of the gains is minimized. The linear, predictive, inverse engine model, which provides the estimated change in throttle from the desired change in torque, is of the form represented in Equation (3.4). Note that this equation is written in the Laplace transform domain to simplify notation.

$$\Delta Th_{req}(s) = \left(\widehat{K}_p(\eta_{ss}, \tau_{ss}) \cdot \frac{(1+T_z \cdot s)}{s \cdot (1+T_p \cdot s)}\right) \cdot \Delta\tau_{des}(s) \tag{3.4}$$

3.1.3 Linear Predictive Drivetrain Model

The goal of this work is to modulate the throttle, and thereby the longitudinal force, so that the Performance Margin does not exceed some threshold. The relationship between the throttle and the engine torque is established (for a particular engine state) by Equations (1) through (4). Next it is necessary to model the drivetrain (i.e., the relationship between the engine torque and the longitudinal force at the tire contact patch). There are several drivetrain sub-systems that influence this relationship (e.g., the tire, torque converter, transmission, and differential gear). Detailed models of these drivetrain sub-systems would be computationally inefficient for real time prediction of the changes in engine torque as a function of changes to the longitudinal force. Instead, a conversion model is developed based on the current state of the engine.

The power from the engine cannot be conserved while it is transferred to the tires. Therefore, the relationship between the engine torque and longitudinal force at the tire contact patch is defined in Equation (3.5) where ϵ defines the overall efficiency of the drivetrain system at the existing state.

$$\epsilon \cdot \eta \cdot \tau = F_x \cdot V_x \tag{3.5}$$

This relationship for small changes to the engine state is given in Equation (3.6), where it is assumed that the changes in the efficiency between the original state and the perturbed state are negligible (a second order term).

$$\epsilon(\eta + \Delta\eta)(\tau + \Delta\tau) = (F_x + \Delta F_x)(V_x + \Delta V_x) \tag{3.6}$$

The first order perturbation of Equation (3.6) is given as Equation (3.7). Note that the equations have been written such that the overall powertrain efficiency is not explicitly required.

$$\Delta\tau(t) = \frac{\tau(t)}{V_x(t)}\Delta V_x(t) + \frac{\tau(t)}{F_x(t)}\Delta F_x(t) - \frac{\tau(t)}{\eta(t)}\Delta\eta(t) \tag{3.7}$$

The change in the longitudinal force a time t_i, $\Delta F_x(t_i)$, is simply the mass of the vehicle times the change in acceleration. This relationship is written as a change in velocity in discrete time steps, from time t_i to time t_{i+1} as in Equation (3.8).

$$\Delta F_x(t_i) = m\left(\frac{\Delta V_i - \Delta V_{i-1}}{t_i - t_{i-1}}\right)$$

$$\Delta V_x(t_i) = \frac{t_i - t_{i-1}}{m}\Delta F_x(t_i) + \Delta V_{i-1} \tag{3.8}$$

It can be shown that this recursive relationship can be rewritten such that the current velocity, $\Delta V_x(t_i)$, is calculated from all the previous changes in the longitudinal force. This formulation assumes that there is a fixed sample time for the system so that $\Delta t = t_i - t_{i-1}$ for all time indices, i. It is also assumed that there is no initial change in velocity. That is, it is assumed that $\Delta V_x(t_1) = 0$. This relationship is described in Equation (3.9).

$$\Delta V_x(t_i) = \frac{\Delta t}{m} \cdot \sum_{j=1}^{i-1} \Delta F_x(t_j) \tag{3.9}$$

The change in engine speed, $\Delta\eta(t)$, is modeled as a function of the velocity. That is, at any moment there is a simple gear reduction, r, (assuming that the vehicle remains in a single gear) and some overall drivetrain efficiency, ε, due to factors such as the tire slip ratio and the possible slippage in the drivetrain (e.g., in the torque converter). This relationship is written as Equation (3.10).

$$V_x(t) = \varepsilon \cdot r \cdot \eta(t) \tag{3.10}$$

The relationship for the perturbed system is captured in Equations (3.11) and (3.12).

$$(V_x + \Delta V_x) = \varepsilon \cdot r \cdot (\eta + \Delta\eta) \tag{3.11}$$

$$\Delta\eta = \frac{\eta}{V_x} \cdot \Delta V_x \tag{3.12}$$

This can be re-written for the discretized system as shown in Equation (3.13).

$$\Delta\eta(t_i) = \frac{\eta(t_i)}{V_x(t_i)} \cdot \Delta V_x(t_i) \tag{3.13}$$

Note that some low-pass filtering may be required if the ratio of current engine speed to longitudinal velocity is derived from experimental data. The final matrix form for the conversion from a change in longitudinal force to vehicle wheel speed is written using the matrix forms shown in Equation (3.14). Note that [S] is simply a lower shift matrix and the vectors are defined similarly to the longitudinal force vector.

$$\{\Delta F_x\} = \begin{bmatrix} \Delta F_x(t_1) \\ \Delta F_x(t_2) \\ \Delta F_x(t_3) \\ \vdots \\ \Delta F_x(t_N) \end{bmatrix} \text{ and } [S] = \begin{bmatrix} 0 & \dots & \dots & 0 \\ 1 & \ddots & \dots & 0 \\ \vdots & \dots & \ddots & 0 \\ 1 & \dots & 1 & 0 \end{bmatrix} \tag{3.14}$$

Diagonal matrices are defined similarly to the following examples in Equation (3.15).

$$[\tau/V_x] = \begin{bmatrix} \ddots & & \\ & \frac{\tau(t_i)}{V_x(t_i)} & \\ & & \ddots \end{bmatrix} \text{ and } [\tau/F_x] = \begin{bmatrix} \ddots & & \\ & \frac{\tau(t_i)}{F_x(t_i)} & \\ & & \ddots \end{bmatrix} \tag{3.15}$$

The final matrix form for the conversion from a change in longitudinal velocity to engine speed is given by Equation (3.16).

$$\{\Delta\eta\} = [\eta/V_x]\{\Delta V_x\} \tag{3.16}$$

And the final matrix form of this transformation from a change in longitudinal force to a change in torque is written as Equation (3.17).

$$\{\Delta\tau\} = \left\{\frac{\Delta t}{m}\left(\left[\frac{\tau}{V_x}\right] - \left[\frac{\eta}{V_x}\right]\left[\frac{\tau}{\eta}\right]\right) + [\tau/F_x]\right\} [S]\{\Delta F_x\} \tag{3.17}$$

Equation (3.17) forms the linear predictive model for the vehicle drivetrain.

The future states of the vehicle can be predicted assuming that knowledge of upcoming terrain and driving conditions are known (see Figure 3.1). This prediction model has both a nonlinear correction model and a linear prediction model forming a feedback control system. Error between the desired longitudinal force and predicted longitudinal force is corrected by predicting the required change in throttle input and resulting predicted longitudinal force. These predictions and corrections are updated at regular intervals that are dictated by the complexity of the models and the on-board computational power. In the examples presented in this work, a 10 second time horizon of future states is predicted and the prediction model is corrected each second.

3.1.4 Simulation Results

A commercial vehicle simulation package is used for the simulation environment. A typical sedan with a 200 kW engine model and a 6-speed automatic transmission is modeled with 15 mechanical degrees of freedom. It is assumed that the desired change in longitudinal force is derived by first calculating the desired change in Performance Margin and that this information is updated every second for the next 10 seconds. The throttle control prediction model estimates the future states in terms of the required change in throttle input and the resulting change in longitudinal force. For a number of computations, there is one nonlinear prediction by the full nonlinear vehicle model, a linear prediction by the simplified inverse engine model, and a correction by the feedback system per second. Implementation of this proposed method is demonstrated in a case study. Consider a sedan traveling at 65 km/hr on a surface with a constant μ of 0.8 navigating a straight road. The generated desired change in longitudinal force as a reference signal is suggested in Figure 3.4.

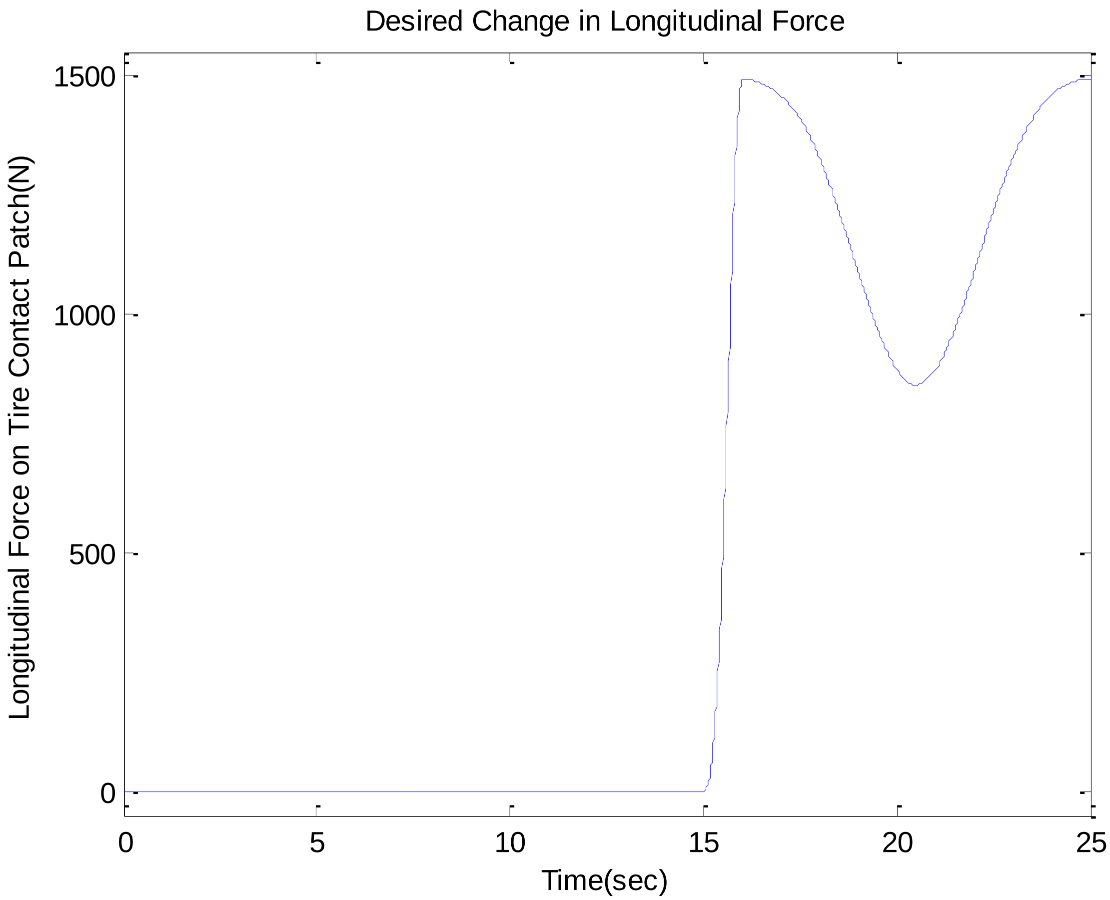

Figure 3.4. Desired change in F_x for a case study

The experiment is conducted in 10-second segments (time segments can also be called time horizons). After simulation results are obtained for the first segment (0-10 seconds), the data are analyzed to determine if any error exists between the desired and predicted longitudinal force and how much throttle correction is necessary. The next 10-second segment (from 1 to 11 seconds) is simulated and analyzed. If the intervention by change in throttle input is necessary at any moment, it is implemented by updating the throttle input in the subsequent steps. This framework is shown in Figure 3.5.

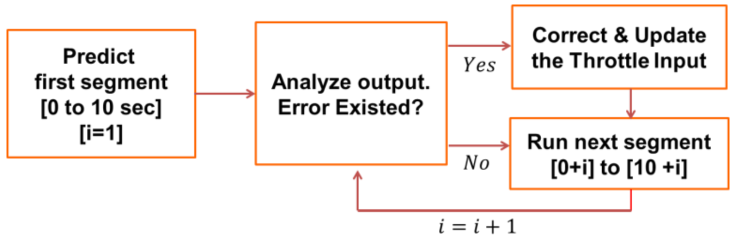

Figure 3.5. Flowchart of Throttle Intervention Process

In this case study, the simulation time is 25 seconds and there is no desired change in longitudinal force until 15 seconds. Therefore, it is expected that the prediction model does not estimate any required change in throttle input until the fifth iteration, when it has upcoming terrain information for the time segment of 5 to 15 seconds. At 15 seconds, there is a desired change in longitudinal force and this leads the prediction model to estimate a required change in throttle input and resulting predicted longitudinal force. This event is detected during the sixth iteration, when the terrain information is updated for the time segment of 6 to 16 seconds. Therefore, the proposed system can begin to prepare for a modest correction to the throttle input 9 seconds before this event. After 9 prediction-correction cycles (from 6 to 15 seconds), the predicted change in throttle input will be ready to apply to the vehicle system at 15 seconds.

3.1.5 Analysis of Simulation Results

During the sixth prediction (6-16 seconds), there is a desired change in longitudinal force (between 15 and 16 seconds). Recall that there is a 10 second window in this implementation of the predictor-corrector algorithm so there is no knowledge of the changes beyond the 16th second at this time step. At the sixth time step there is an error between the desired and predicted longitudinal forces. This initiates the throttle intervention strategy and begins to correct the throttle input, so that the desired change in longitudinal force is generated after 9 seconds. From 6 to 15 seconds, there are 9 prediction-correction cycles to the throttle input which determine the necessary throttle input alternation to be enforced at the 15 second mark. Eventually, as shown in Figure 3.6, the predicted throttle input generates a longitudinal force close to the desired response. From 22 to 25 seconds, the result shows large errors between the predicted and desired longitudinal forces. This can be corrected by further iterating the prediction-correction process.

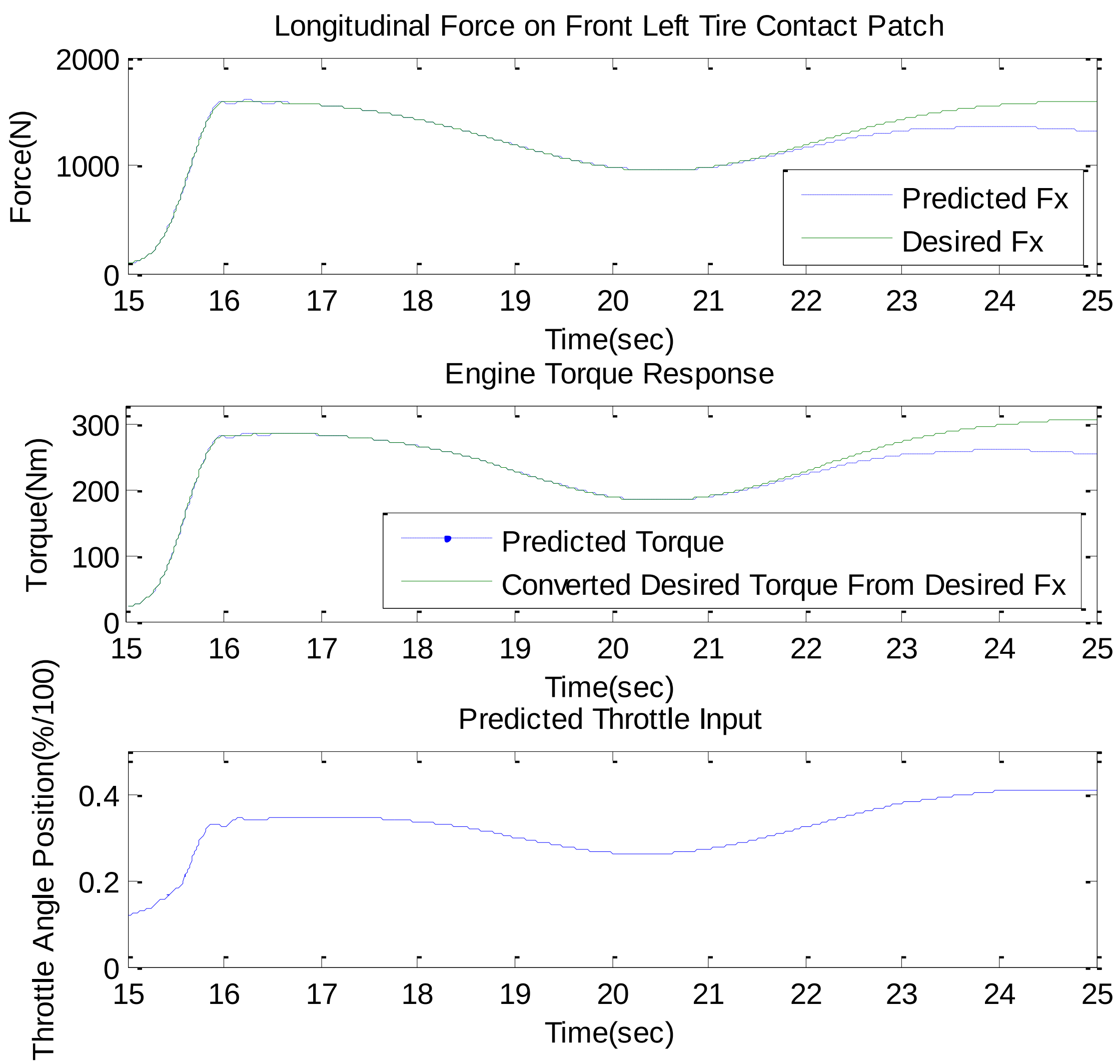

Figure 3.6. Predicted change in throttle input and resulting predicted longitudinal force at 15 seconds

3.1.6 Conclusions

The modulation of longitudinal force at the tire contact patch as a critical index of vehicle handling capability proved effective in the development of a throttle manipulation for this work. Within 10 prediction-correction iterations, the required change in throttle input which can generate the desired longitudinal force is determined. The number of predictions and corrections is a tunable condition; this iteration process can be optimized based on specific requirements for error tolerance between predicted and desired longitudinal force. The most distinctive feature of this system when compared with current ESC systems is its ability to continuously predict and prepare throttle modulations while maintaining the vehicle's handling capability. Lateral and vertical forces at the tire contact patches also affect the handling capabilities; a model to generate these forces from longitudinal force is under development.

3.2 Model-Based Predictive Brake Control

The objective of this section (3.2) is to develop a prediction model that estimates the required brake modulation to deliver the desired longitudinal force. This work proceeds as follows. First, the switching model between the throttle-only control strategy and the use of the brake is developed. This model is used to determine whether the system can reach the desired change in longitudinal force by decreasing the throttle input without braking. Next, a simplified brake model is developed to estimate the required brake modulation to achieve the desired change in longitudinal force. Last, the prediction model to estimate the required brake modulation and the resulting change in longitudinal force is developed. The integration of these contributions is demonstrated through a case study wherein a desired change in longitudinal force is prescribed and the brake modulation required to achieve this change in force is predicted. The accuracy and limitations of the method are discussed followed by concluding remarks.

3.2.2 Background

The intent of the LAAVD research is to avoid the situation in which current Driver Assistance Systems would become active. One method of achieving this intent is to modulate the longitudinal force at the tire contact patch by controlling the throttle input to the engine [49]. Cho, et al. demonstrates, however, that the engine has limited performance in the steady-state range. In addition, the ability to develop negative changes in the longitudinal force from throttle manipulation alone, and the resulting engine braking, is limited. To compensate, a method to modulate longitudinal force by brake control is developed here. It is assumed that brake intervention can be unfavorable for driver comfort; throttle intervention will be the preferred mode of deceleration, relying only minimally on brake modulation.

The linear prediction-nonlinear correction process outlined by Bandy, et al. is fundamental to this work [4]. The system flowchart is reproduced here as Figure 3.1. A linear chassis model first determines the relationship between a desired change in performance margin and the necessary change in longitudinal force, followed by the linear powertrain model discussed by Cho [49]. This work adds the possibility of brake manipulation to this powertrain model, resulting in the throttle and brake commands represented in the Linear Predictions box in Figure 3.1.

The success of the Intervention Strategy relies on an accurate and computationally efficient inverse brake model which can estimate the required brake modulation necessary to deliver a desired change in longitudinal force at the tire contact patch. A significant amount of recent brake control research has focused on achieving such performance goals. Yi and Chung offer an approach for nonlinear brake control by developing a nonlinear computer model and a linear model of the hydraulic brake actuator system [50]. Liang, et al. concentrate on a vehicle's longitudinal brake control by developing a modified sliding control with variable control parameter [51]. Trachtler proposes the steering and suspension system as well as brake intervention scheme for optimized and integrated vehicle control [52]. Ioannou and Xu suggest vehicle speed control by controlling the throttle and brake input with sliding mode control [47]. Gerdes and Hedrick suggest an adaptive controller to handle the throttle and brake input [48]. Presently, a linear prediction and non-linear correction approach is developed in this work.

3.2.3. Switching Model between Throttle and Brake

In typical driving, the throttle and brake control tasks are decoupled in that a typical driver will close the throttle before beginning to apply the brakes. Since the Intervention Strategy is developed to act in harmony with the driver's control authority, the switching point between a throttle-only control approach and a braking approach (with closed throttle) is explored. Consider the case in which the engine torque is quickly decreased by instantaneously closing the throttle as shown in Figure 3.7. Here the throttle angle is closed from 12% throttle to zero (see the lower plot) and the resulting change in engine torque is plotted in the upper plot. For this particular example, the engine torque reaches a new steady-state value in less than one second.

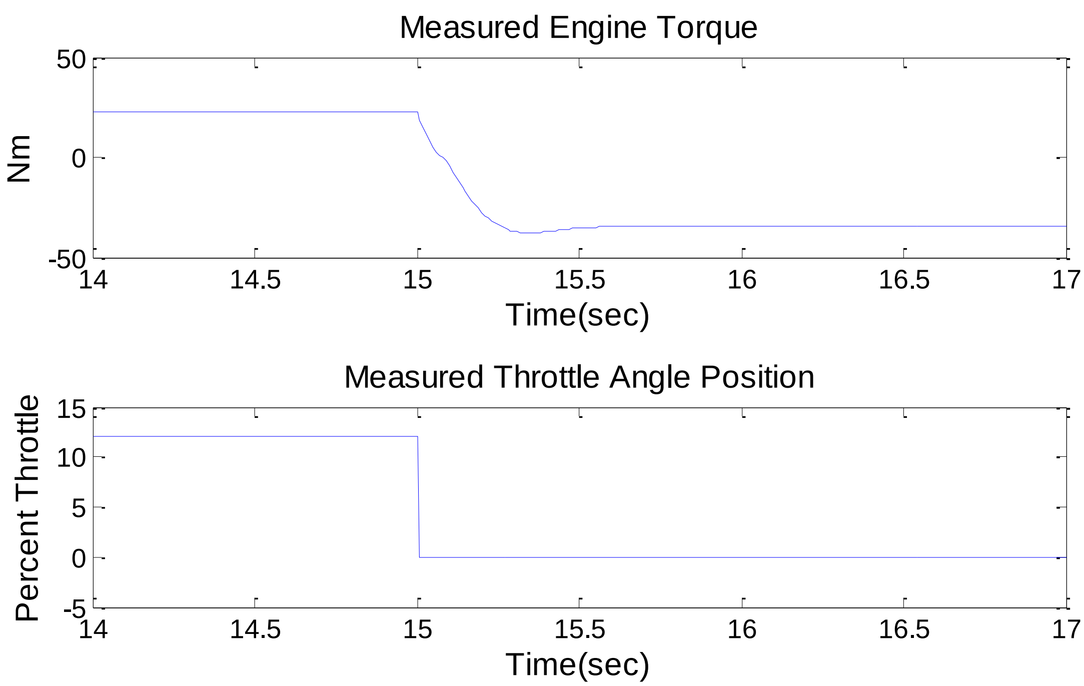

Figure 3.7. Results of closed throttle at 15 seconds

In this work, a time-step of one second is used to assure that the system has reached a new steady-state torque for all possible initial states (η_0, τ_0). It is possible to create an efficient map of the steady state engine torque, $\tau_{ss}(\Delta t)$, after closing the throttle angle as a function of the engine state. Calibration points at numerous engine states distributed over a range from 870 to 6000 rpm and -10 to 400 Nm are considered. Next τ_{ss} as a function of the steady-state engine state is approximated by a polynomial of the form represented in Equation (3.18).

$$\hat{\tau}_{ss}(\eta_{cal},\tau_{cal}) = \beta_0 + \beta_1\eta_{cal} + \beta_2\tau_{cal} + \beta_3\eta_{cal}^2 + \beta_4\tau_{cal}^2 + \beta_5\eta_{cal}^3 + \beta_6\tau_{cal}^3$$

$$+\beta_7\eta_{cal}^{-1} + \beta_8\tau_{cal}^{-1} + \beta_9\eta_{cal}^{-2} + \beta_{10}\tau_{cal}^{-2} \tag{3.18}$$

The coefficients are found using a generalized inverse approach such that the squared error in the estimate of τ_{ss} is minimized. Finally, it is possible to estimate the maximum change in engine torque at closed throttle with Equation (3.19).

$$\Delta\tau_{max} = \tau(t_0) - \hat{\tau}_{ss}(\eta_{cal},\tau_{cal}) \tag{3.19}$$

Then ΔF_{x-des} can be converted to $\Delta\tau_{des}$ by the linear predictive drivetrain model developed by Cho, et al. in Cho's references [29] as shown in Equation (3.20).

$$\{\Delta\tau_{des}\} = \left\{\frac{\Delta t}{m}\left(\left[\frac{\tau}{V_x}\right] - \left[\frac{\eta}{V_x}\right]\left[\frac{\tau}{\eta}\right]\right) + [\tau/F_x]\right\}\ [S]\{\Delta F_{x-des}\} \tag{3.20}$$

The criteria which necessitate a switch from throttle to brake manipulation are simply defined by Equation (3.21).

$$|\Delta\tau_{max}| > |\Delta\tau_{des}| \Rightarrow \text{Throttle Control}$$

$$|\Delta\tau_{max}| < |\Delta\tau_{des}| \Rightarrow \text{Brake Control} \tag{3.21}$$

3.2.4 Simplified Brake Model

A typical brake system is complex and difficult to model. A simplified brake model is developed in this work by system identification. The system exhibits a proportional gain response up to 10Hz. Therefore, the highest frequency that is applicable to the simple brake model is 10Hz. In a similar manner, Cho, et al. [53] demonstrate that the cutoff frequency for throttle control is 1.5 Hz. If throttle-only control is preferable to brake control, as is the case in the current definition of the Intervention Strategy, then the effective brake control frequency range is 1.5 to 10 Hz.

Though the causality is such that a change in the brake command causes the change in longitudinal force, the inverse relationship is desirable in developing the Intervention Strategy. From this observation, the inverse FRF is defined as a function of frequency, f, as shown in Equation (3.22) .

$$H(f)_{inv-brk} = \frac{Brk(f)}{F_x(f)} \tag{3.22}$$

This FRF is linearly approximated by the transfer function shown in Equation (3.23).

$$G_{inv-brk}(s) = K_b \cdot \frac{s+T_z}{s} \tag{3.23}$$

Next, the proportional gain, K_b, and time constants, T_z, are determined by analyzing the bode plot of the FRF.

3.2.5 Prediction Model

In this section (3.2), it is assumed that the future states of the vehicle can be predicted, given the upcoming terrain and driving conditions (provided by GPS or satellite information systems). If it is deemed necessary to modulate the brake as well as the throttle, this prediction model estimates the required brake modulation and resulting predicted longitudinal force. These predictions and corrections are updated at regular intervals that are dictated by the complexity of the models and the on-board computational power. In this work, specifically, the prediction model has a one second update rate and a ten second time horizon for future prediction.

It is assumed that the desired change in longitudinal force is derived from some desired change in Performance Margin. Future states are predicted by the brake control prediction model. At each time step, there is one nonlinear prediction by the full nonlinear vehicle model, a linear prediction by the simplified brake model, and a correction by the feedback system (see Figure 3.1).

Likewise the previous work in section (3.1), it is assumed that there is a ten second preview of data and that this preview information is updated each second. At the initial time step, the simulation results are obtained for the first segment (0-10 seconds), the data are analyzed to determine if any error exists between the desired and predicted longitudinal force and how much throttle or brake correction is necessary. The next 10-second segment (from 1 to 11 seconds) is then simulated and analyzed. This concept is shown schematically in Figure 3.8.

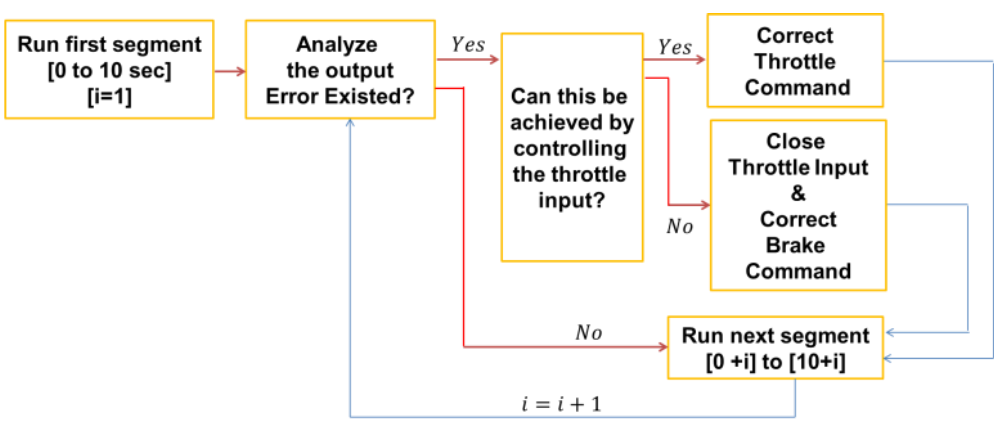

Figure 3.8. Flowchart of Throttle and Brake Modulation Process

3.2.6 Simulation Results

Implementation of this proposed method is demonstrated in a case study. Consider a typical sedan with a 200 kW engine and a 6-speed automatic transmission modeled with 15 mechanical degrees of freedom traveling at 65 km/hr on a surface with a coefficient of friction of 0.8 traveling a straight road. Next consider a situation in which the desired longitudinal force drops instantaneously from 100N to -300 N and this drop occurs 15 seconds from the beginning of the simulation. It is assumed that the driver does not change the throttle or brake positions during this simulation.

The prediction model does not estimate any required change in throttle input until the sixth prediction (5-15 seconds). At 15 seconds, there is a desired change in longitudinal force and this leads the prediction model to estimate a required change in throttle input and resulting predicted longitudinal force. This initiates the Intervention Strategy.

First, the change in longitudinal force achievable by closing the throttle is predicted. In this scenario, the desired change in longitudinal force is greater than the maximum achievable change in longitudinal force by closing throttle. The switching model initiates the brake intervention strategy and closes the throttle. As a result, throttle input is turned off during the seventh prediction (6-16 seconds), as shown in Figure 3.9. Note that the decrease in longitudinal force is due only to closing the throttle, without any braking being initiated. There is a substantial delay in the response and the minimum force does not achieve the desired level, as expected.

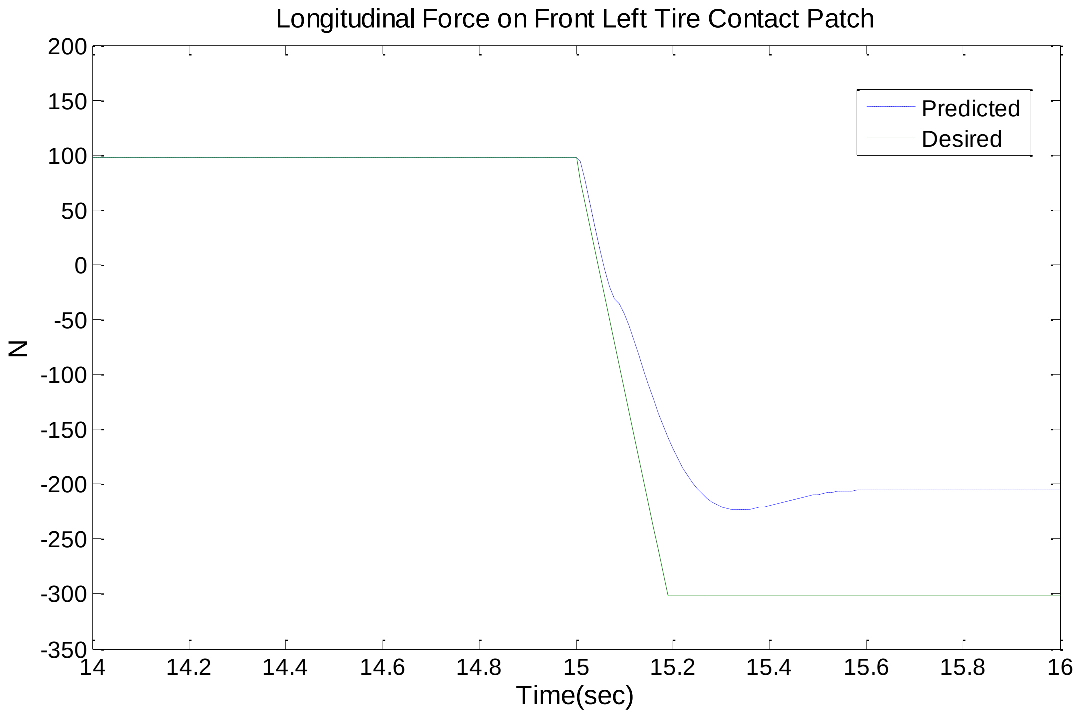

Figure 3.9. Longitudinal force from first iteration – throttle only

For the eighth prediction (7-17 seconds), the brake control model is used to estimate the required brake modulation. This can compensate the delay and magnitude error between desired and predicted longitudinal forces as shown in Figure 3.10. Note that the response time is much faster and that the predicted steady-state force is much closer to the desired value.

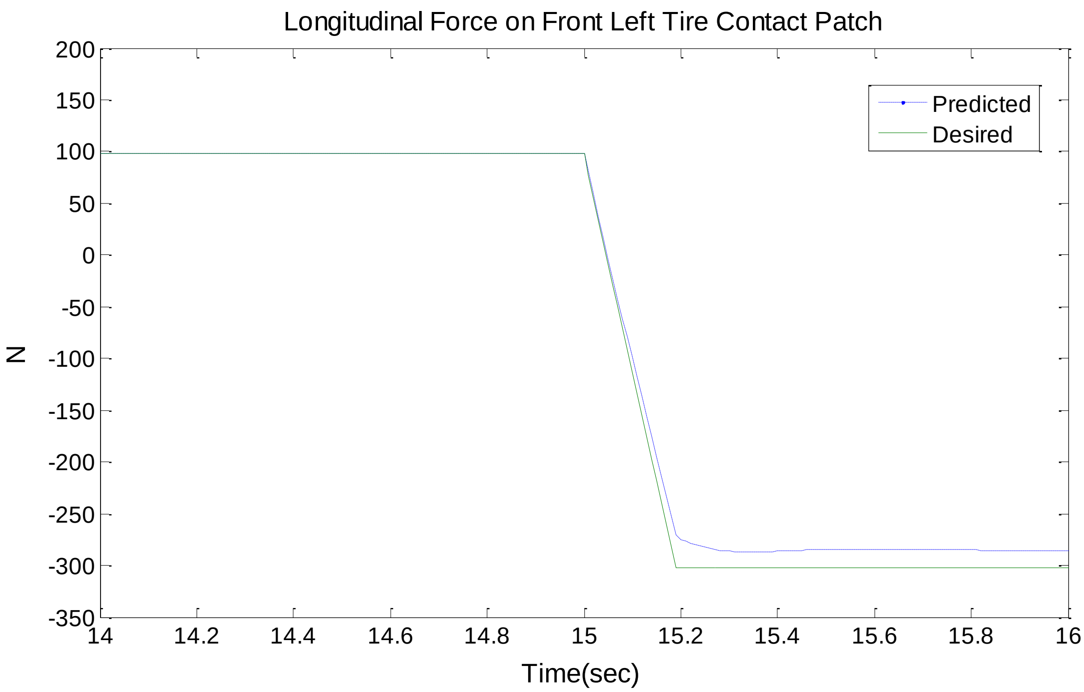

Figure 3.10. Longitudinal force from first iteration – throttle only

From 8 to 15 seconds, there are eight prediction-correction iterations to sufficiently alter for brake wheel pressure at 15 seconds. Finally, as shown in Figure 3.11, the predicted brake commands combined with a closed throttle input generates the desired longitudinal force.

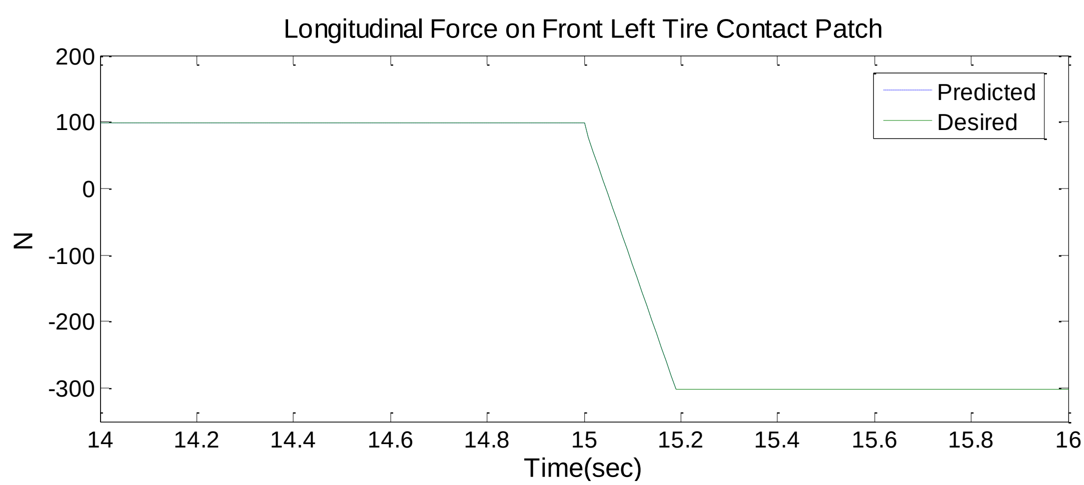

Figure 3.11. Longitudinal Force at final iteration

3.2.7 Conclusions

A prediction model that estimates the required brake modulation to deliver the desired longitudinal force is developed. This prediction is then used in a predictor-corrector algorithm within a proposed Intervention Strategy that is still under development. It is demonstrated through an example that the linear prediction-nonlinear correction process is effective in affecting large changes in longitudinal force. The simplicity of the model is encouraging for future implementation of this strategy in real-time applications. The ability to predictively adapt the vehicle dynamics separates this work from current reactive technologies such as TCS and ESC systems.

4. Yaw Perturbation Cancellation by Sliding Mode Control after the Intervention Strategy

Throttle and brake modulation techniques are developed in Chapter 3 to maintain the handling capability. These are one of critical sides to modulate the control index, PM. Another way to manipulate the PM is controlling the yaw motion of the vehicle. For achieving this, yaw motion control technique is developed in this chapter. Therefore, this work proceeds as follows: First of all, background for developing a vehicle model for the purpose of yaw motion control is provided. Next the active steering control concept is suggested. Last the simulation result and future plan is provided.

4.1. Background

In this section, the basic vehicle dynamics for bicycle model and pneumatic tire model are introduced that will be used for future development.

4.1.1. Tire-Road Interaction

One seminal question of pneumatic tires is how they can interact with road surfaces for generating the forces at the tire contact patch to navigate the vehicle. Actually, pneumatic tire is very complex structures and thus it is also hard to figure out the frictional interaction between the tire's rubber and road surface. Under these reasons, it is difficult to estimate the capability with respect to the generating force of tire.

Since the scope of the work in this section focuses on developing the yaw perturbation cancellation control model after applying the Intervention Strategy, analysis of vehicle dynamics under small perturbations will be considered by the simplified and linearized tire force generation. This assumes the vehicle usually maintains the handling capability and stability after the Intervention Strategy and only generate small perturbation in terms of yaw direction.

4.1.2. Lateral Forces at the Tire Contact Patch and Side slip

If each wheel supports a weight of the vehicle, the normal force can be considered that is applied between tire contact patch and road. If the small force to the lateral direction is applied to the wheel, the corresponding force will be generated at the tire contact patch. In this case, the wheel does not follow the path anymore that is directed. Instead, the wheel may have lateral velocity as well as the longitudinal velocity. Therefore, the direction of the resultant vector of the velocities indicates the different direction to compare with the center line of the wheel. The angle between the centerline of the wheel and the direction that is caused by the lateral force to the wheel is called the Slip angle,α. This is illustrated in Figure 4.1.

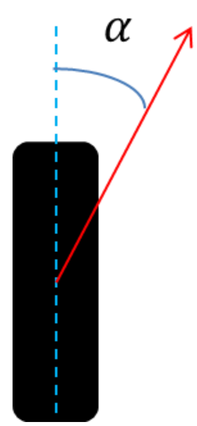

Figure 4.1. The Slip angle between the centerline of the wheel and the direction of resultant vector of velocities

The Intervention Strategy usually bring back the Performance Margin value below the threshold and sometimes Performance Margin stays around the boundary value that can cause small perturbation of yaw motion. This perturbation is usually very small and thus it is reasonable to consider the linearized model for defining the relationship between the lateral force at the tire contact patch and side slip angle. It is very well known that there is almost linear proportional relationship between the lateral force at the tire contact patch and the slip angle up to some slip angles. Therefore, in this work, the cornering stiffness, C_α, is used that is defined the linearized relationship between the lateral force and the slip angle. If the slip angle hold large value, the tire shows the nonlinear relationship between the force and the slip angle. Please refer about this from Figure 4.2.

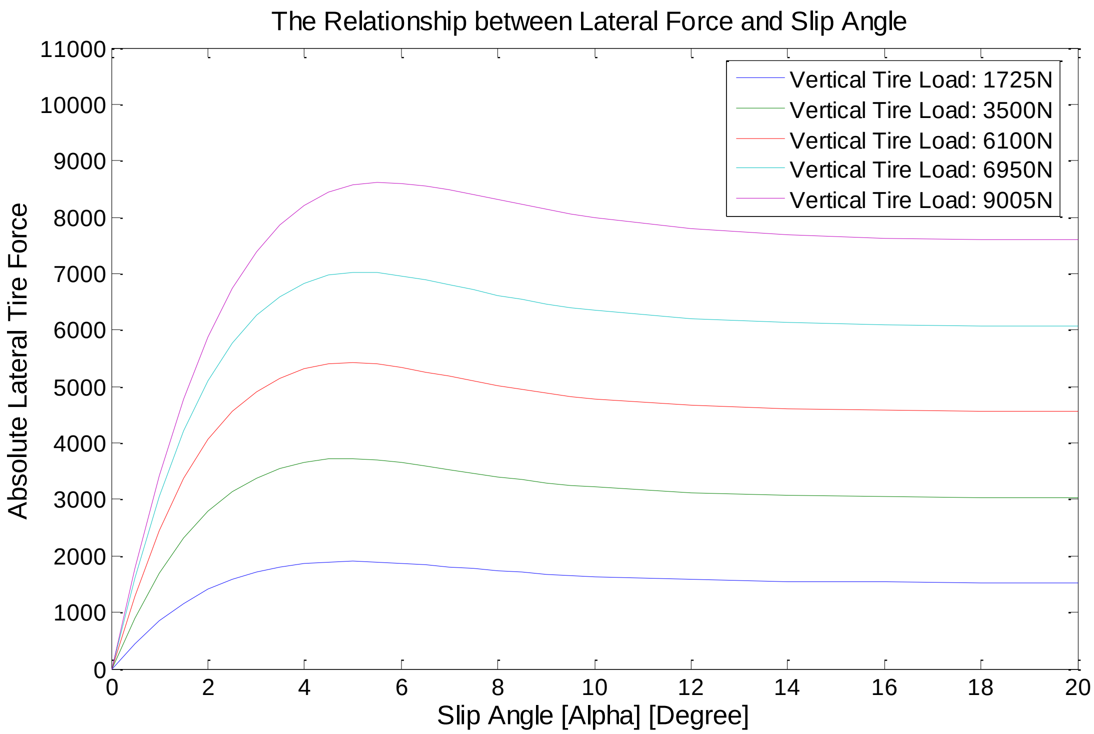

Figure 4.2. The lateral force as a function of slip angle for different vertical tire load

From the observation of Figure 4.2, it is reasonable to approximate the relationship between force and side slip angle up to 5 degrees. This is equivalently represented in Equation (4.1).

$$C_\alpha = \frac{F_y}{\alpha} \tag{4.1}$$

4.1.4 Bicycle Model of Vehicle

The bicycle model of the vehicle is suggested in Figure 4.3.

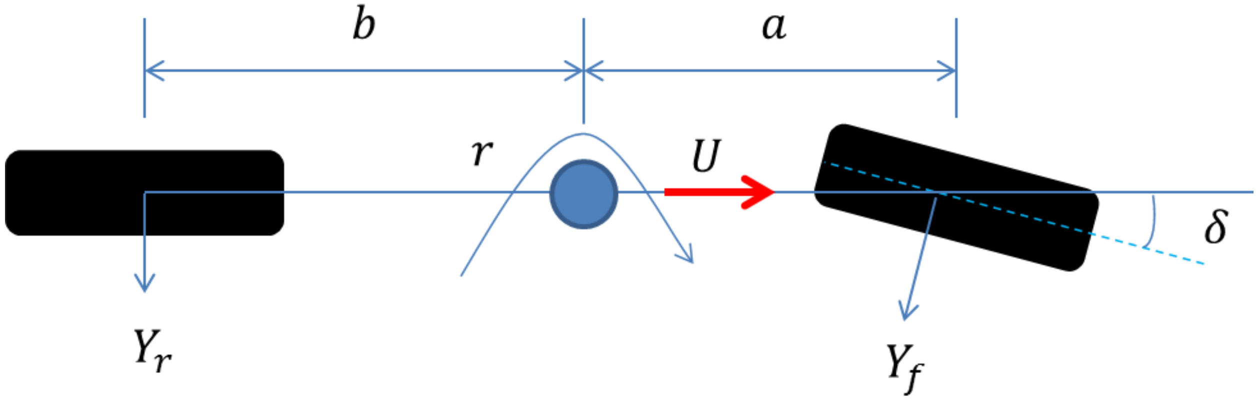

Figure 4.3. The bicycle model of the vehicle with respect to the body centered coordinate system.

U represents the longitudinal velocity and V represents the lateral velocity. When the bicycle model is developed, it is assumed that the longitudinal velocity is constant for the normal motion and small perturbed motion. Therefore, this can be considered as one of the parameters. The lateral velocity and yaw rate are varying parameters which can describe the vehicle's motion in terms of lateral direction and yaw direction. The equation of motion can be set up from the Figure 4.3.

$$m(\dot{V} + rU) = Y_f + Y_r \tag{4.5}$$

$$I_z\dot{r} = aY_f - bY_r \tag{4.6}$$

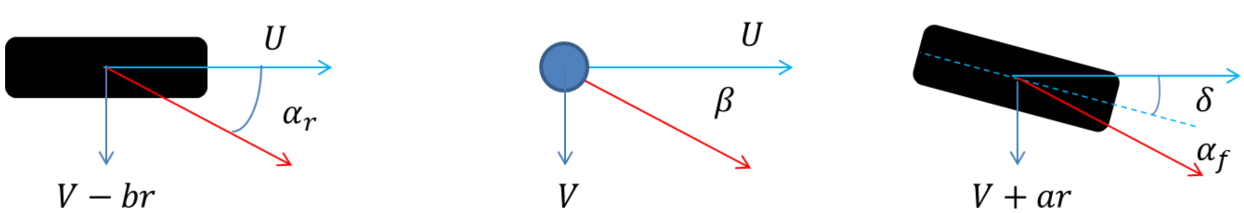

Figure 4.4. Slip angle calculations

From the Figure 4.4, slip angle can be calculated as Equation (4.7).

$$\alpha_f = \frac{V+ar}{U} - \delta\ ,\ \alpha_r = \frac{V-br}{U} \tag{4.7}$$

From the Equation (4.1), it is available to define the lateral force for front and rear as Equation (4.8).

$$-Y_f = C_f\alpha_f\ ,\quad -Y_r = C_r\alpha_r \tag{4.8}$$

By combining the Equation (4.5) ~ Equation (4.8), the equation of motion for the bicycle model can be represented in Equation (4.9) and (4.10).

$$m(\dot{V} + rU) = -\frac{(C_f+C_r)V}{U} - \frac{(aC_f-bC_r)r}{U} + C_f\delta \tag{4.9}$$

$$I_z\dot{r} = -\frac{(aC_f-bC_r)V}{U} - \frac{(a^2C_f+b^2C_r)r}{U} + aC_f\delta \tag{4.10}$$

4.2. Electronic Stability Enhancement

The yaw perturbation cancellation can comes from the yaw motion control technique in the automotive industry. There could be some ways to construct the control architecture for controlling the yaw motion. The differential braking control is a kind of way for controlling the vehicle's yaw motion. This is an effective way but it arises the energy dissipation due to the friction between brake pad and the wheel disk. One of the other ways to consist of yaw motion control is an active steering control scheme. If the side slip angle is very large, this cannot be considered for the yaw perturbation cancelling since it cannot cover the nonlinear area when the bicycle model is used. However, after the Intervention Strategy, the most of the cases maintain vehicle stability and handling capability. Therefore, there is no much perturbation after the Intervention Strategy and it is reasonable to assume that the slip angle can stay within linear range. For this reason, the active steering control is appropriate control scheme for cancelling the yaw perturbation after the Intervention Strategy since active steering control does not dissipate the energy much to compare with differential braking control method.

4.2.1. Model Reference Control

The concept of model reference control for active steering is illustrated in Figure 4.5.

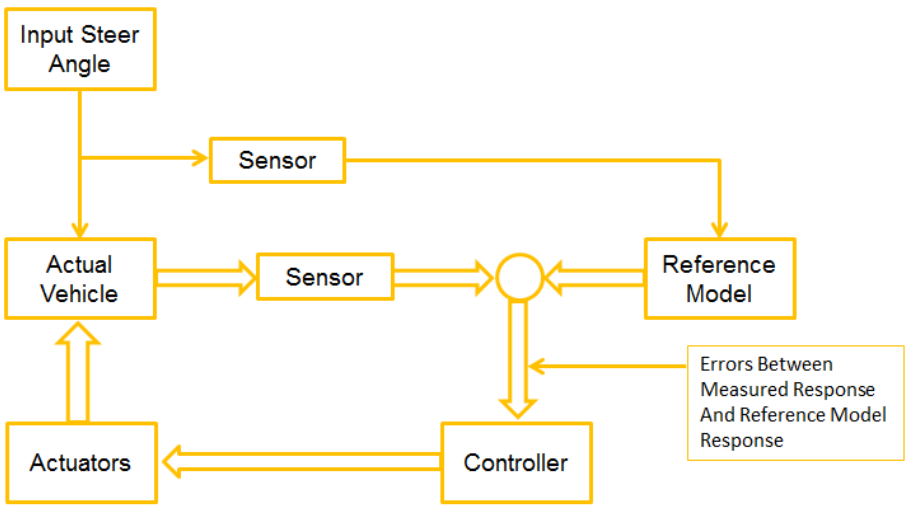

Figure 4.5. Model Reference Control scheme for active steering control

4.2.2. Sliding Mode Control

One of the robust controls are the sliding mode control and this is considered to consist of control architecture in developing of yaw perturbation cancellation. In this work, the active steering control only uses the front steering angle for the input and bicycle model that is developed in previous section 4.1 for the reference model.

To understand about the concept of the sliding mode control, it is required to consider the dynamic system that is represented by the state space representation form as shown in Equation (4.11).

$$\dot{x} = Ax + bu + d \tag{4.11}$$

where x represents a n-dimensional states vector, u represents a single input, and d represents a vector disturbances. Then the sliding surface is defined by the Equation (4.12).

$$\mathrm{S} = \mathrm{C}^{\mathrm{T}}(\mathrm{x} - \mathrm{x_d}) \tag{4.12}$$

where C^{T} is an n-dimensional row vector and $\mathrm{x_d}$ represents the desired trajectory that the states, x, try to follow.

The sliding surface can be defined when the states is equal to the desired states which drives S is equal to zero. Then the sliding mode controller can be constructed that tries to drive S to the zero. This can be equivalently understood that the control system pushes the states try to follow the desired states. In this work, the desired trajectory comes from the electronic reference model that takes the same steering angle input which also goes into the real vehicle system by the driver. If the sliding surface can be driven to the zero, the real vehicle shows the response that is identical to the reference model.

To prove the convergence of the sliding mode control system, Lyapunov function approach can be considered.

Let $\dot{\mathrm{S}}$ as described in Equation (4.13):

$$\dot{\mathrm{S}} = -\mathrm{k_1 S} - \mathrm{k_2 sgnS} = -\mathrm{k_1 S} - \mathrm{k_2}\left(\frac{|\mathrm{s}|}{\mathrm{s}}\right) \tag{4.13}$$

where $\mathrm{k_1}$ and $\mathrm{k_2}$ are positive constants.

It is available to choose $\mathrm{k_1}$ as zero like below.

$$\dot{\mathrm{S}} = -\mathrm{k_2 sgnS} = -\mathrm{k_2}\left(\frac{|\mathrm{s}|}{\mathrm{s}}\right) \tag{4.14}$$

This also enables for S to converge to zero. Though this is one of the possible behavior for $\dot{S}$, it is slow than Equation (4.13). So, Equation (4.13) is chosen for the active steering control architecture. The derivative of S^2 is suggested in Equation (4.15) by considering the Equation (4.13)

$$\frac{d}{dt}\left(\frac{S^2}{2}\right) = S\dot{S} = -k_1 S^2 - k_2|S| \tag{4.15}$$

Equation (4.15) shows that the derivative square of S is always negative regardless of the sign of S.

This is sufficient condition to guarantee that S converges to zero.

Next, the control law is considered. The Equation (4.16) can be derived by differentiating the Equation (4.12) and substituting the result into the Equation (4.13).

$$\dot{S} = C^T(\dot{x} - \dot{x}_d) = -k_1 S - k_2 \mathrm{sgn} S \tag{4.16}$$

$\dot{x}$ can be represented by using the Equation (4.11) which has zero disturbance. S can be represented by using the Equation (4.12). Then the Equation (4.17) can be derived by substituting these Equations into the Equation (4.16).

$$C^T Ax + C^T bu - C^T \dot{x}_d = -k_1 C^T(x - x_d) - k_2 \mathrm{sgn}(C^T(x - x_d)) \tag{4.17}$$

A control law can be derived by rearranging the Equation (4.17) in terms of u.

$$u = -\frac{1}{C^T b}[C^T Ax - C^T \dot{x}_d + k_1 C^T(x - x_d) + k_2 \mathrm{sgn}\left(C^T(x - x_d)\right) \tag{4.18}$$

By observing the Equation (4.18), it can be understood that the chattering problem may occur. This problem comes from the signum function that dither between +1 and -1 whenever S changes the sign.

This is especially undesirable for the active steering control. For correcting the steering angle to follow the desired trajectory, the control system cannot generate the compensated steering angle input that jump back and forth around nominal value.

More detailed information about this will be discussed in section 4.4.

The last remaining task is choosing the elements of C^T so that it can make rational behavior for the system when it is forced to remain on the surface $S = 0$ in the state space. If k_2 is equal to zero, then only linear part of the control law can be considered. Then it is able to choose C^T which can make the system has a good stability if it is assumed that x_d and d are equal to zero. Based on these assumptions, the Equation (4.19) can be obtained by substituting the control law, Equation (4.18), into the Equation (4.11).

$$\dot{x} = \left[A - \frac{bC^T}{C^T b}A - k_1 \frac{bC^T}{C^T b}\right] x \tag{4.19}$$

It is clear that one eigenvalue hold $-k_1$ since $k_2 = 0$. The rest eigenvalues can be determined by choosing C^T appropriately.

4.2.4. Active Steering Applied to the Bicycle Model for the Vehicle

The bicycle model is developed in previous section to describe the lateral dynamics of the vehicle. The front steering angle represents the control input and this is denoted δ here. Since the system pursues the active steering control, the steering angle is represented by the sum of a driver command steering angle, δ_f, and a compensated steering angle by the control system, δ_c. This is equivalently represented in Equation (4.20).

$$\delta = \delta_f + \delta_c \tag{4.20}$$

The Equation (4.21) can be derived by substituting the Equation (4.9) and (4.10) into the form of state space representation like Equation (4.11).

$$\begin{bmatrix}\dot{V}\\ \dot{r}\end{bmatrix} = \begin{bmatrix}A_{11} & A_{12}\\ A_{21} & A_{22}\end{bmatrix}\begin{bmatrix}V\\ r\end{bmatrix} + \begin{bmatrix}\frac{C_f}{m}\\ \frac{aC_f}{I_z}\end{bmatrix}(\delta_f + \delta_c) + \begin{bmatrix}d_1\\ d_2\end{bmatrix} \tag{4.21}$$

where

$$A_{11} = -\frac{C_f + C_r}{mU}, \quad A_{12} = \left[-\frac{aC_f - bC_r}{mU} - U\right]$$

$$A_{21} = -\frac{aC_f - bC_r}{I_z U}, \quad A_{22} = -\frac{a^2 C_f + b^2 C_r}{I_z U} \tag{4.22}$$

The electronic reference model can be represented by similar equations with different parameters like Equation (4.23).

$$\begin{bmatrix}\dot{V}_d\\ \dot{r}_d\end{bmatrix} = \begin{bmatrix}A_{11d} & A_{12d}\\ A_{21d} & A_{22d}\end{bmatrix}\begin{bmatrix}V_d\\ r_d\end{bmatrix} + \begin{bmatrix}\frac{C_{fd}}{m}\\ \frac{aC_{fd}}{I_z}\end{bmatrix}\delta_f \tag{4.23}$$

The parameters can be chosen freely to represent the electronic reference model so that it can generate the desired response. The neutral steer is often considered as an optimized vehicle with respect to the steer. Therefore, this can be one of the choices for representing the electronic reference model.

The Equation (4.24) is valid for the neutral steer.

$$aC_f = bC_r \tag{4.24}$$

From Equation (4.24), C_r can be represented by C_f. Then the parameters in Equation (4.23) can be derived like below Equation (4.25).

$$A_{11d} = -\frac{a+b}{bmU} C_f, \quad A_{12d} = -U$$

$$A_{21d} = 0, \; A_{22d} = \frac{a(a+b)}{I_z U} C_f \tag{4.25}$$

Though the sliding surface, S, can contain all the state variables, only a pure yaw rate controller will be developed in this section. Because the yaw rate is easy to measure and many vehicles have a yaw rate sensor recently while the lateral velocity is difficult to measure directly.

4.2.5. Active Steering Yaw Rate Controller

The state variables for the vehicle and electronic reference model by bicycle model are represented by the Equation (4.26).

$$x = \begin{bmatrix} V \\ r \end{bmatrix}, \; x_d = \begin{bmatrix} V_d \\ r_d \end{bmatrix} \tag{4.26}$$

The pure yaw rate controller can be designed by choosing an appropriate C^T that can derive the sliding surface which is a only function of yaw rate. This is equivalently represented by the Equation (4.27).

$$S = C^T(x - x_d) = (r - r_d) \tag{4.27}$$

In this case, C^T can be set up like the Equation (4.28).

$$C^T = [0\ 1] \tag{4.28}$$

Then some terms in the control law can be derived as the Equation (4.29).

$$C^T b = \frac{aC_f}{I_z}, \quad C^T Ax = A_{21}V + A_{22}r \tag{4.29}$$

The Equation (4.30) represents the final form of yaw rate control law that is derived by using the Equation (4.27) ~ Equation (4.29).

$$u = \delta_f + \delta_c = -\frac{I_z}{aC_f}[(A_{21}V + A_{22}r) - \dot{r}_d + k_1(r - r_d) + k_2 sgn(r - r_d)] \tag{4.30}$$

The concept of the yaw rate control by active steering is illustrated in Figure 4.6 with the vehicle and the electronic reference model. Though the real vehicle is suggested in Figure 4.6, it cannot be accurate for all the cases since the bicycle model is used to capture the behavior of the real vehicle. Especially, this is indeed when the vehicle operates in a nonlinear region.

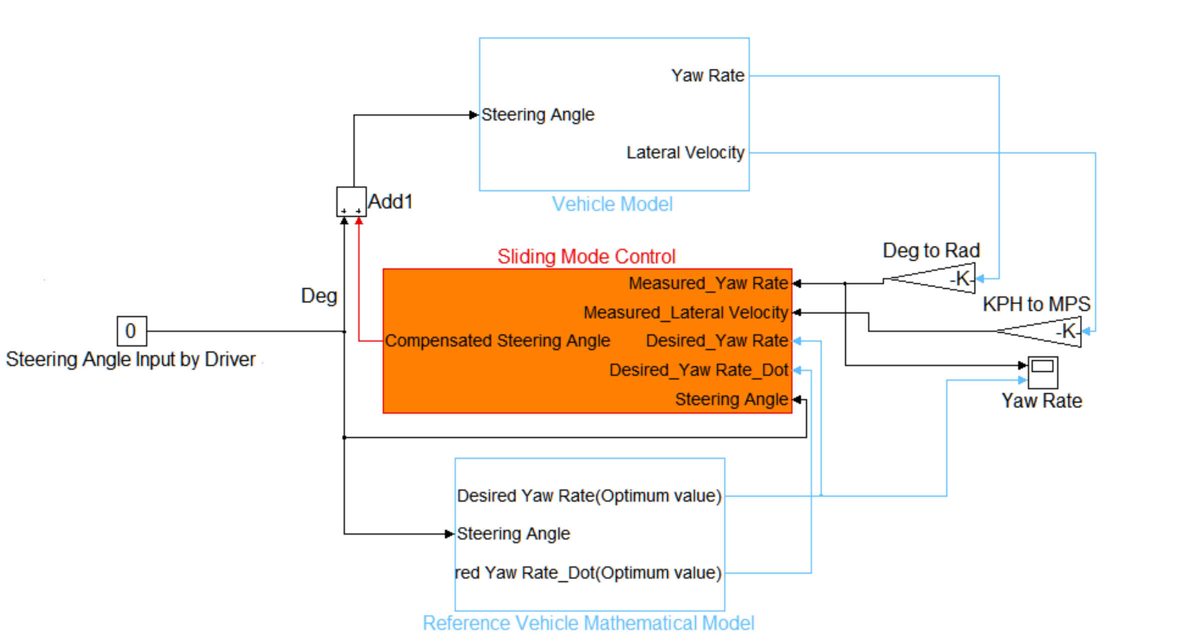

Figure 4.6. The Simulink model of the yaw rate control together with the vehicle and the reference model

Another aspect that is available from the Simulink model in Figure 4.6 is deriving the parameters for the sliding mode controller by running the simulation with the vehicle model and electrical reference vehicle model.

After running the simulation and deriving all the needed parameters for the controller, the real vehicle model is attached to the pure yaw rate control model instead of general mathematical vehicle model. By doing this, it is available to check how sliding mode control works well for the system and make the system to be stable. From Figure 4.7, it is possible to look into the Simulink diagram for the pure yaw rate control model for real vehicle. The commercial program package, Carsim, is replaced and used for representing the real vehicle.

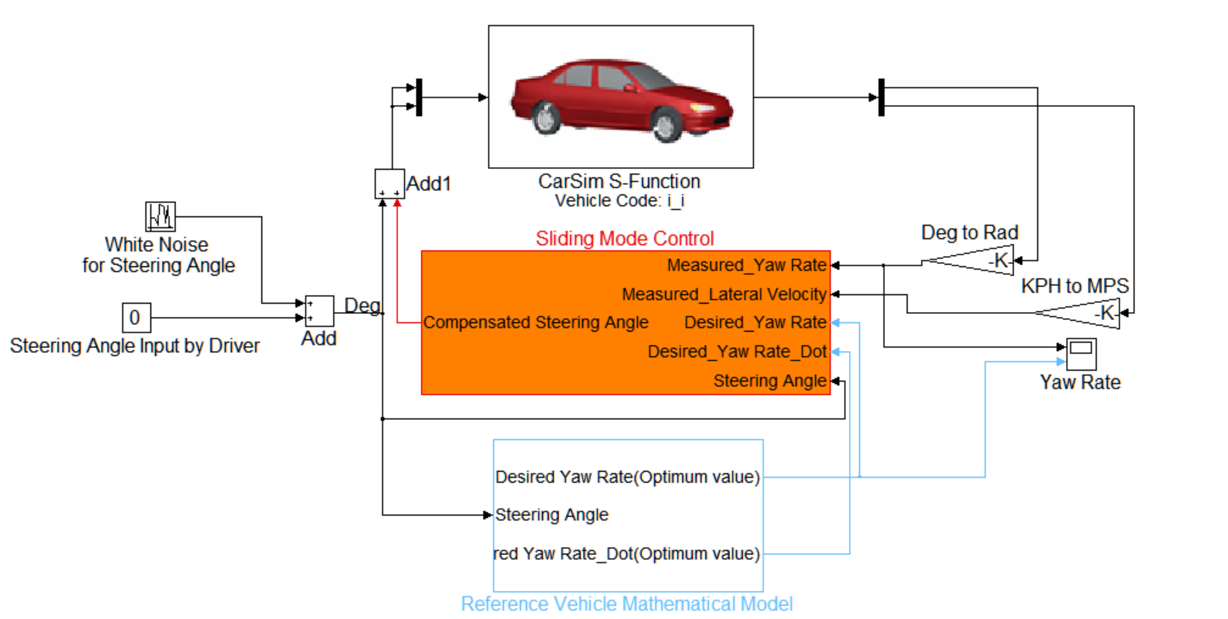

Figure 4.7. The Simulink model of the yaw rate control with the Carsim and the reference model

It is required to look into the Equation (4.19) to see whether the system will be stable when sliding surface considers only the linear part of the control law since the stability depends on the choice of C^T. The column vector b can be found from the Equation (4.21).

$$b = \begin{bmatrix} \frac{C_f}{m} \\ \frac{aC_f}{I_z} \end{bmatrix} \tag{4.31}$$

and by using the Equation (4.28),

$$bC^T = \begin{bmatrix} 0 & \frac{C_f}{m} \\ 0 & \frac{aC_f}{I_z} \end{bmatrix} \tag{4.32}$$

The terms in the Equation (4.19) can be evaluated by using the Equation (4.29) and (4.32).

$$\begin{bmatrix} A_{11} & A_{12} \\ A_{21} & A_{22} \end{bmatrix} - \begin{bmatrix} 0 & \frac{I_z}{am} \\ 0 & 1 \end{bmatrix} \begin{bmatrix} A_{11} & A_{12} \\ A_{21} & A_{22} \end{bmatrix} - k_1 \begin{bmatrix} 0 & \frac{I_z}{am} \\ 0 & 1 \end{bmatrix} = \begin{bmatrix} s - A_{11} + \frac{A_{21}I_z}{am} & -A_{12} + \frac{A_{22}I_z}{am} + k_1 I_z am \\ 0 & -k_1 \end{bmatrix}$$

(4.33)

Eigenvalues for the Equation (4.33) can be found out by using a characteristic equation.

$$\det\begin{bmatrix} s - A_{11} + \frac{A_{21}I_z}{am} & -A_{12} + \frac{A_{22}I_z}{am} + k_1 I_z am \\ 0 & s + k_1 \end{bmatrix} = 0 \tag{4.34}$$

By rearranging the above Equation (4.34), Equation (4.35) can be derived.

$$(s + k_1)\left(s - A_{11} + \frac{A_{12}I_z}{am}\right) = 0 \tag{4.35}$$

From the Equation (4.35), the eigenvalues can be found out intuitionally.

$$s_1 = k_1,\ s_2 = A_{11} - \frac{A_{21}I_z}{am} \tag{4.36}$$

One eigenvalue only depends on the control parameter k_1 and that is related with the convergence speed to the sliding surface $\mathrm{S} = 0$. Another eigenvalue, which is related with the stability of the system when it is in the surface, can be derived by using parameters from the Equation (4.22).

$$s_2 = -\frac{(a+b)C_r}{amU} \tag{4.37}$$

By observing the Equation (4.37), it can be understood that this eigenvalue is negative since all the vehicle parameters are positive. Therefore, the yaw rate control system is stable.

4.3 Analysis of Simulation Results

From the simulation with sliding mode controller, electronic reference model and Carsim, it is available to check the result how controller shows the performance for undesired situations.

For testing the algorithm and running the simulation, the road condition was set up first. From the Figure 4.8, it shows the simulation condition. Three vehicles will run on the road at the same time where there is road which has low friction coefficient and strong wind like gust from the left side and right side.

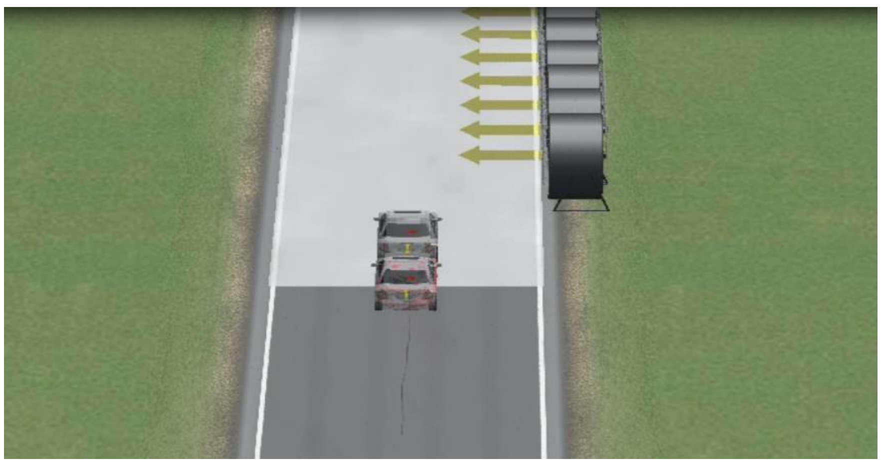

Figure 4.8. Simulation and Road Condition. Dark grey road has normal friction coefficient and light grey road has low friction coefficient.

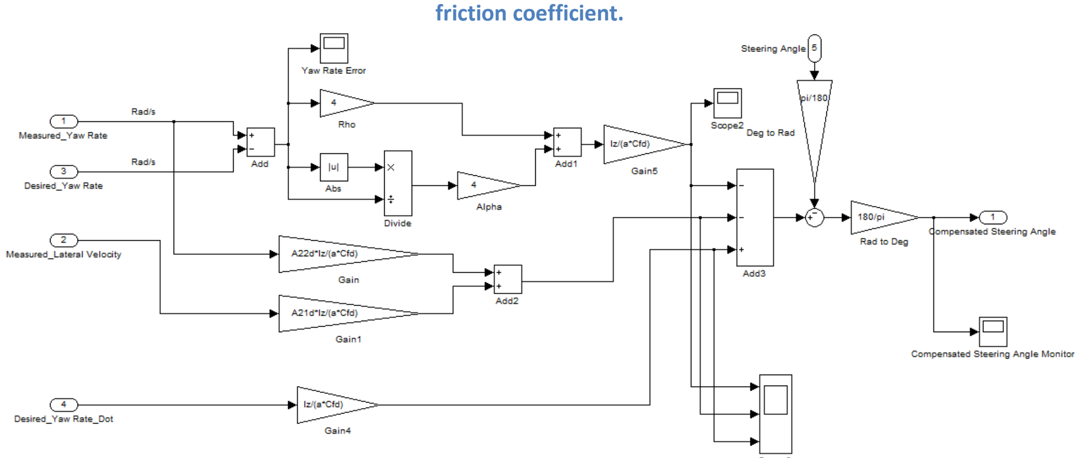

Figure 4.9. Sliding Mode Controller for Pure Yaw Rate Control Model

After running the simulation from Simulink, the error of yaw rate between desired value from electronic reference model and measured value from real vehicle (Carsim) model was compared to each other. The plot is suggested below.

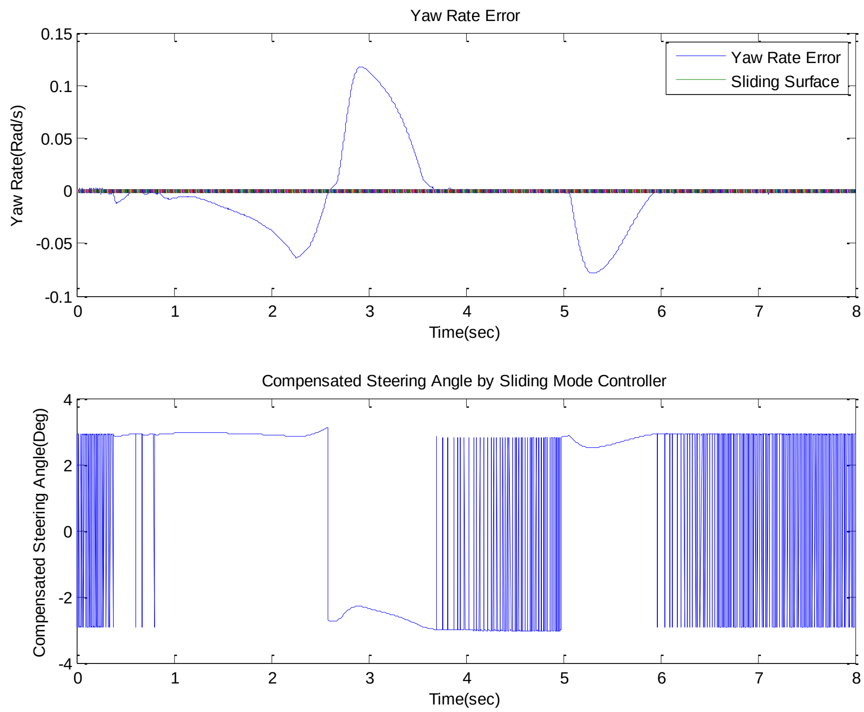

Figure 4.10. Plot for Yaw rate error and Compensated steering angle by Sliding Mode Controller

From Figure 4.10, it looks clear that the yaw rate error perturbed a little before there is gust from right side. Thus, the response of the compensated steering angle by Sliding Mode Controller chattered back and forth because signum function was used while defining the sliding surface. This chattering problem might be undesirable and so should be eliminated by modifying the sliding surface. To solve this problem, some modified and alternative approach is suggested at next following section.

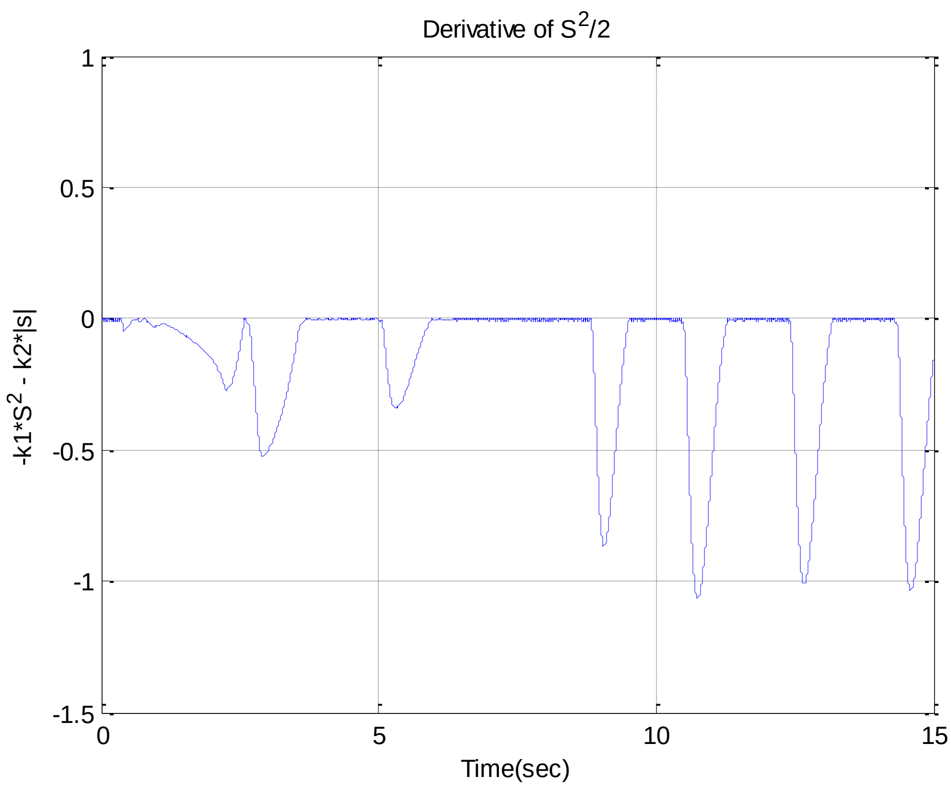

Figure 4.11. The confirmation of system's stability.

Finally, from Figure 4.12, it is available to compare three vehicle's motion how they behave on the low friction road with gust from side.

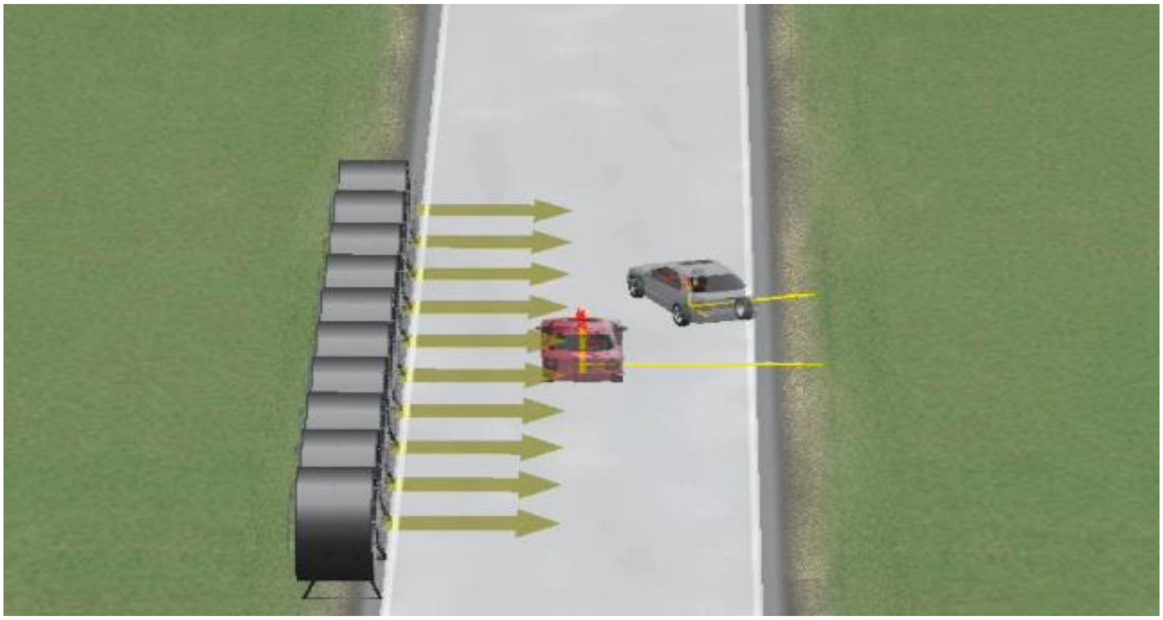

Figure 4.12. Comparing Vehicle's Behavior. Red vehicle has an active steering system.

From the Figure 4.12, it is clear that vehicles which has Electronic Stability Control (ESC) or Active Steering Control (Advised method in this chapter) show stable motion under the condition where there is low friction coefficient and gust from the right or left side. In contrast, the vehicle which does not have any ESC or Active Steering Control system shows unstable motion under the same condition.

4.4 Alternative Solution for Chattering Problems by Signum Function

From Figure 4.10, it looks clear that there is chattering problem. To solve this problem, alternative approach for switching function was adapted which is Saturation Function that can be defined by tangent hyperbolic function.

After replacing the switching function, the chattering problem was solved though vehicle's response was a little slower than before. However, the vehicle finds out its stability eventually. The result is plotted below.

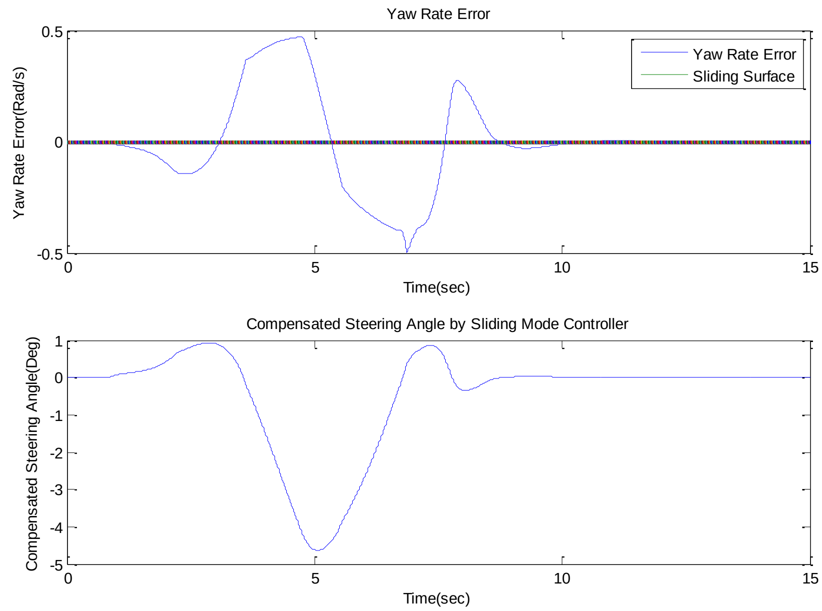

Figure 4.13. Plot for Yaw rate error and Compensated steering angle by Sliding Mode Controller after replacing new switching function, tangent hyperbolic.

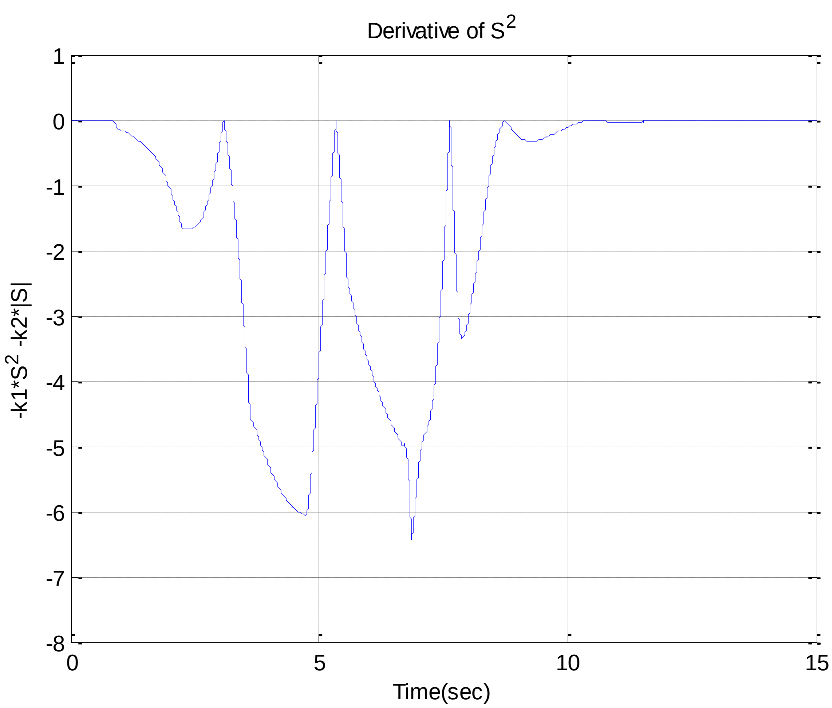

Figure 4.14. The confirmation of system's stability. Chattering problem is reduced much by comparing with Figure 4.11.

5. Intervention Strategy

Since one of the system's goals is to be minimally intrusive (silent) so that the driver is more comfortable while driving, it is of importance to consider this in the development of the LAAVDS. This can lead to considering the minimization of the jerk motion of the vehicle since it is closely related with driving comfort [55]. Constrained optimization is considered in this work to solve this problem. Satisfying the Performance Margin criteria and quasi static dynamics of the powertrain are considered as constraints and the objective goal is to minimize the jerk motion of the vehicle. The procedure in terms of integrating all these processes is developed to form the completed intervention strategy.

Note that there are some assumptions while developing the Intervention Strategy. First of all, it is assumed that a validated full-vehicle model exists for predicting future vehicle states. The next is a valid driver model for predicting future driver commands. The last assumption is the computer processing capabilities which will advance in the near future to allow real-time implementation.

5.1. Introduction

The previous two decades has seen numerous achievements in the vehicle control area. One of the successful products is the Electronic Stability Control (ESC) system, an indispensable item for recent vehicles since the 2012 NHTSA regulation that the every vehicle in the United States must have it. ESC systems have clearly demonstrated their effectiveness as witnessed by the NHTSA report describing the reduction in accidents [1]. However there might be some situations in which the ESC system cannot correct the vehicle's yaw error perfectly. Similarly, there may be insufficient time to take some vehicle control actions. To address these undesirable situations, the concept of the Location Aware Adaptive Vehicle Dynamics System (LAAVDS) is introduced by Bandy [4].

The purpose of Location-Aware Adaptive Vehicle Dynamics (LAAVD) research is to develop a system to help the driver in maintaining vehicle handling capabilities through various driving maneuvers. The proposed method is predictive, estimating the ability of the vehicle to successfully navigate upcoming terrain, and it is assumed that the future vehicle states and local driving environment is known. A predictive vehicle control strategy must be developed such that the vehicle is navigated successfully through a corner via appropriate changes to the driver's commands and do so in a manner that is in harmony with the driver's intentions and not in a distracting or irritating manner. In addition, this control strategy should use a novel measure of handling capability, the Performance Margin, to evaluate the need to intervene [2]. Clearly this research depends on the numerous new technologies being developed to capture and convey information about the local driving environment (e.g., bank angle, elevation changes, curvature, and friction coefficient) to the vehicle and driver.

As part of the predictive control strategy, the vehicle control system must estimate the appropriate modulation of throttle and brake. At the same time, the driver should remain comfortable, as measured by the vehicle's jerk motion. To achieve system performance that is minimally intrusive (silent) yet achieves the desired Perfomance Margin requirements, the Intervention Strategy is an integration of constrained optimization and adaptive learning control.

The objective of this work is to develop the Intervention Strategy(IS) which can guarantee the vehicle's handling capability continuously while minimize the vehicle's jerk motion. The rest of the chapter proceeds as follows. First, an optimal design process is developed. This includes the concept of the active constraints area for the Intervention Strategy, objective function, and constraints. Updating the control law that can compensate the linearized models' error is suggested. Next, the simulation results will be provided that can demonstrate the effectiveness of the IS. The accuracy and limitations of the method are discussed followed by concluding remarks.

5.2. Background

The feasibility of the proposed method relies on the ability to predict vehicle states and the availability of information about the local driving environment (location, friction, banking, etc.). The information available to the vehicle and the driver continues to grow and research continues in both fields. An overview of the practicality of implementing a Global Positioning System (GPS)-based control system into ground vehicles is discussed by Beiker et al. [38]. Furthermore, Ahn proposes both longitudinal and lateral dynamics based algorithms to estimate friction using measurements from sensors that are available on typical commercial vehicles [39]. Hsu also provides the method to estimate the side slip angle and friction by using steering torque [43]. Lee develops a method to estimate the maximum tire-road friction coefficient by designing tractive force estimator, a brake gain estimator, and a normal force observer [40]. Based on these successful studies, it is assumed in this work that information about the current vehicle state and local driving environment are available.

The predictive vehicle control strategy, outlined by Bandy, et al., and employed in the LAAVDS features a linear predictor, nonlinear corrector strategy as shown in Figure 5.1 [4]. Nonlinear corrector (simulation) takes a role to predict the future vehicle status from the highly accurate full nonlinear vehicle model. Linear prediction takes a role to estimate the desired change in throttle or brake as a control input to the vehicle system.

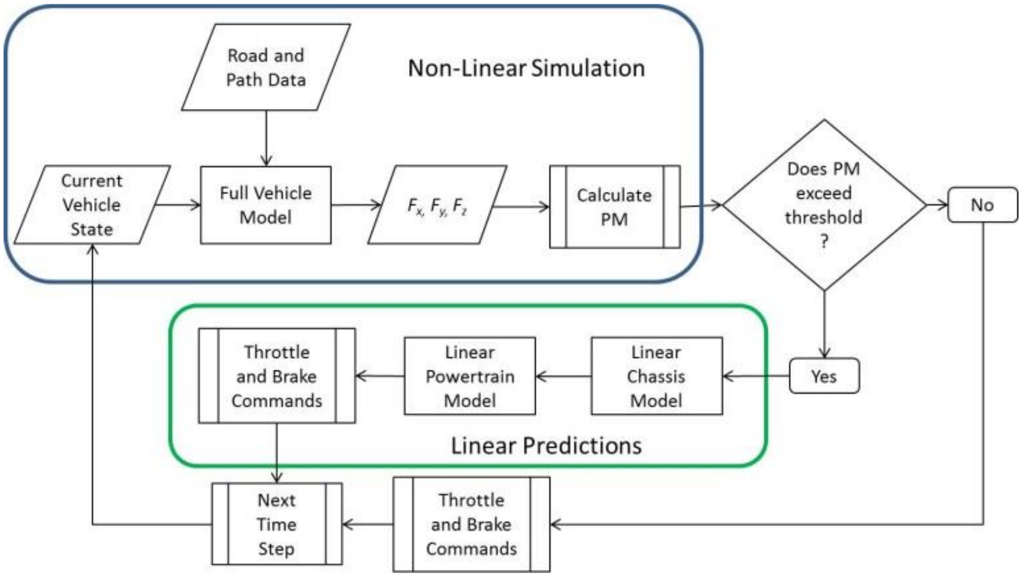

Figure 5.1. Overview of the predictive vehicle control strategy Implementation in Simulation

One critical aspect of this work is the implementation of a means to characterize the state of the vehicle with respect to its available handling capability. This characterization is needed when considering control schemes to ensure that the handling capabilities of the vehicle are not exceeded. In this work, the Performance Margin (PM) is used [2]. The PM is defined as the ratio of the required tractive effort to complete the maneuver to the available tractive effort at the front and rear axles respectively as shown in Equation (5.1), (5.2), where the front tires are indexed by i=1,2 and the rear tires by i=3,4.

$$\mathrm{PM}_{\mathrm{Front}} = \frac{\Sigma_{i=1}^{2}\sqrt{F_{xi}^{2}+F_{yi}^{2}}}{\Sigma_{i=1}^{2}\mu F_{zi}} \tag{5.1}$$

$$\mathrm{PM}_{\mathrm{Rear}} = \frac{\Sigma_{i=3}^{4}\sqrt{F_{xi}^{2}+F_{yi}^{2}}}{\Sigma_{i=3}^{4}\mu F_{zi}} \tag{5.2}$$

The linear steady-state model developed by Cho [49] is used in this work to estimate the required change in the throttle command from the desired change in longitudinal force ($\Delta u = P \cdot \Delta F_x$). The parameters for this linear model are developed at each time step based on the current state of the vehicle.

Similarly, a linear chassis model developed by Bandy [54] is used to estimate the desired change in longitudinal force at the tire contact patch from the desired change in PM. This model enables the system only needs to handle the longitudinal force for affecting the change in PM since it defines the relationship between longitudinal force, lateral force, and vertical force at the tire contact patch.

5.3. Optimal Design for the Intervention Strategy

In this section, the condition for initiating the Intervention Strategy is suggested and the active constraint area for the Performance Margin is defined for this Intervention Strategy. The optimal design process is also developed for setting up the objective function and its constraints for the constrained optimization.

5.3.1. Define the Active Constraint

When the Performance Margin does not exceed its threshold, there is no reason to initiate the intervention strategy. However, it should be started once there is such an event that the Performance Margin exceeds its threshold.

From the vehicle future prediction, it is able to estimate the vehicle's future Performance Margin status as illustrated in Figure 5.2.

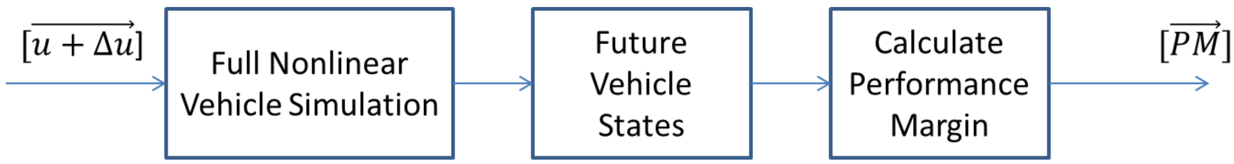

Figure 5.2. Future Prediction by Full Nonlinear Vehicle Simulation and Calculating the Performance Margin.

As a next step, check the Performance Margin to determine there is any time range where the Performance Margin exceeds its threshold. Then such a time range can be defined as an 'active constraint area' and this is illustrated in Figure 5.3. The way to derive this active constraint area mathematically from the times series data is explained below.

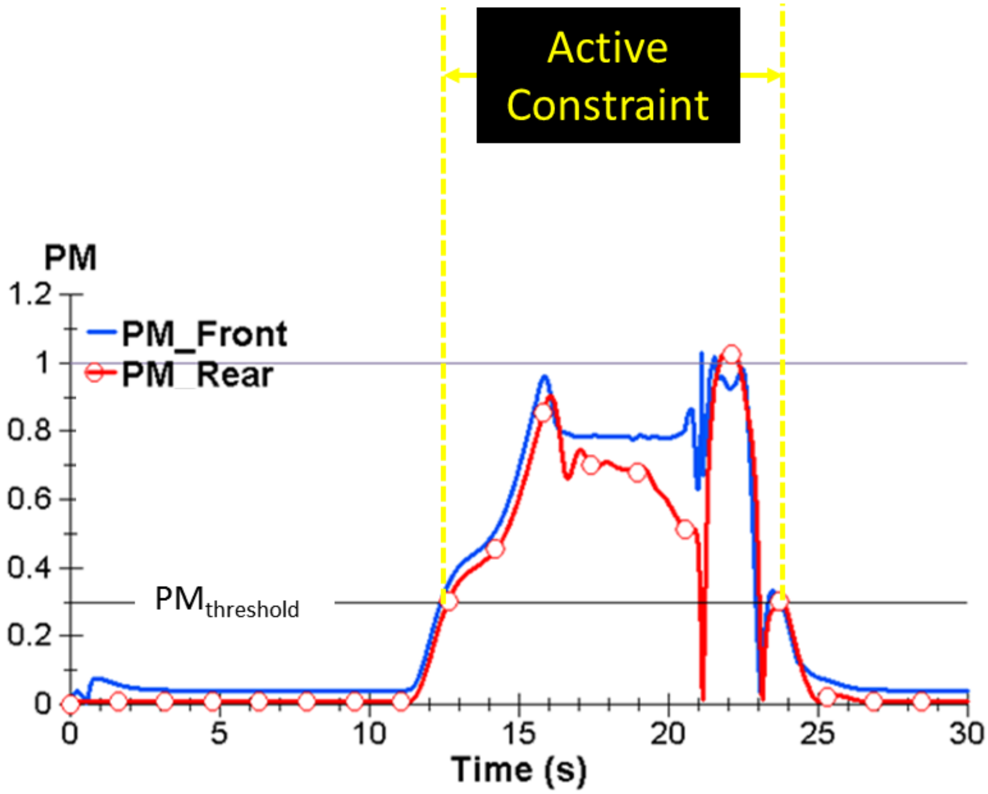

Figure 5.3. Performance Margin for Active Constraint Area

Let $\vec{x}$ be a vector in which the elements are indexed by k and $\vec{x}$ spans all the times being considered in the future prediction, and $\mathrm{k} = 1,2,3, \ldots.$

Let $\vec{y}$ be a vector spanning the space of active constraints. The number of elements in $\vec{y}$ is m.

Then define matrix M, comprising elements of zeros and ones, forming a mask such that

$$\vec{y} = M\vec{x} \tag{5.3}$$

This concept can be applied to the Performance Margin for deriving the active constraint area. Then the active constraints on the ΔPM can be written as

$$[\Delta \mathrm{PM}^{\mathrm{active}}]_{m\times 1} = M_{m,n}\left[\Delta PM \quad \right]_{n\times 1} \tag{5.4}$$

5.3.2. Objective Function

Next, if there are N number of sample points in the 'active constraint area', then the jerk motion of the vehicle in this active constraint area can be set up like the below Equation (5.5).

$$\boldsymbol{J'_{jerk}} = \begin{bmatrix} \frac{(F'_x[n+1]-F'_x[n])}{\Delta t} \\ \frac{(F'_y[n+1]-F'_y[n])}{\Delta t} \\ \frac{(F'_z[n+1]-F'_z[n])}{\Delta t} \\ \frac{(\theta'[n+1]-\theta'[n])}{\Delta t} \\ \frac{(\phi'[n+1]-\phi'[n])}{\Delta t} \\ \frac{(\psi'[n+1]-\psi'[n])}{\Delta t} \end{bmatrix} = \begin{bmatrix} J_x(1) & J_x(2) & \cdots & J_x(N) \\ J_y(1) & J_y(2) & \cdots & J_y(N) \\ J_z(1) & J_z(2) & \cdots & J_z(N) \\ J_\theta(1) & J_\theta(2) & \cdots & J_\theta(N) \\ J_\phi(1) & J_\phi(2) & \cdots & J_\phi(N) \\ J_\psi(1) & J_\psi(2) & \cdots & J_\psi(N) \end{bmatrix} \tag{5.5}$$

The system needs to manipulate the throttle or the brake input to minimize the jerk motion of the vehicle. Then it is required to represent $F'_x, F'_y, F'_z, \theta', \phi', \psi'$ as a function of Δu which consists of change in throttle angle and brake pressure. These can be arranged like below.

$$F'_x = F_x + \Delta F_x = F_x + P \cdot \Delta u \tag{5.6}$$

Where

$$\Delta F_x = P \cdot \Delta u \tag{5.7}$$

$$P: Linearized\ Powertrain\ Model$$

F'_y, F'_z can also be defined as

$$F'_y = F_y + \Delta F_y \tag{5.8}$$

$$F_z' = F_z + \Delta F_z \tag{5.9}$$

Bandy suggests a linearized chassis model and this can help to represent $\Delta F_y, \Delta F_z$ as a function of ΔF_x [54]. Based on the linearized chassis model theory, ΔF_y *and* ΔF_z can be converted into ΔF_x like below.

$$\Delta F_x = C_Y \cdot \Delta F_y \tag{5.10}$$

$$\Delta F_x = C_Z \cdot \Delta F_z \tag{5.11}$$

Where $\mathrm{C_Y}$ and $\mathrm{C_z}$ represent

$$\mathrm{C_Y} = \text{Linear Chassis Model for } 'y' \text{direction to } 'x' \text{direction} \tag{5.12}$$

$$\mathrm{C_Z} = \text{Linear Chassis Model for } 'z' \text{direction to } 'x' \text{direction} \tag{5.13}$$

Therefore F_y' and F_z' can be rewritten like below.

$$F_y' = F_y + C_Y^{-1} \cdot \Delta F_x = F_y + C_Y^{-1} \cdot P \cdot \Delta u \tag{5.14}$$

$$F_z' = F_z + C_Z^{-1} \cdot \Delta F_x = F_z + C_Z^{-1} \cdot P \cdot \Delta u \tag{5.15}$$

θ', ϕ', ψ' can also be derived like below.

$$\theta' = \theta + \Delta\theta \tag{5.16}$$

$$\phi' = \phi + \Delta\phi \tag{5.17}$$

$$\psi' = \psi + \Delta\psi \tag{5.18}$$

The linearized chassis model can help to represent $\Delta\theta, \Delta\phi, \Delta\psi$ as a function of ΔF_x.

$$\Delta F_x = C_Y \cdot (C_P \cdot \Delta\theta) \rightarrow \Delta\theta = (C_Y \cdot C_P)^{-1} \cdot \Delta F_x \tag{5.19}$$

$$\Delta F_x = (C_R \cdot \Delta\phi) \rightarrow \Delta\phi = C_R^{-1} \cdot \Delta F_x \tag{5.20}$$

$$\Delta F_x = C_{Yaw} \cdot \Delta\psi \rightarrow \Delta\psi = C_{Yaw}^{-1} \cdot \Delta F_x \tag{5.21}$$

Where C_p, C_R, C_{Yaw} represent

$$C_p = pitch\ stiffness$$

$$C_R = Roll\ stiffness$$

$$C_{Yaw} = \frac{\rho \cdot m}{(\Delta t)^2} \begin{bmatrix} 1 & & \\ \vdots & \ddots & \\ 1 & \dots & 1 \end{bmatrix}^{-1}$$

Therefore, θ', ϕ', ψ' can be rewritten like below.

$$\boldsymbol{\theta' = \theta + C_p^{-1} \cdot \Delta F_x = \theta + C_p^{-1} \cdot P \cdot \Delta u} \tag{5.22}$$

$$\boldsymbol{\phi' = \phi + C_R^{-1} \cdot \Delta F_x = \phi + C_R^{-1} \cdot P \cdot \Delta u} \tag{5.23}$$

$$\boldsymbol{\psi' = \psi + C_{Yaw}^{-1} \cdot \Delta F_x = \psi + C_{Yaw}^{-1} \cdot P \cdot \Delta u} \tag{5.24}$$

Therefore, the jerk motion in terms of direction, $\mathrm{F_x}, F_y, F_z, \theta, \phi, and\ \psi$, now can be expressed as a function of change in throttle and brake. Next, the objective function should be considered and two contributions can be counted to set up the objective function. The first contribution to the objective function is from the vehicle's jerk motion and this has the highest priority of any other contributions to the objective function. The weighting matrix to the components in terms of 6 directions of jerk motion can be represented by Equation (5.25).

$$\mathrm{W_f'} = \begin{bmatrix} a_1' & & & \\ & a_2' & & \\ & & \ddots & \\ & & & a_6' \end{bmatrix}_{6\times 6} \tag{5.25}$$

a_1 affects to the weighting of the jerk motion of longitudinal direction. a_2 affects to the weighting of the jerk motion of lateral direction. a_3 affects to the weighting of the jerk motion of vertical direction. a_4 affects to the weighting of the jerk motion of pitch direction. a_5 affects to the weighting of the jerk motion of roll direction. a_6 affects to the weighting of the jerk motion of yaw direction.

The relative importance of the time series elements can be different. Therefore, the weighting matrix to the elements in terms of time series can be represented by Equation (5.26).

$$\mathrm{W}_\mathrm{r}' = \begin{bmatrix} b_1' & & & \\ & b_2' & & \\ & & \ddots & \\ & & & b_N' \end{bmatrix}_{N\times N} \tag{5.26}$$

b_1 affects to the weighting of the 1st time elements for 6 direction elements. b_2 affects to the weighting of the 2nd time elements for 6 direction elements. In this way, $b_N$affects to the weighting of the N^{th} time element for 6 direction elements.

Eventually, the first cost function can be represented by Equation (5.27).

$$J_1 = ||W_f' \cdot \mathrm{J}_{\mathrm{jerk}}' \cdot W_r'||_2 \tag{5.27}$$

where $||W_f' \cdot \mathrm{J}_{\mathrm{jerk}}' \cdot W_r'||_2$ represents the square root of the largest eigenvalue of

$\left(W_f' \cdot \mathrm{J}_{\mathrm{jerk}}' \cdot W_r'\right) \cdot \left(W_f' \cdot \mathrm{J}_{\mathrm{jerk}}' \cdot W_r'\right)^T$.

Then the second objective function can be considered as is a kind of penalty cost function for the brake manipulation by the driver and the system. The total brake pressure is the sum of the brake pressure from driver command and vehicle control system. This can be equivalently represented by Equation (5.28).

$$\mathrm{BR} = Br_{driver} + Br_{system} \tag{5.28}$$

Let $\mathrm{J}_{\mathrm{BR}}''$ as a matrix that represents all the brake pressure information in the time range of active constraint area. Then it can be expressed like Equation (5.29).

$$\mathrm{J}_{\mathrm{BR}}'' = \begin{bmatrix} BR_{FL}(1) & BR_{FL}(2) & \cdots & BR_{FL}(N) \\ BR_{FR}(1) & BR_{FR}(2) & \cdots & BR_{FR}(N) \\ BR_{RL}(1) & BR_{RL}(2) & \cdots & BR_{RL}(N) \\ BR_{RR}(1) & BR_{RR}(2) & \cdots & BR_{RR}(N) \end{bmatrix} \tag{5.29}$$

Let weighting matrix for each brake wheel pressure as $\mathrm{W}_{\mathrm{f}}''$

$$\mathrm{W}_{\mathrm{f}}'' = \begin{bmatrix} a_1'' & & & \\ & a_2'' & & \\ & & a_3'' & \\ & & & a_4'' \end{bmatrix}_{4\times4} \tag{5.30}$$

a_1'' affects to the weighting of the brake pressure of front left side. a_2'' affects to the weighting of the brake pressure of front right side. a_3'' affects to the weighting of the brake pressure of rear left side. a_4'' affects to the weighting of the brake pressure of rear right side.

Let weighting matrix for time series elements as $\mathrm{W}_{\mathrm{r}}''$.

$$\mathrm{W}_{\mathrm{r}}'' = \begin{bmatrix} b_1 & & & \\ & b_2 & & \\ & & \ddots & \\ & & & b_N \end{bmatrix}_{N\times N} \tag{5.31}$$

Therefore, the cost function which represents the penalty by using a brake can be expressed by Equation (5.32).

$$\mathrm{J}_2 = ||W_f'' \cdot J_{BR}'' \cdot W_r''||_2 \tag{5.32}$$

where $\left|\left|W_f'' \cdot \mathrm{J}_{\mathrm{jerk}}'' \cdot W_r''\right|\right|_2$ represents the square root of the largest eigenvalue of

$\left(W_f'' \cdot \mathrm{J}_{\mathrm{jerk}}'' \cdot W_r''\right) \cdot \left(W_f'' \cdot \mathrm{J}_{\mathrm{jerk}}'' \cdot W_r''\right)^T$.

Finally, the integrated form of the objective function can be represented by Equation (5.33).

$$\boldsymbol{J} = \boldsymbol{J_1} + \boldsymbol{J_2} \tag{5.33}$$

5.3.3 Constraints for the Optimization

1. Active Constraints on Performance Margin: As the active constraints area is already explained in the section 5.3.1, the Performance Margin, with respect to the front and rear tires, for active constraint area can be derived from using the Equation (5.4). This Performance Margin for active constraint area can consist of Equation (5.34).

$$\begin{bmatrix} \Delta PM_{front} \\ \Delta PM_{rear} \end{bmatrix}_{2N\times 1} = [L.C.M][D.T][P.T]\begin{bmatrix} \Delta Th \\ \Delta Br \end{bmatrix}_{2N\times 1} \tag{5.34}$$

Where

$[L.C.M]$: Linearized Chassis Model

$[D.T]$: Linearized Drivetrain Model

$[P.T]$: Linearized Powertrain Model

The above equation sets up the relationship between the change in Performance Margin and the change in throttle and brake inputs.

2. $Freq < Freq_{threshold}$: Since the system considers the quasi-static dynamics of the engine and brake, it is required to create the desired change in throttle or brake that is always smaller than the frequency threshold bound. For achieving this goal, the Discrete Sine Transform (DST) can be considered to generate the desired change in throttle or brake input that can decompose a function of time (a signal) into the frequencies. This enables the system to generate the throttle or brake

input by combining the sinusoidal functions that have smaller frequencies than the threshold frequency.

If the frequency threshold of the engine is $\omega_{\mathrm{M\_Thr}}$, then the desired change in throttle input can be represented by summation of sine functions which all have smaller frequencies than this threshold frequency. This is equivalently represented in Equation (5.35).

$$[\Delta Th]_{N\times 1} = \sum_{i=1}^{M\_Thr} a_i \cdot \sin\left(\frac{\omega_i}{2\cdot\pi}\right)\left(\frac{k}{N}\right) \tag{5.35}$$

This can be rearranged in matrix form.

$$[\Delta Th]_{N\times 1} = \left[\mathrm{S}_{k,i}\right]_{N\times M\_Thr} \cdot \begin{bmatrix} a_1 \\ a_2 \\ \vdots \\ a_{M\_Thr} \end{bmatrix}_{M\_Thr\times 1} \tag{5.36}$$

$$\text{where } \mathrm{S}_{k,i} = \sin\left(2\pi k \cdot \left(\frac{i}{N}\right)\right)$$

Likewise, with engine control, if the frequency threshold of the brake is $\omega_{\mathrm{M\_Brk}}$, then the desired change in brake input can be represented by summation of sine functions which all have smaller frequencies than this threshold frequency. This is equivalently represented in Equation (5.37).

$$[\Delta Br]_{N\times 1} = \sum_{i=1}^{M\_Brk} b_i \cdot \sin\left(\frac{\omega_i}{2\cdot\pi}\right)\left(\frac{k}{N}\right) \tag{5.37}$$

This can be rearranged in matrix form.

$$[\Delta \mathrm{Br}]_{N\times 1} = \left[S_{k,i}\right]_{N\times M\_Brk} \cdot \begin{bmatrix} b_1 \\ b_2 \\ \vdots \\ b_{M\_Brk} \end{bmatrix}_{M\_Brk\times 1} \tag{5.38}$$

$$\text{where } \mathrm{S}_{k,i} = \sin\left(2\pi k \cdot \left(\frac{i}{N}\right)\right)$$

3. The above two suggested constraints can be integrated and represented in one Equation. From Equation (5.4), Equation (5.34), Equation (5.36), and Equation (5.38), it is able to represent the final constraint equation like below.

$$\begin{bmatrix} \Delta PM_{front} \\ \Delta PM_{rear} \end{bmatrix}_{2N,1} = [Q]_{2N,2N} \begin{bmatrix} S_{N,K\_Thr} & 0 \\ 0 & S_{N,K\_Brk} \end{bmatrix} \begin{bmatrix} a_{K\_Thr,1} \\ \beta_{K\_Brk,1} \end{bmatrix}$$

$$\begin{bmatrix} \Delta PM_{front} \\ \Delta PM_{rear} \end{bmatrix}_{M,1}^{\text{active}} = [M]_{M,2N} \begin{bmatrix} \Delta PM_{front} \\ \Delta PM_{rear} \end{bmatrix}_{2N,1} \tag{5.39}$$

Where

$$[Q] = [L.C.M][D.T][P.T]$$

Then the compensated PM should be brought below PM threshold. This is equivalently represented in Equation (5.40).

$$\begin{bmatrix} \boldsymbol{PM_{front}} \\ \boldsymbol{PM_{rear}} \end{bmatrix}_{\boldsymbol{M,1}}^{\boldsymbol{active}} + \begin{bmatrix} \boldsymbol{\Delta PM_{front}} \\ \boldsymbol{\Delta PM_{rear}} \end{bmatrix}_{\boldsymbol{M,1}}^{\textbf{active}} < \begin{bmatrix} \boldsymbol{PM_{front-threshold}} \\ \boldsymbol{PM_{rear-threshold}} \end{bmatrix} \tag{5.40}$$

5.3.4. Update Law for the Learning Controller (Linearized Powertrain Model)

There are in total 3 linearized prediction models. They are linear powertrain model, drive train model, and chassis model. Since these models are linearized from totally nonlinear model, they always show somewhat errors to compare with full nonlinear vehicle model. Therefore, it is required to compensate this error by updating the linear model continuously whenever the error comes out from the difference between linearized model and full nonlinear model. In this section, the detailed method to update the linear prediction model from the error is suggested.

First of all, the integrated linear powertrain model and drive-train model can be updated continuously from the error. Let linear powertrain model as Γ_{PT}. From Chapter 3, the design method for engine and brake model is already provided. These models are represented as a Frequency Response Function in the frequency domain. In general form of the Iterative Learning Control, models are usually represented in the time domain. Therefore, by taking the inverse Fast Fourier Transform, it is able to get its impulse response in the time domain. Since the system is discretized, this impulse response can consist of the lower triangular toeplitz matrix for the convolution integral with the error vector and equivalently represented in Equation (5.41).

$$\Gamma_{\mathrm{PT}} = \begin{bmatrix} h_1 & & & & \\ h_2 & h_1 & & & \\ \vdots & \vdots & \ddots & & \\ h_{n-1} & h_{n-2} & \dots & h_1 & \\ h_n & h_{n-1} & \dots & h_2 & h_1 \end{bmatrix} \tag{5.41}$$

Where h_i represents the element of the impulse response that comes from taking the Inverse Fast Fourier Transform of the linearized powertrain model.

Therefore, it can be understood that the linear powertrain model, Γ_{PT}, takes a form of the lower triangular toeplitz matrix. By reviewing the Section 3.1.3 (Linear Predictive Drivetrain Model) and the Equation (3.17), it can be understood that the linear drivetrain model also takes the form of shifted lower triangular toeplitz matrix since terms, $\left[\frac{\tau}{\mathrm{V_x}}\right], \left[\frac{\eta}{V_x}\right], \left[\frac{\tau}{\eta}\right], and\ \left[\frac{\tau}{F_x}\right]$, in Equation (3.17) take a diagonal matrix form and [S]in Equation (3.17) takes a shifted lower triangular toeplitz matrix. Then the integration form of linear powertrain model and drive-train model also takes a same form, lower triangular toeplitz matrix. Integrated model can be represented simply in Equation (5.42).

$$\Gamma_{\mathrm{integrated}} = \Gamma_{PT} \times \Gamma_{DT} \tag{5.42}$$

Then the input for the linear prediction model can be expanded by the following procedures.

$$\vec{u}_k = \vec{u}_{k-1} + \Delta\vec{u}_k = \vec{u}_{k-1} + \Gamma_{\mathrm{integrated}} \cdot \vec{e}_k \tag{5.43}$$

$$\vec{u}_{k+1} = \vec{u}_k + \Delta\vec{u}_{k+1} = \vec{u}_k + \Gamma_{\text{integrated}} \cdot \vec{e}_{k+1} \tag{5.44}$$

$$\vdots$$

Where $\mathrm{e_k}$ represents the error force at the tire contact patch between actual from full nonlinear model and estimated from linearized prediction model at k^{th} trial, and $\mathrm{u_k}$ represents the throttle input to the system at k^{th} trial. Note that $\Gamma_{\text{integrated}}$ is independent from the number of iterations (k) since the fixed control law is used in Equation (5.43) and (5.44). Therefore, it is independent from the 'k'. The updated control law will be derived below that shows this gamma depends on 'k' since it is updated continuously from the error.

From the Equation (5.43) and (5.44), compensated change in throttle input is equivalently represented in Equation (5.45).

$$\Delta\vec{u}_k = \Gamma_{\text{integrated}} \cdot \vec{e}_k$$

$$\Delta\vec{u}_{k+1} = \Gamma_{\text{integrated}} \cdot \vec{e}_{k+1}$$

$$\vdots \tag{5.45}$$

By adding the Equation (5.43) and the Equation (5.44), the Equation (5.46) can be set up like below.

$$\Delta\vec{u}_k + \Delta\vec{u}_{k+1} = \Gamma_{\text{integrated}} \cdot (\vec{e}_k + \vec{e}_{k+1}) = \Gamma'_{\text{integrated}} \cdot (\vec{e}_{k+1}) \tag{5.46}$$

Equation (5.46) shows the relationship between the fixed control law and the updated (adaptive) control law. Note that the term, $\Gamma'_{\text{integrated}}$, is an updated control law from the previous (k^{th}) error.

Equation (5.46) can be rearranged like below.

$$\Gamma_{\text{integrated}} \cdot (\vec{e}_k + \vec{e}_{k+1}) = \Gamma'_{\text{integrated}} \cdot (\vec{e}_{k+1}) = \left(\Gamma_{\text{integrated}} + \Gamma_{\text{u}}\right) \cdot (\vec{e}_{k+1}) \tag{5.47}$$

where Γ_{u} represents the change in control law based on the error.

Then the updated law for the linearized model can be derived like the Equation (5.48).

$$\Gamma_{\mathrm{integrated}} \cdot e_k = \Gamma_u \cdot e_{k+1} \tag{5.48}$$

Since $\Gamma_{\mathrm{integrated}}, e_k, e_{k+1}$ are known and the control law, $\Gamma_{\mathrm{integrated}}$ and Γ_{u} are the lower triangular toeplitz matrix, it is able to estimate the undetermined update control law, Γ_{u}, by forward substitution method.

Therefore, it is able to update the control law continuously, in terms of the integrated linear powertrain and drivetrain model, for every iteration of the intervention strategy.

5.4. Simulation Results

A commercial vehicle simulation package is used for the simulation environment. A typical sedan with a 200 kW engine model and a 6-speed automatic transmission is modeled with 15 mechanical degrees of freedom. The road is designed that is a straight road and then a sharp corner as suggested in Figure 5.4. This can naturally make an environment that the vehicle may lose its handling capability if the vehicle runs with high speed (above 100Km/h). Each sharp corner has its own characteristic. The first corner is the simplest corner with a 50m curve radius. The second corner has up and down hill so that the vehicle pass through the downhill at the corner. The third corner has a bank that is skewed toward the outside of the road. The fourth corner has a split μ condition.

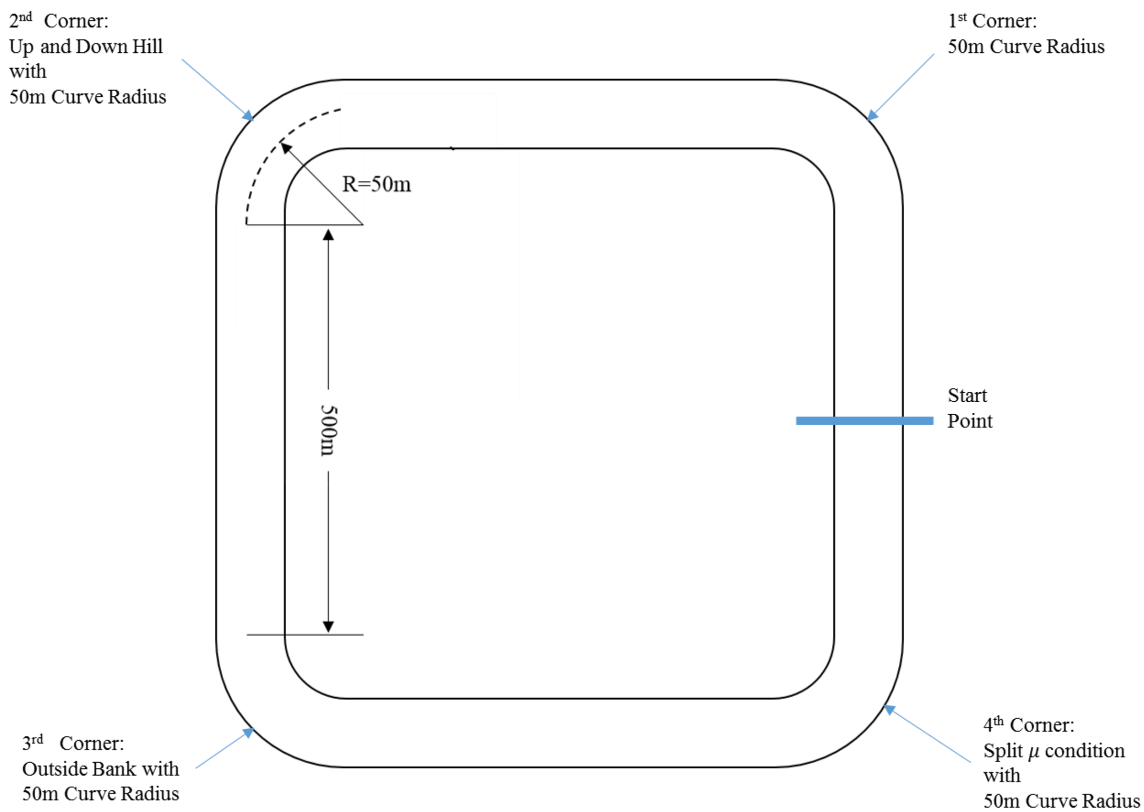

Figure 5.4. The Top View of the Track for the Simulation

The initial speed of the vehicle is 110Km/h and this speed is maintained by conventional cruise control system. The simulation package also provides the driver model where the vehicle try to maintain its lateral position in the center line of the road.

Since the LAAVDS is model based predictive control system, the future prediction is performed for every second after starting the simulation. The system has 10 second time horizon for future prediction and one second update rate. Since these time horizon and update rate are user defined parameters, they can be adjusted later based on the request of the user. The PM prediction result for next 10 seconds before entering the 1st corner is suggested in Figure 5.5. As it can be seen from the Figure 5.5, the vehicle exceeds its PM after approximately 9 seconds from the moment when it predicts the next future 10 seconds. This means that this vehicle may lose its handling capability around this moment and thus it is required to modulate the throttle and brake to bring it back below the threshold.

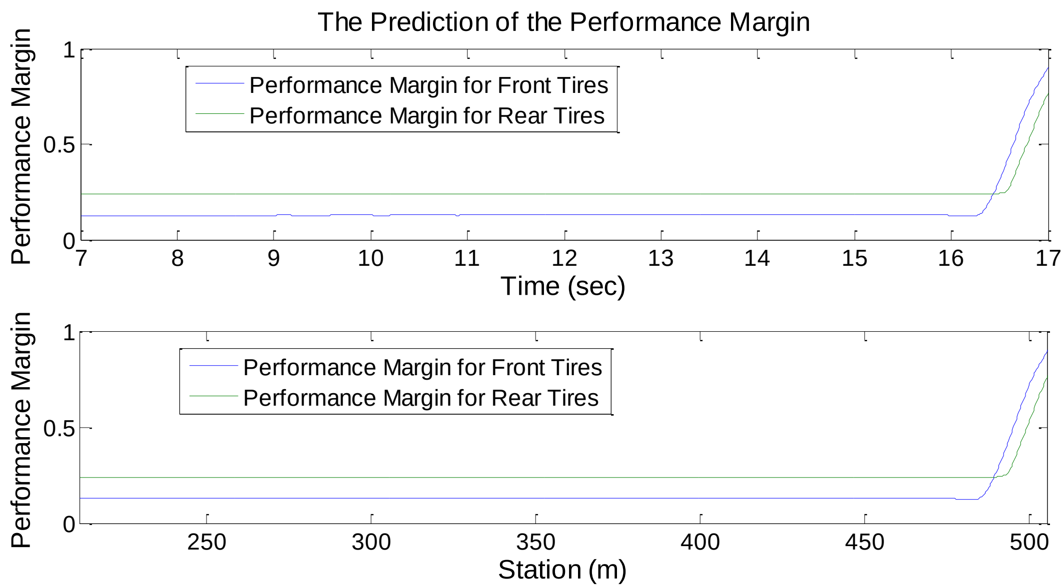

Figure 5.5. The Prediction of the Performance Margin for next 10 seconds before entering the 1st Corner

The Intervention Strategy is initiated to generate the desired change in throttle and brake pressure. During the Intervention Strategy, the constrained optimization is executed and optimal throttle and brake input is prepared to compensate the current vehicle's throttle and brake status so that the vehicle can recover the handling capability in near future.

After updating the throttle and brake input by the Intervention Strategy continuously for every 1 second, the vehicle can pass the 1st corner successfully. The corresponding PM is suggested in Figure 5.6. For the 1st corner, more detailed information in terms of the history for throttle, brake, and velocity during the Intervention Strategy is provided in Appendix. The change in longitudinal, lateral, and vertical forces during cornering are also suggested consecutively in Appendix.

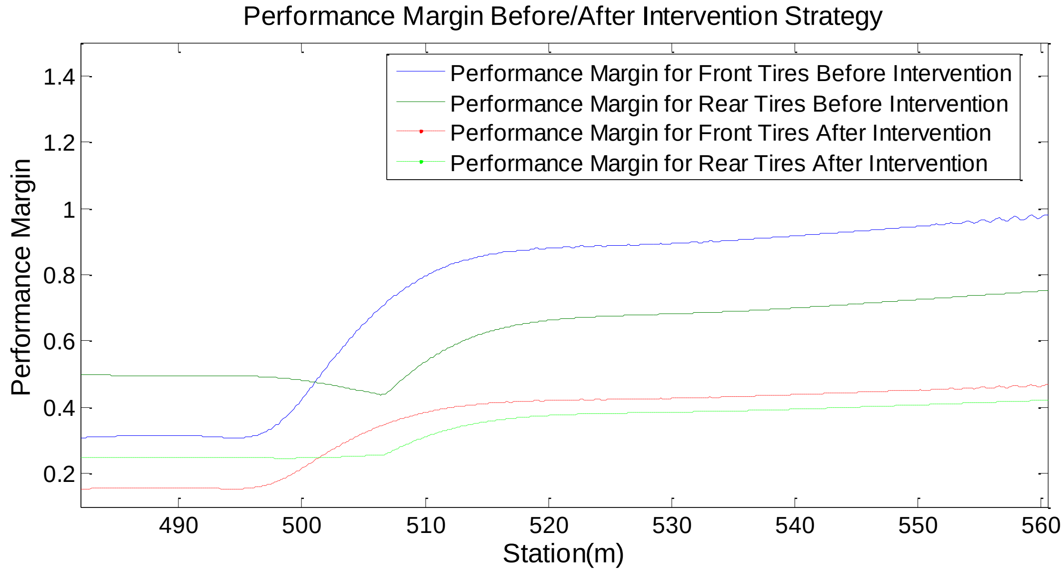

Figure 5.6. The Comparison of the Performance Margin Before and After Intervention Strategy at the 1st Corner

The illustration of the simulation animation for comparing the handling capability is suggested in Figure 5.7 and Figure 5.8.

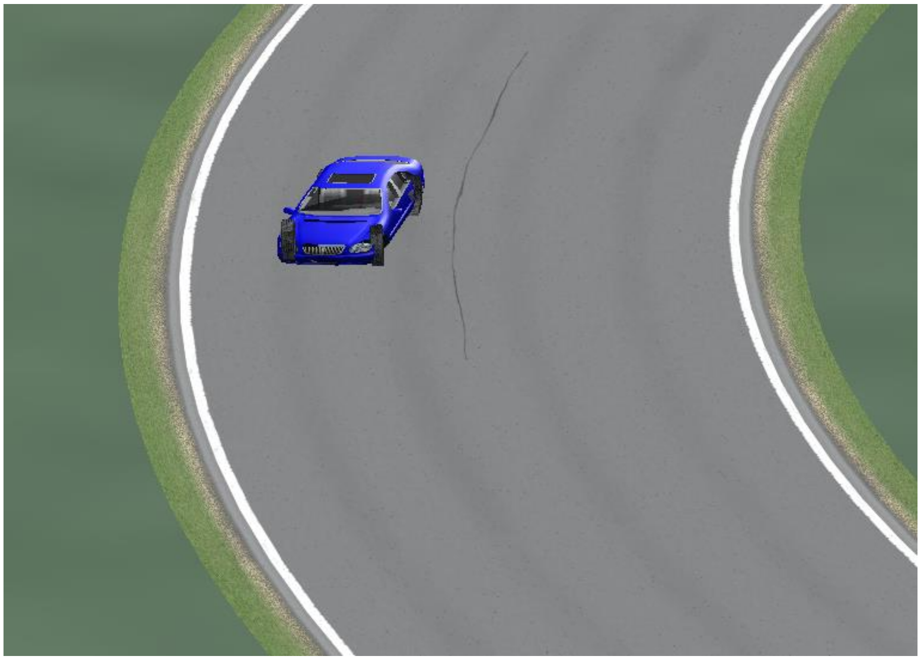

Figure 5.7. The Vehicle Behavior without the Intervention Strategy

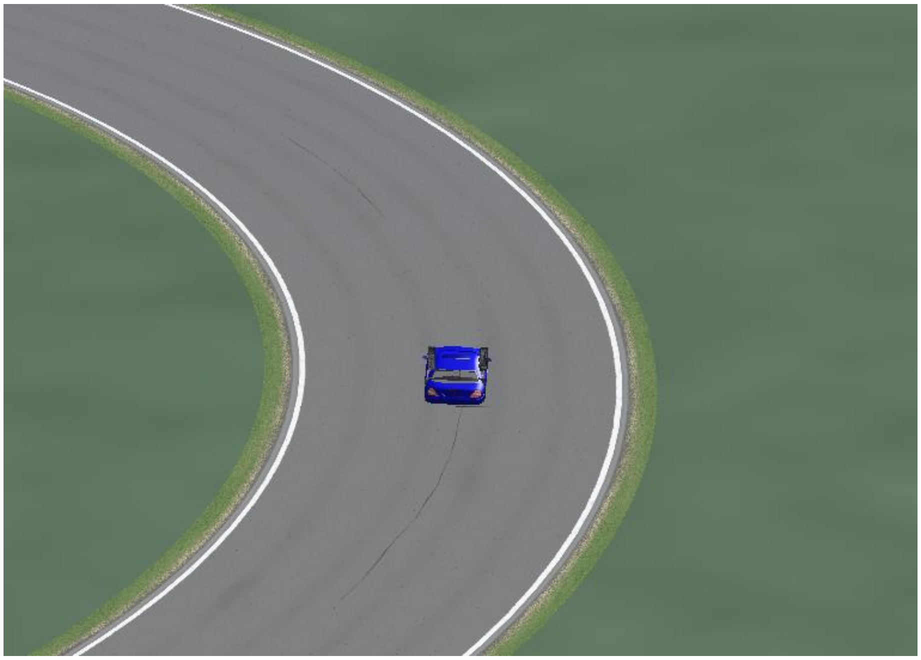

Figure 5.8. The Vehicle Behavior after Applying the Intervention Strategy

The Performance Margin without the Intervention Strategy at the 2nd corner is suggested in Figure 5.9.

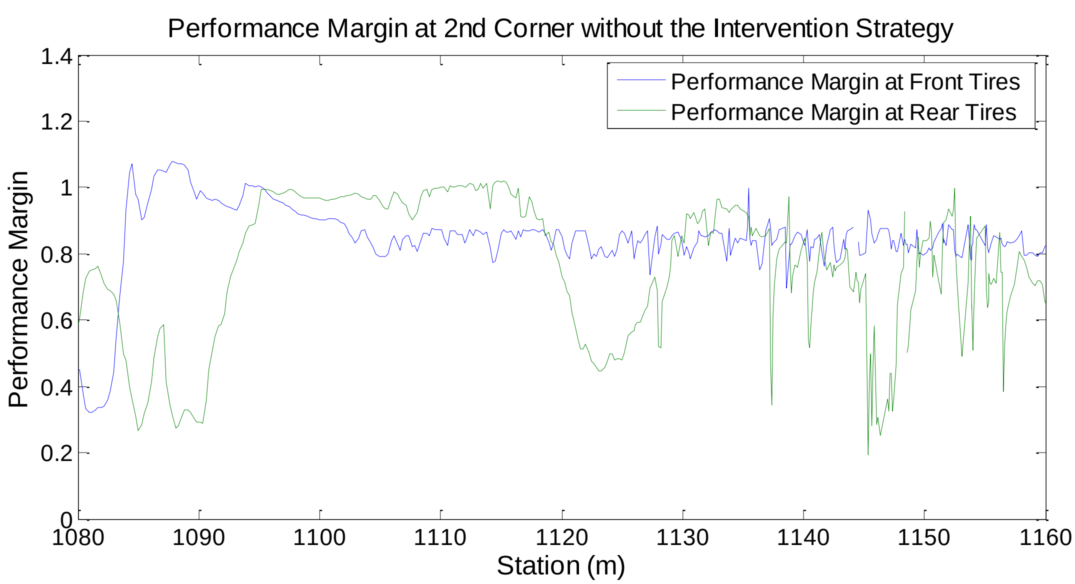

Figure 5.9. Performance Margin at 2nd corner without the Intervention Strategy

After updating the throttle and brake by the Intervention Strategy continuously until control goal is satisfied, the vehicle can pass the 2nd corner successfully. The corresponding PM is suggested in Figure 5.10. For the 2nd corner, more detailed information in terms of the history for throttle, brake, and velocity during the Intervention Strategy is provided in Appendix. The change in longitudinal, lateral, and vertical forces during cornering are also suggested consecutively in Appendix.

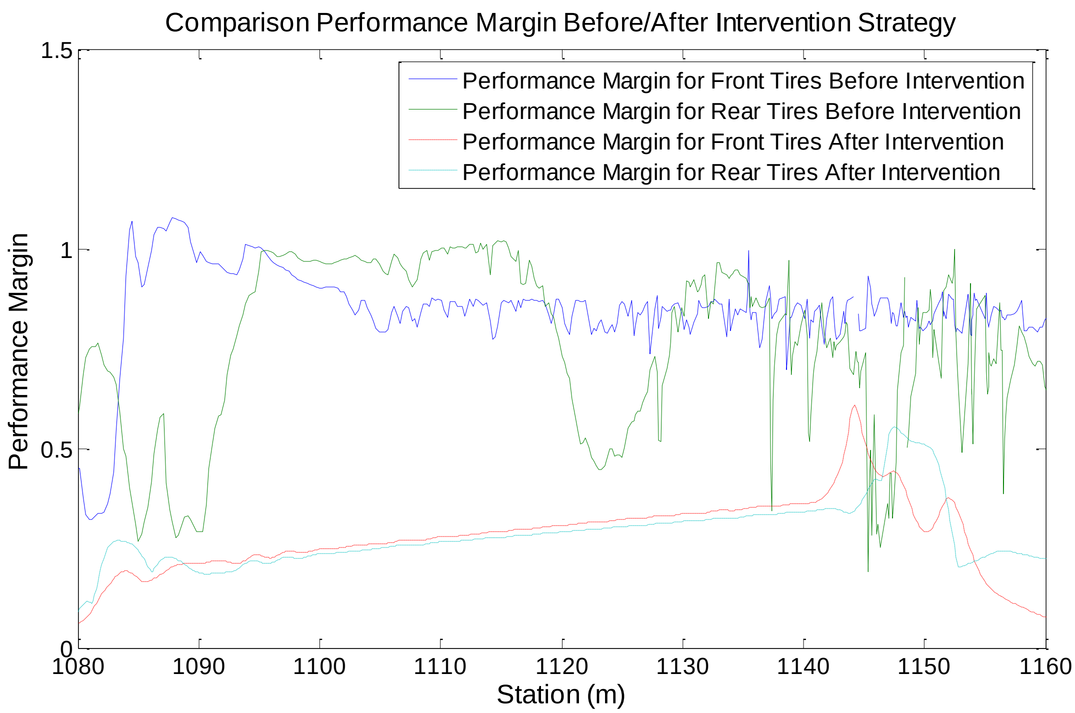

Figure 5.10. The Comparison of the Performance Margin Before and After Intervention Strategy at 2nd Corner

The illustration of the simulation animation is suggested in Figure 5.11 and 5.12 for comparing the effectiveness of the Intervention Strategy.

Figure 5.11. The illustration of the simulation animation without the Intervention Strategy

Figure 5.12. The illustration of the simulation animation with the Intervention Strategy

For the 3rd corner, the PM is suggested in Figure 5.13 if the vehicle runs without the Intervention Strategy.

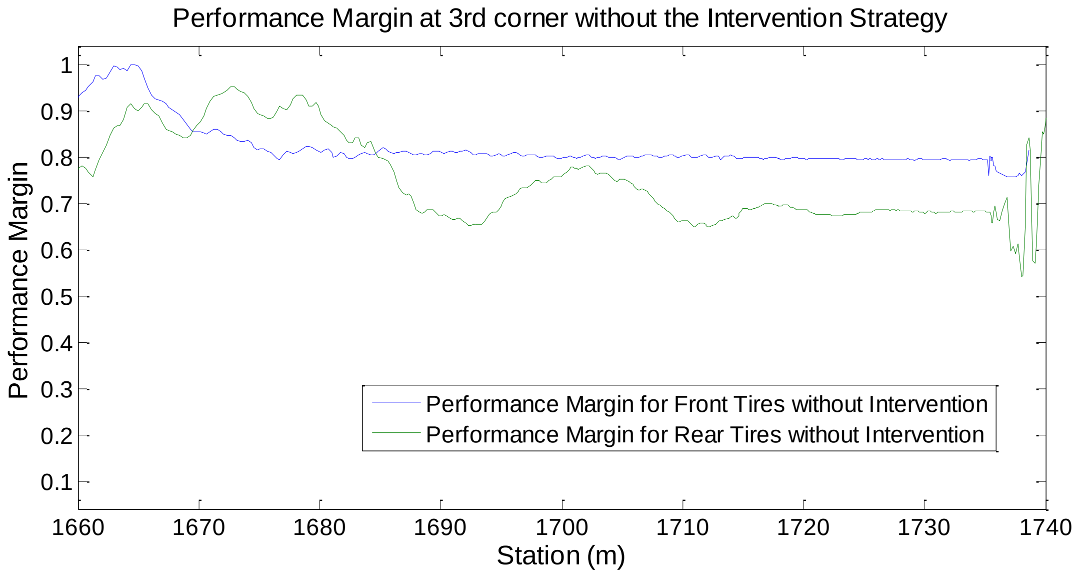

Figure 5.13. Performance Margin at the 3rd corner without the Intervention Strategy

After updating the throttle and brake input by the Intervention Strategy continuously for every 1 second, the vehicle can pass the 3rd corner successfully. The corresponding PM is suggested in Figure 5.14. For the 3rd corner, more detailed information in terms of the history for throttle, brake, and velocity during the Intervention Strategy is provided in Appendix. The change in longitudinal, lateral, and vertical forces during cornering are also suggested consecutively in Appendix.

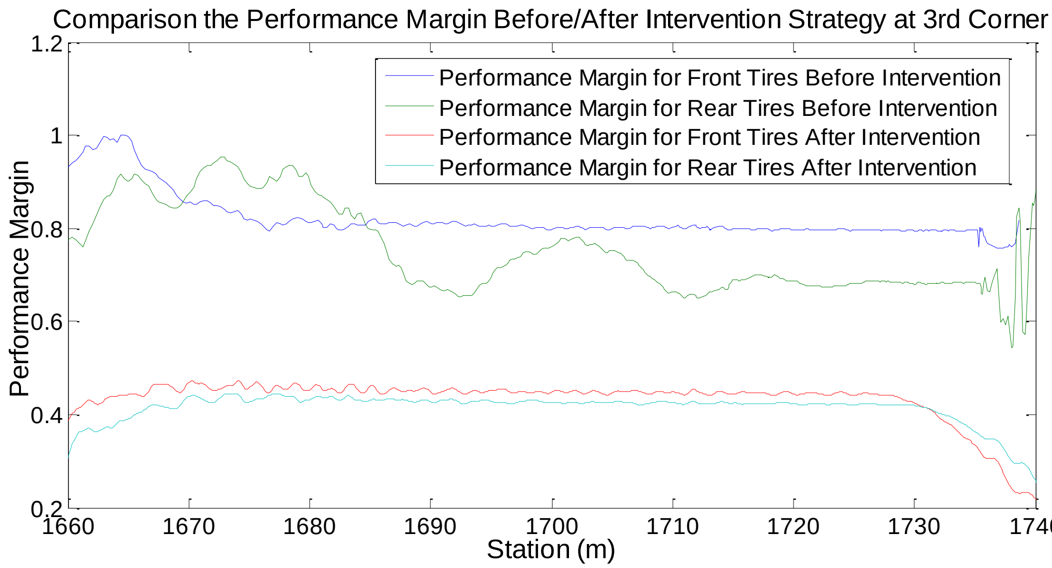

Figure 5.14. The comparing of the Performance Margin at the 3rd corner after applying the Intervention Strategy

For the 4th corner, it is a split μ condition and the PM without the Intervention Strategy is suggested in Figure 5.15.

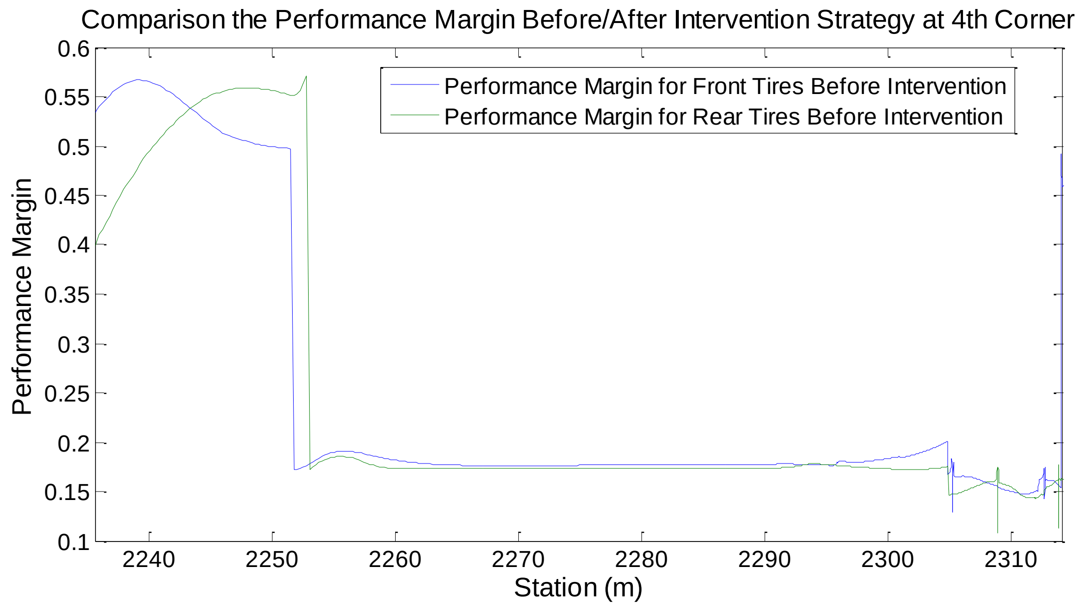

Figure 5.15. The Performance Margin at the 4th corner without the Intervention Strategy

Throughout the Intervention Strategy, the throttle and brake is updated continuously. The PM comparison after applying the Intervention Strategy is suggested in Figure 5.16. For the 4th corner, more detailed information in terms of the history for throttle, brake, and velocity during the Intervention Strategy is provided in Appendix. The change in longitudinal, lateral, and vertical forces during cornering are also suggested consecutively in Appendix.

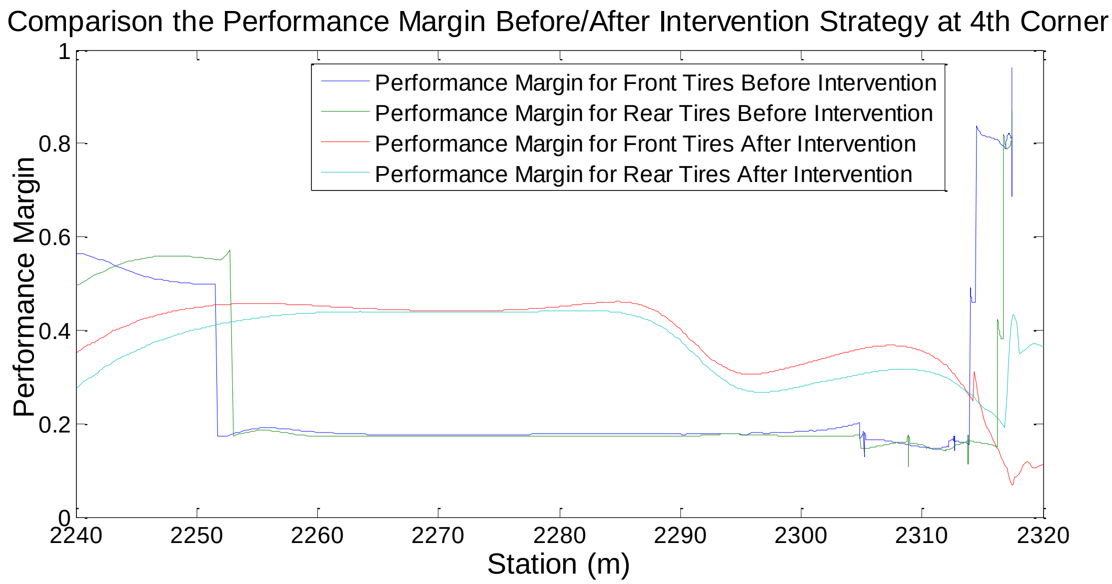

Figure 5.16. The comparing of the Performance Margin at the 4th corner after applying the Intervention Strategy

As can be seen from Figure 5.16, it can be understood that the vehicle passes the 4th corner successfully after applying the Intervention Strategy.

5.5. Nomenclature

PM	Performance Margin
IS	Intervention Strategy
P	Linearized Powertrain
C_Y	Linearized Chassis Model for y direction to x direction
C_Z	Linearized Chassis Model for z direction to x direction
u	Current Throttle or Brake Input to the System
Δu	Compensated Throttle or Brake Input to the System by Controller
θ	Pitch Angle
Φ	Roll Angle
ψ	Yaw Angle
C_p	Pitch Stiffness
C_R	Roll Stiffness
C_{Yaw}	Yaw Stiffness
ΔPM	Compensated Performance Margin by Compensated Throttle or Brake Input
ΔTh	Compensated Throttle Input
ΔBr	Compensated Brake Input

Γ_{PT}	Representation of the Linear Powertrain Frequency Response Function in the Time Domain for the Convolution Integral
$\Gamma_{\text{Integrated}}$	Representation of the Integrated Model of the Linear Powertrain and Drivetrain Models in the Time Domain for the Convolution Integral
u_k	Throttle or Brake Input to the System at kth iteration
Δu_k	Compensated Throttle or Brake Input to the System by the Controller at kth iteration

6. Future Works

6.1. Simulation Validation with More Various and Complex Track

The simulation result is suggested in previous section and it shows the effectiveness of the Intervention Strategy. However it is required to consider more various racing tracks so that the vehicle can face more extreme condition. For example, the winding road will be designed that changes the curvature continuously. The track design process that contains not only x,y,z information but also bank, elevation and curvature information is not simple process. For this reason, the Track Builder Software is developed by VTPL. This software will be used to design the road and implemented into the Carsim for validation.

6.2. Design of Software In the Loop Simulation (SILS), the Size of the Time Horizon and Update Rate

There are still remaining works in this dissertation. One of the issue can be the size of the time horizon for future prediction and its update rate. The interesting range of future prediction for the control of vehicle motion depends on road profile and ego vehicle's speed. Cho, in his patent, provides the concept how to adjust the size of the interesting range for vehicle control based on the vehicle speed [56]. If the vehicle runs at high speed, then the interesting range of future prediction is greater than the low speed. Vice versa can be established. The frequencies for update rate can also be adjusted based on road profile. For example, the winding road or complex racing track may request higher frequencies for update rate since the curvature is continuously changed and thus can affect to the driving condition frequently.

To determine the reasonable size of time horizon and frequency for update rate, it is required to perform numerous simulation. Manually, it is hard to achieve this goal and thus need to make a loop simulation. There could be two ways to make a loop simulation. One is to consider the Hardware in the Loop Simulation (HILS). By adding a real hardware in the loop simulation, it can monitors the performance of the algorithm before implementing it into the real vehicle system. However, this can cost much. Another way is to consider the Software in the Loop Simulation (SILS). Without any hardware platform, it is able to validate the algorithm and tune parameters by consisting of loop simulation.

Once SILS is constructed, it will be available to find out the reasonable size of time horizon for future prediction and update rate. And it will also can find out the limit size of the time horizon and update rate from performing various and numerous simulations. But, there is some conditions to achieve this goal. The first task is that it requires a lot of various tracks. The second is that there is big difference between the simulation and real vehicle test. Thus, even if reasonable size of time horizon and update rate is found out by the simulation, it still needs to do a real vehicle test to reduce the gap between simulation and real vehicle test. Currently, the size of time horizon can be suggested by the Equation (6.1).

$$\mathrm{T}_{\mathrm{size}} = K_1(V_x) + K_2(\rho) \tag{6.1}$$

Where

$\mathrm{T}_{\mathrm{size}}$: The size of time horizon

$K_1(V_x)$: 1st Decision Factor, as a function of velocity, for the size of time horizon

$K_2(\rho)$: 2nd Decision Factor, as a function of curvature, for the size of time horizon

The functions and parameters in Equation (6.1) can be determined by numerous simulation with various tracks.

6.3. The development of the Full Vehicle Model.

The commercial program, Carsim, is currently used for predicting the future vehicle states. This provides a highly accurate full nonlinear vehicle model and thus is reasonable to use it as a future prediction model. However, the biggest problem of using this program is that it is impossible to implement it into the real vehicle system since it does not provide the auto-code generation tool-kit for the vehicle model. Therefore, the full vehicle model is required if it needs to be implemented into the real vehicle. Currently, the study about the full nonlinear vehicle model is performed in VTPL. This model contains from engine dynamics to tire mechanics. Though there were a lot of efforts to improve this model, it still needs to consider a lot of factors that is currently not implemented. Those are listed below.

a. Bank of Road: This can affect to the longitudinal force, lateral force, and vertical force at the tire contact patch and thus it is required to be considered for performing an accurate nonlinear vehicle simulation.

b. Driver Model: Current vehicle model assumes that the vehicle model only runs on the straight road. This can be a problem when the vehicle undergoes the cornering. Without the adequate driver model, it is not able to run the simulation for various and complex road tracks.

The biggest challenging part is the accuracy to compare with the result from the Carsim. Currently, the simulation is performed on the straight road without any bank so that it can avoid the effect of the bank angle of the road and driver model. The throttle input is given as a constant value. Under this simulation environment, the lateral force and vertical force at the tire contact patch show big error to compare with the result that comes from the Carsim. Therefore it is required to carry out the fine-tuning for parameters so that the vehicle model can emulate the nonlinear behavior of the Carsim. One available method for the fine tuning is a manual tuning from numerous simulations. Another way is to consider the self-tuning method by combining of the optimization method.

Since all these works can be a topic for the master thesis, it is remained as a future work.

6.4. The Consideration for the Change of Center of Gravity

Currently, the Intervention Strategy considers the quasi static (low frequency) interruption for vehicle control. This means that the vehicle’s motion can be manipulated smoothly and thus there can be no much change in Center Of Gravity (COG) during the Intervention Strategy. However, if there is quick change in vehicle control motion, the change of COG should be considered. Sol suggests a method to estimate the change of COG [57]. The estimator uses averaged displacement measurements to estimate changes in vehicle body mass, vehicle COG location, and vehicle pitch moment of inertia, due to variations in fuel load, passenger load, and cargo load. More and a lot of literature review is required if this topic is considered for implementing into full vehicle model and LAAVDS.

7. Conclusions

The development of the LAAVDS focuses on improving the vehicle's handling capability. The ultimate goal of this system is to take some vehicle control actions, like modulating the throttle and brake, in advance if it seems that the vehicle may fall into the dangerous situations for the upcoming road profile. This can help the vehicle to be ready for passing through the unexpected, dangerous road profile successfully by taking active vehicle control actions.

This ADAS system, the LAAVDS, has a distinctive point to compare with recent cutting edge ADAS technology. While most of the current ADAS system focuses on real time vehicle control, the LAAVDS adapts the model based predictive control system. This enables the vehicle to predict the future vehicle dynamics status and take an action in advance. The development of the Intervention Strategy for the LAAVDS demonstrates the effectiveness of this system. The simulation results suggest the necessity of the LAAVDS beyond the ESC system. From 2012, all the vehicles in the U.S. begin to equip the ESC system. The statistics, from the NHTSA, already shows the improvement of the safety by the ESC system. Though there is no doubt that the ESC system enhances safety, the LAAVDS can be positioned beyond this system. The evolution speed of the hardware and sensor is faster than any time in the past, and this will lead the vehicle to equip a safety oriented system, like the LAAVDS, that relies on the high performance hardware and sensor. Therefore, in near future, it is expected this kind of system can be equipped to the vehicle so that it can raise up the stability and safety.

Appendix

The history of throttle, brake, and vehicle velocity, with the Intervention Strategy are provided for each corner. The change in longitudinal force, lateral force, and vertical force are also suggested consecutively.

1st Corner

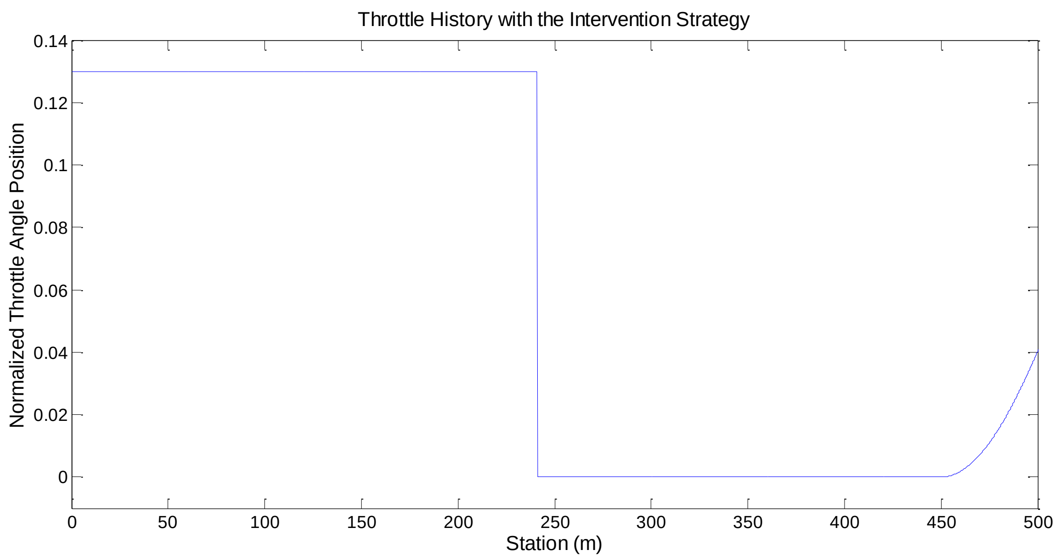

Figure A.1. The Throttle History before Entering the 1st Corner

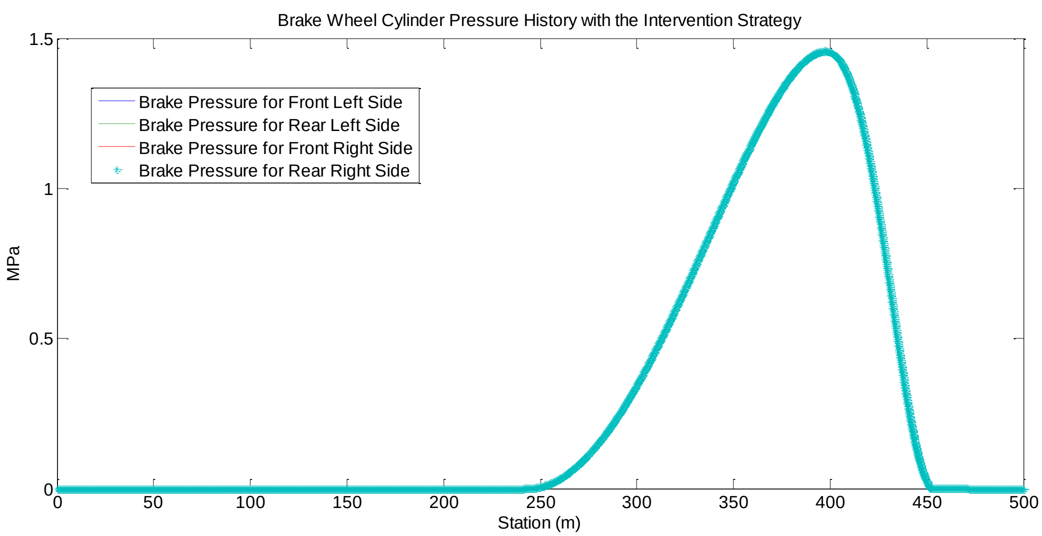

Figure A.2. The Brake History before Entering the 1st Corner

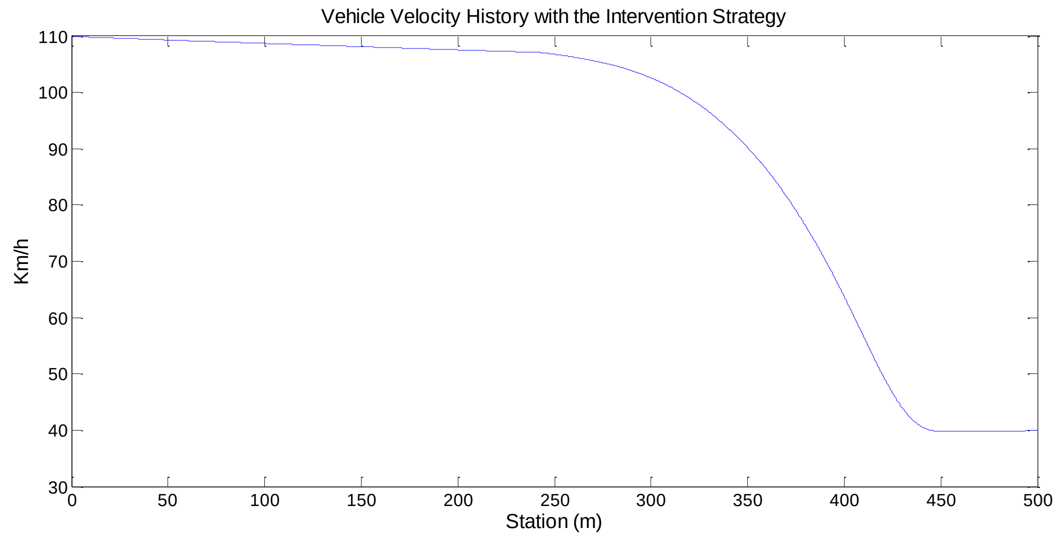

Figure A.3. The Velocity before Entering the 1st Corner

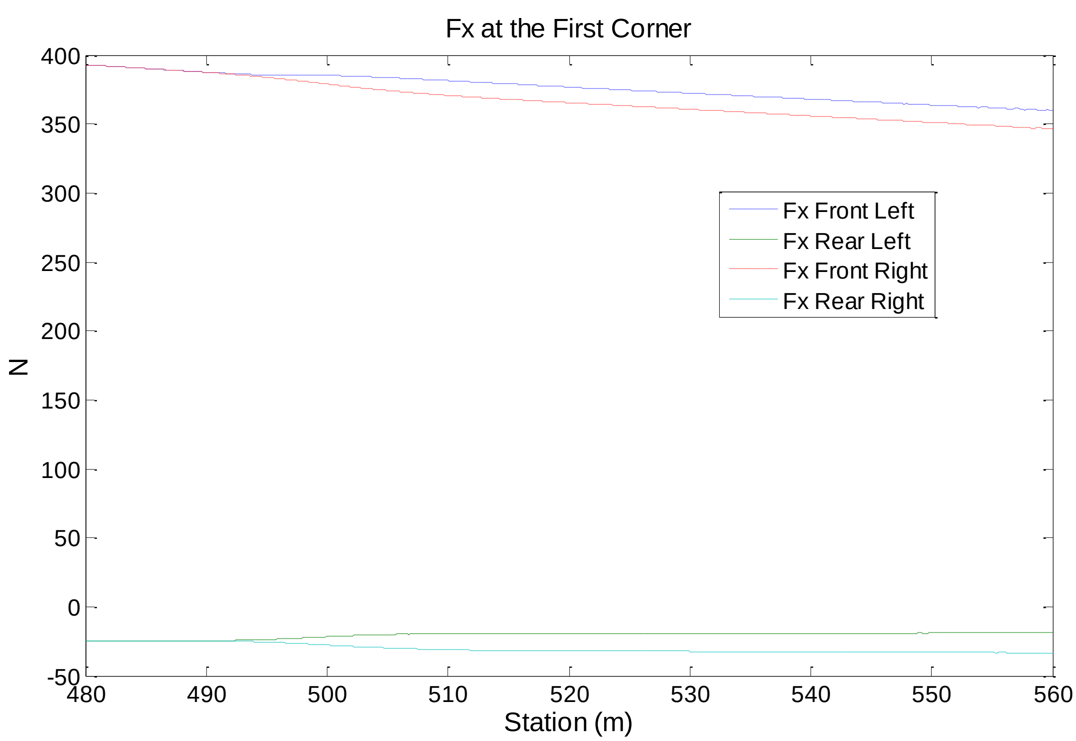

Figure A.4. The Change in Fx during cornering for the 1st Corner

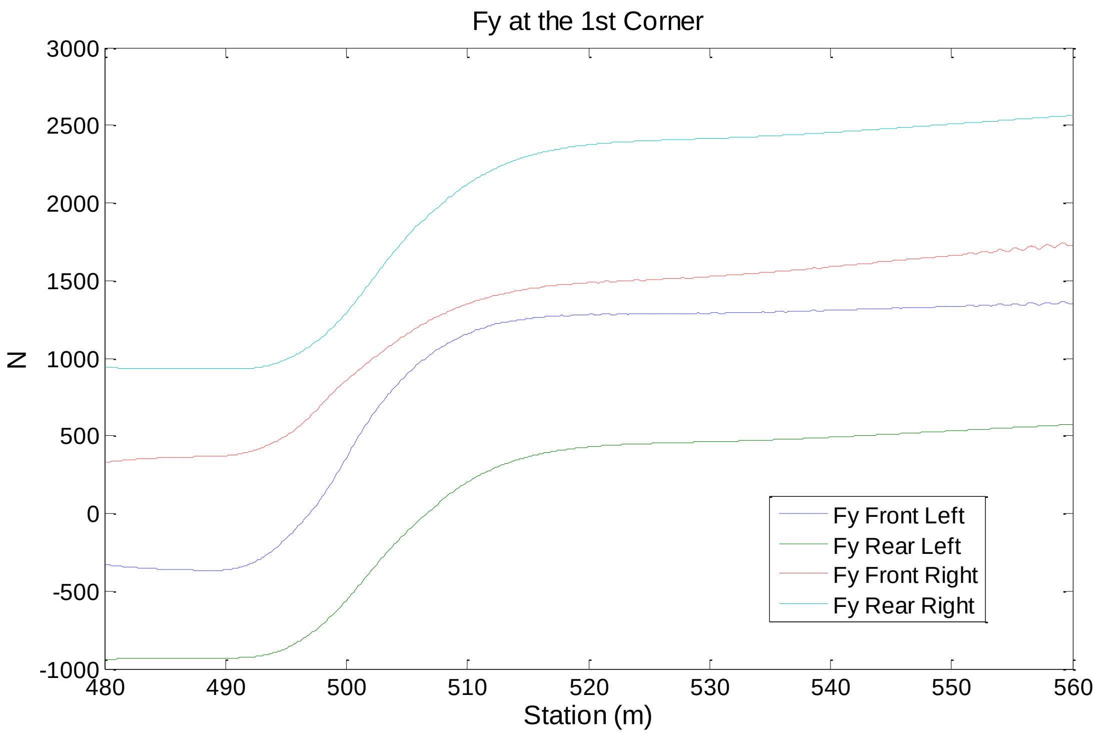

Figure A.5. The Change in Fy during cornering for the 1st Corner

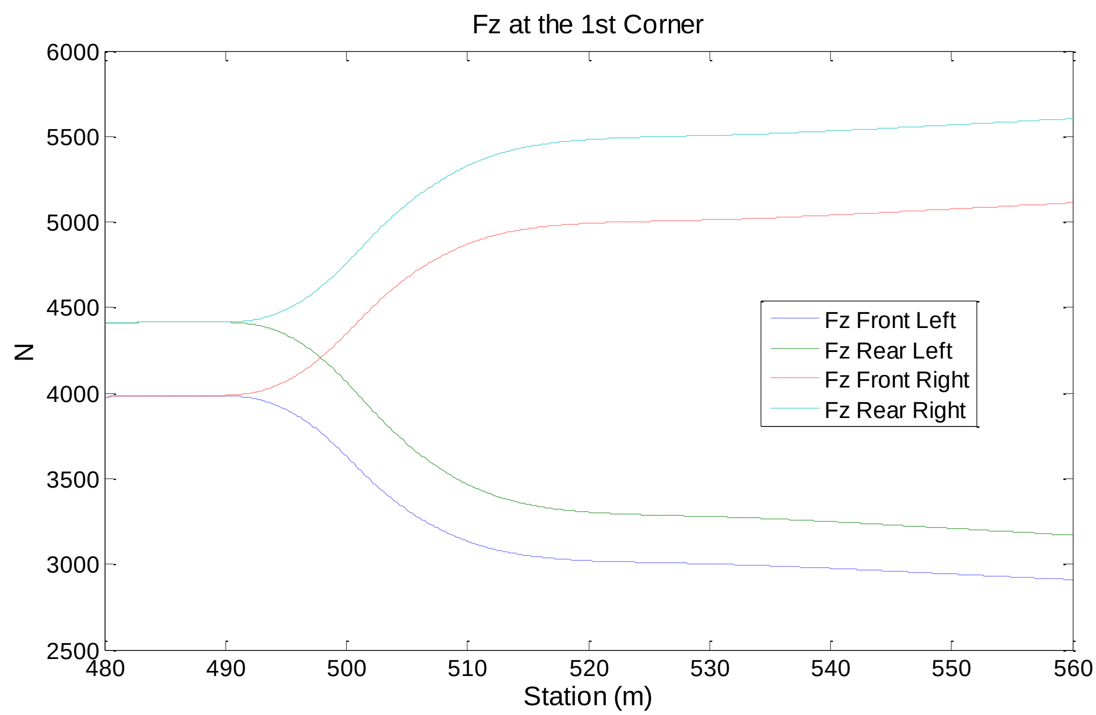

Figure A.6. The Change in Fz during cornering for the 1st Corner

2^{nd} Corner

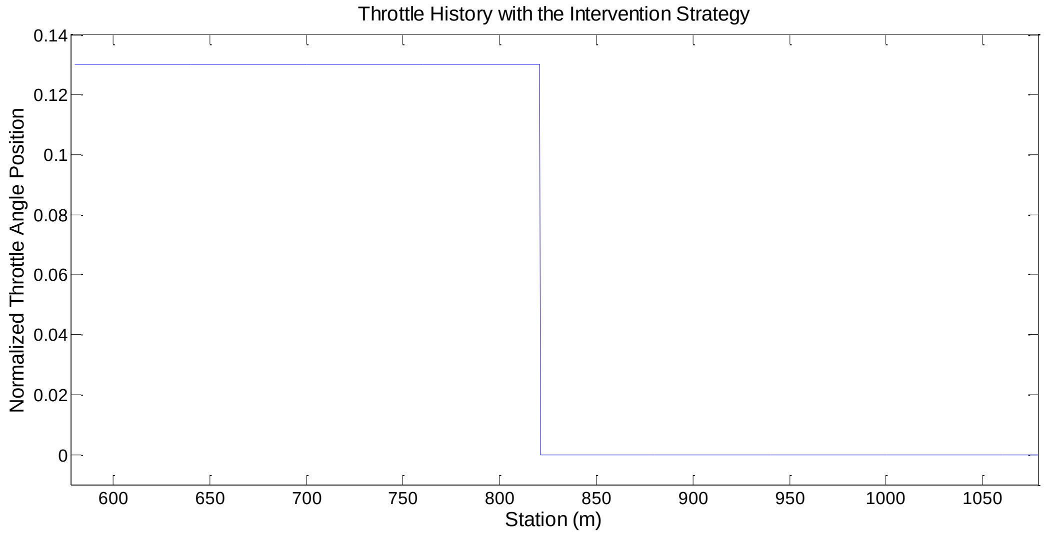

Figure A.7. The Throttle History before Entering the 2^{nd} Corner

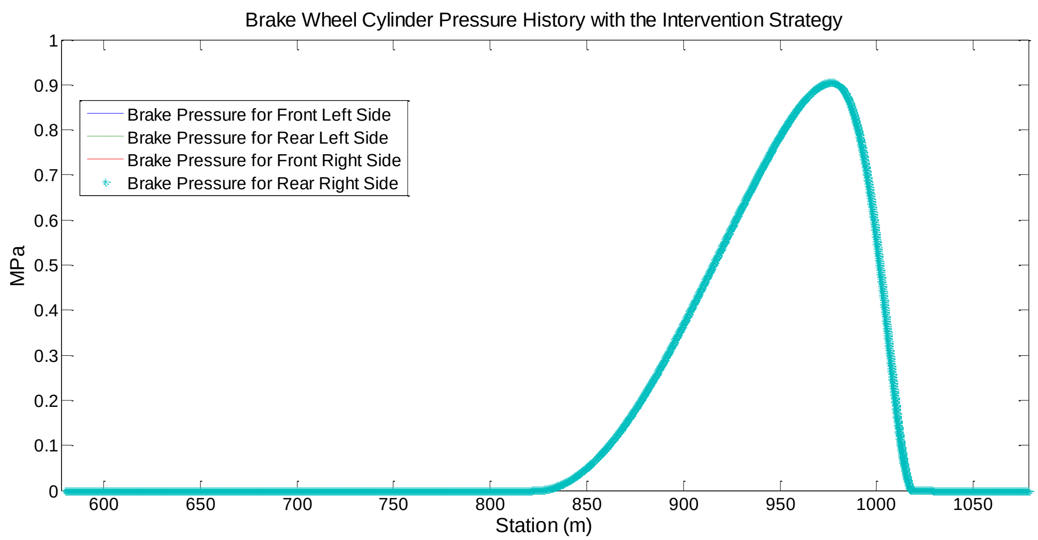

Figure A.8. The Brake History before Entering the 2^{nd} Corner

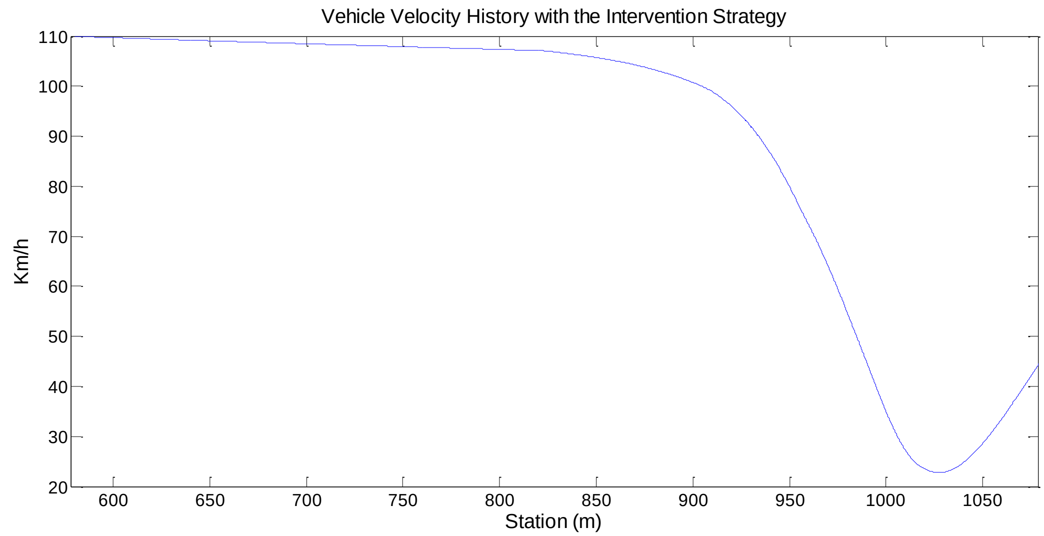

Figure A.9. The Velocity before Entering the 2nd Corner

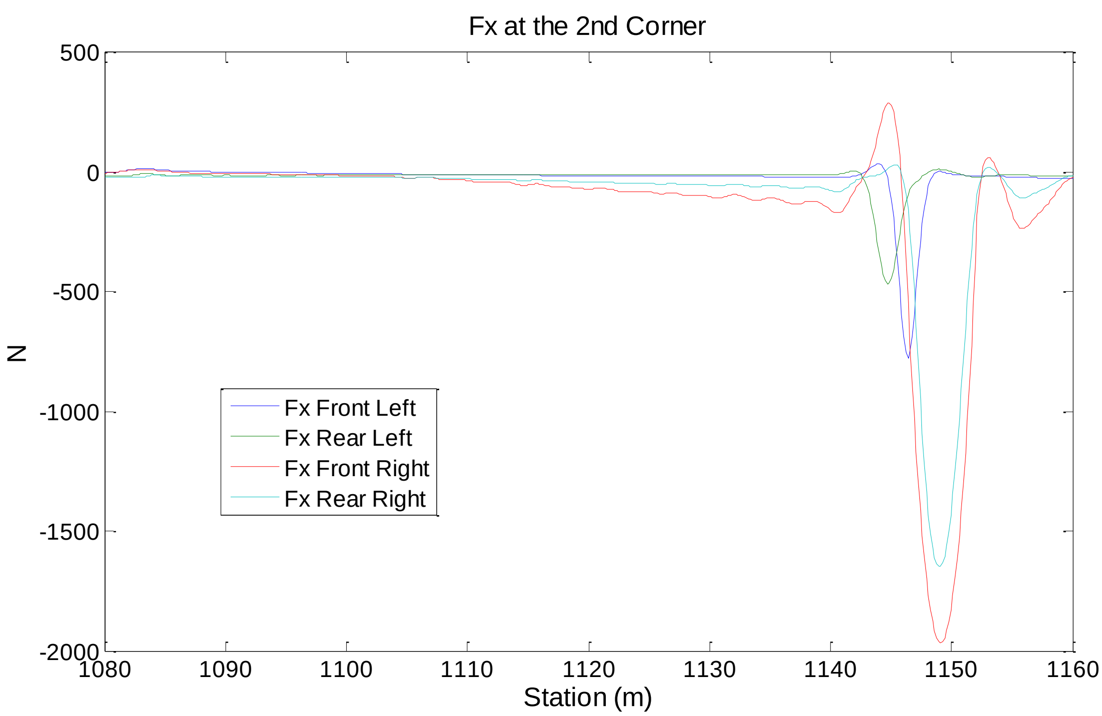

Figure A.10. The Change in Fx during cornering for the 2nd Corner

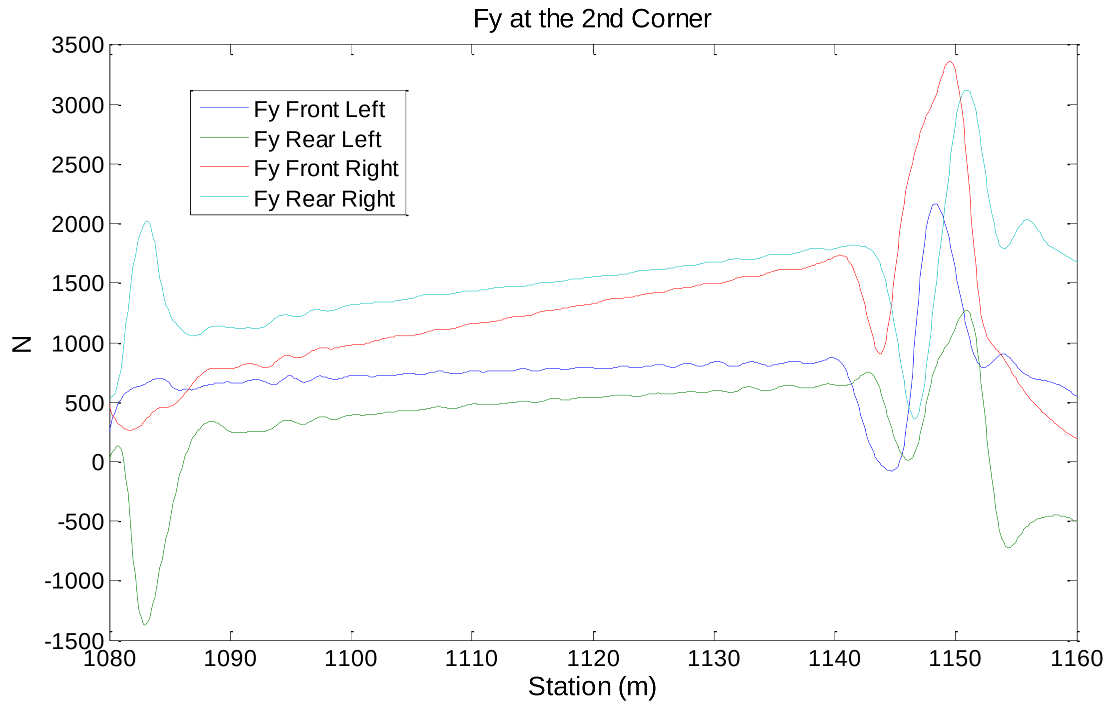

Figure A.11. The Change in Fy during cornering for the 2nd Corner

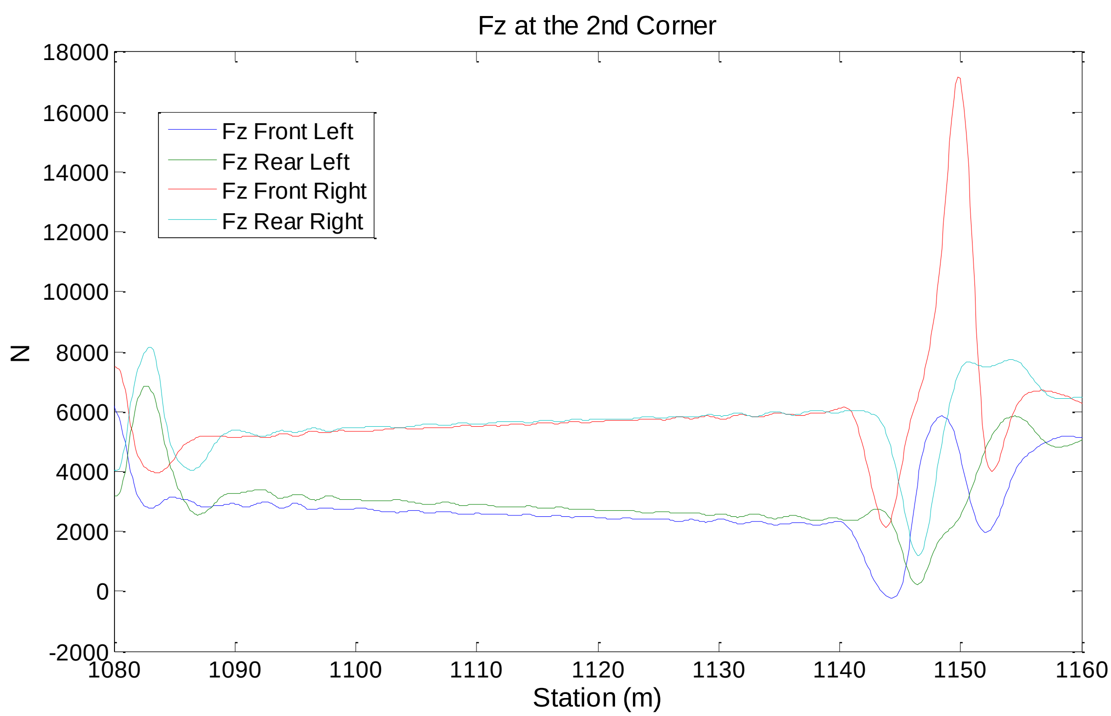

Figure A.12. The Change in Fz during cornering for the 2nd Corner

3rd Corner

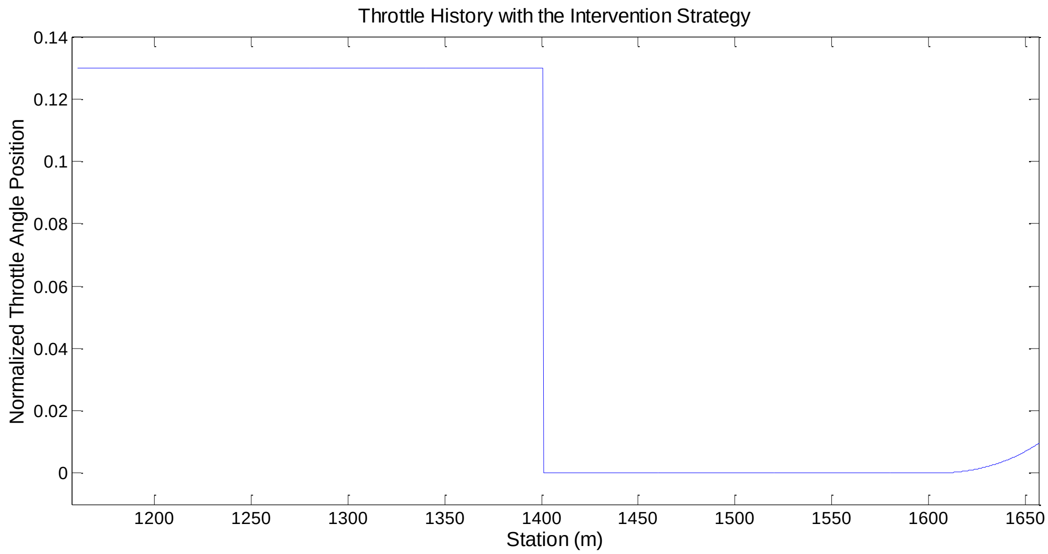

Figure A.13. The Throttle History before Entering the 3rd Corner

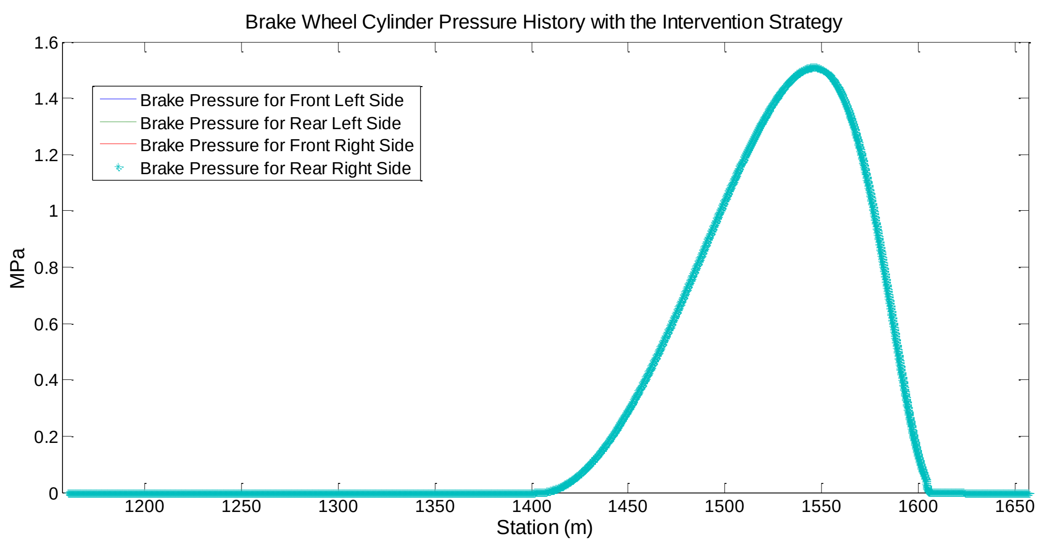

Figure A.14. The Brake History before Entering the 3rd Corner

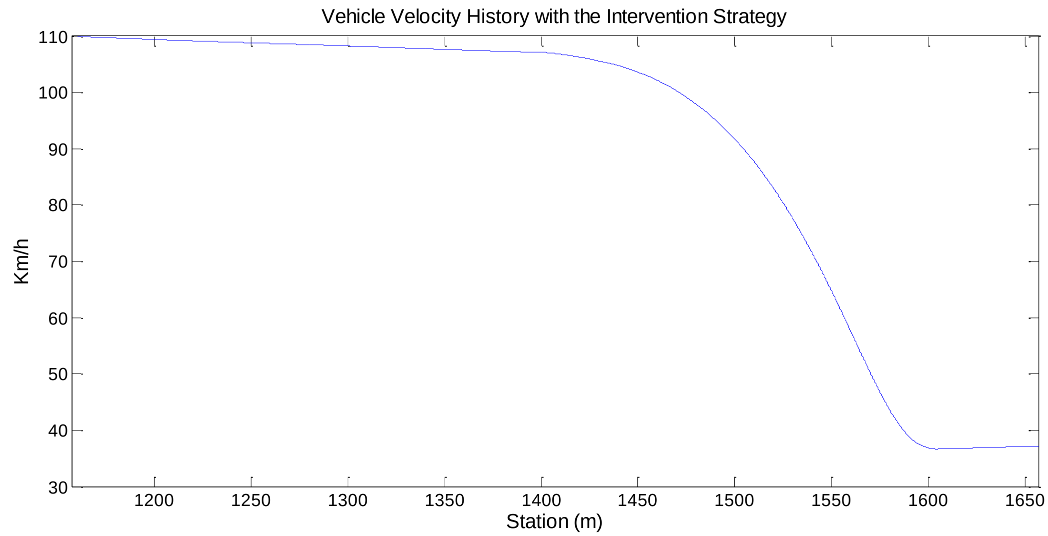

Figure A.15. The Velocity before Entering the 3rd Corner

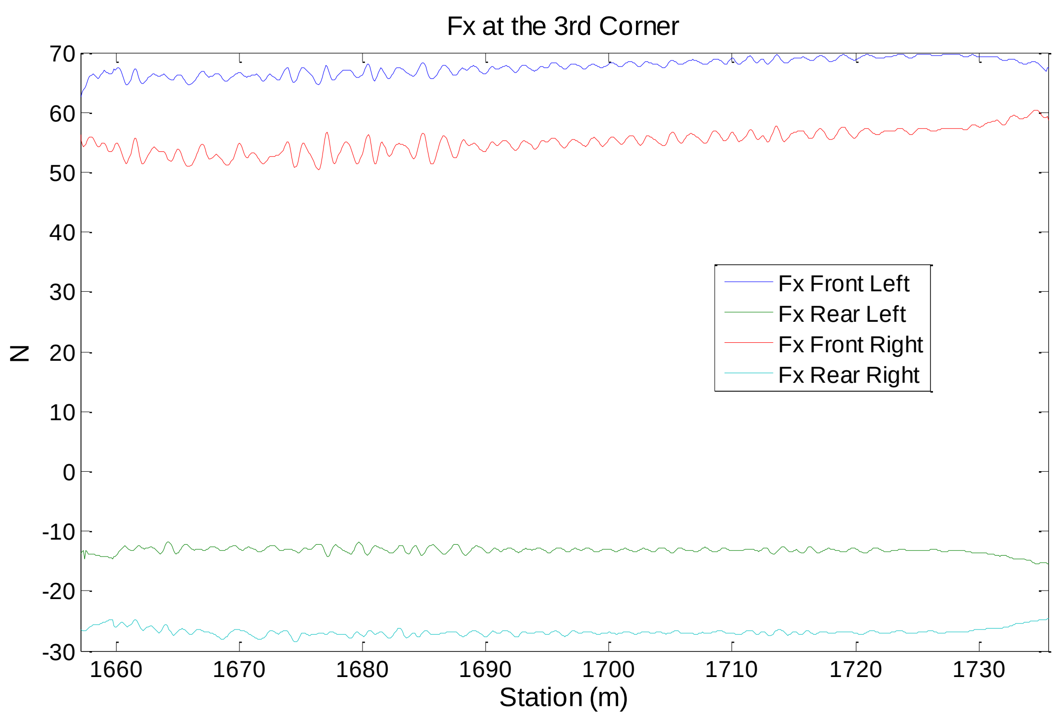

Figure A.16. The Change in Fx during cornering for the 3rd Corner

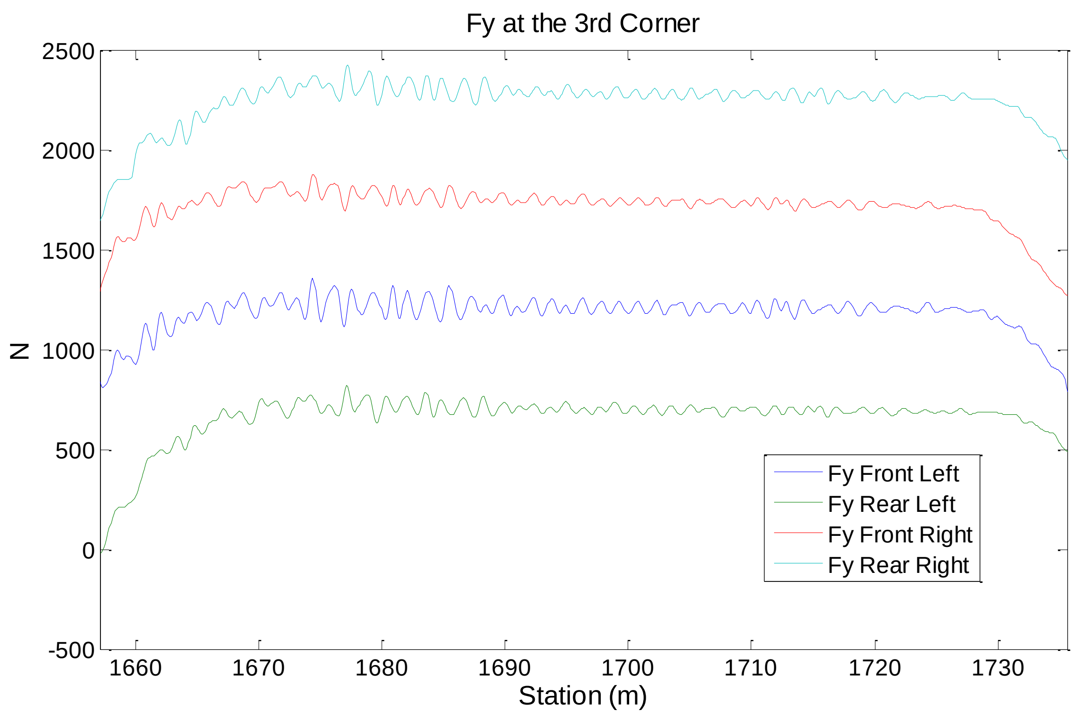

Figure A.17. The Change in Fy during cornering for the 3rd Corner

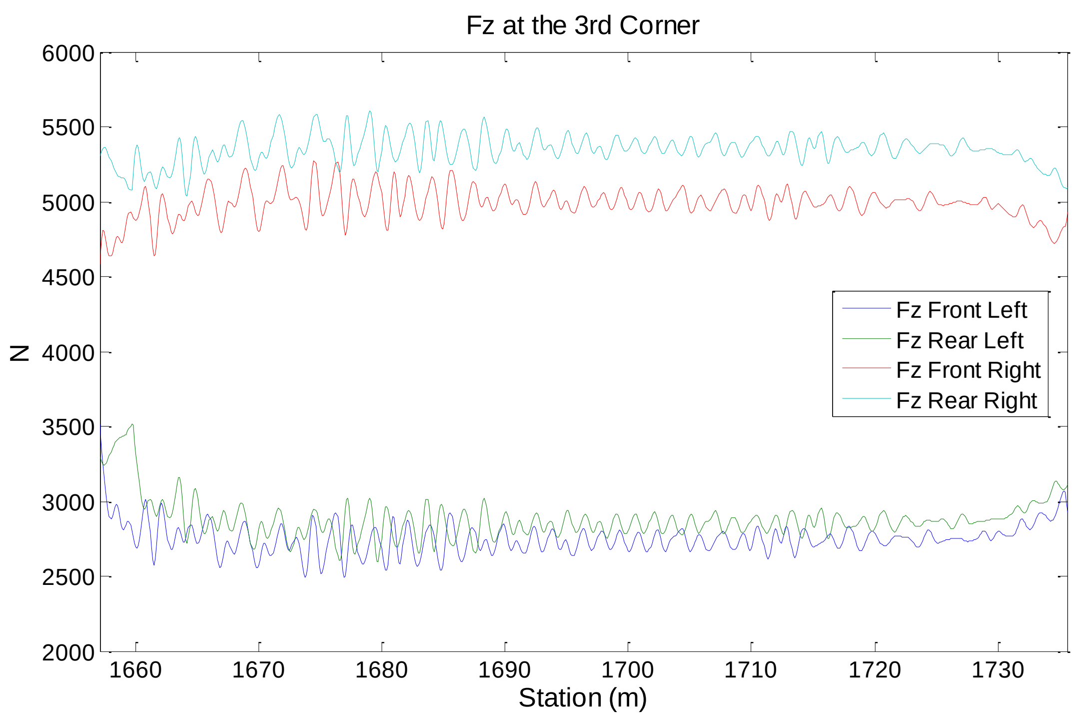

Figure A.18. The Change in Fz during cornering for the 3rd Corner

4th Corner

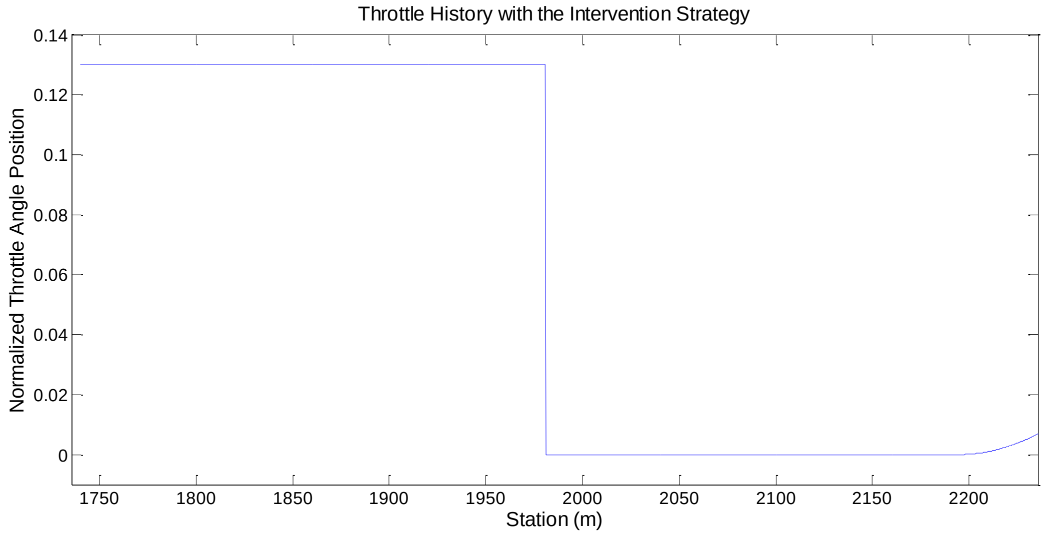

Figure A.19. The Throttle History before Entering the 4th Corner

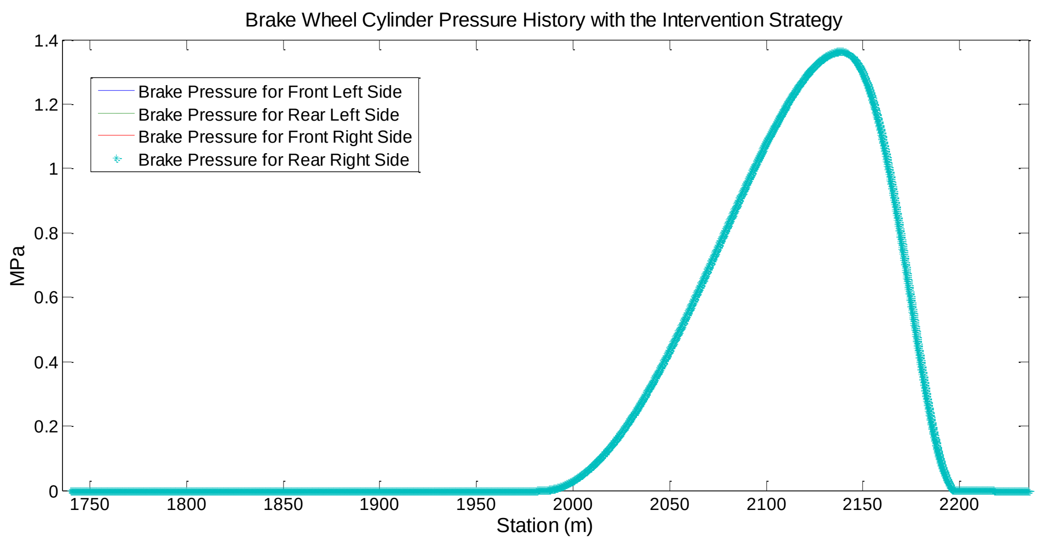

Figure A.20. The Brake History before Entering the 4th Corner

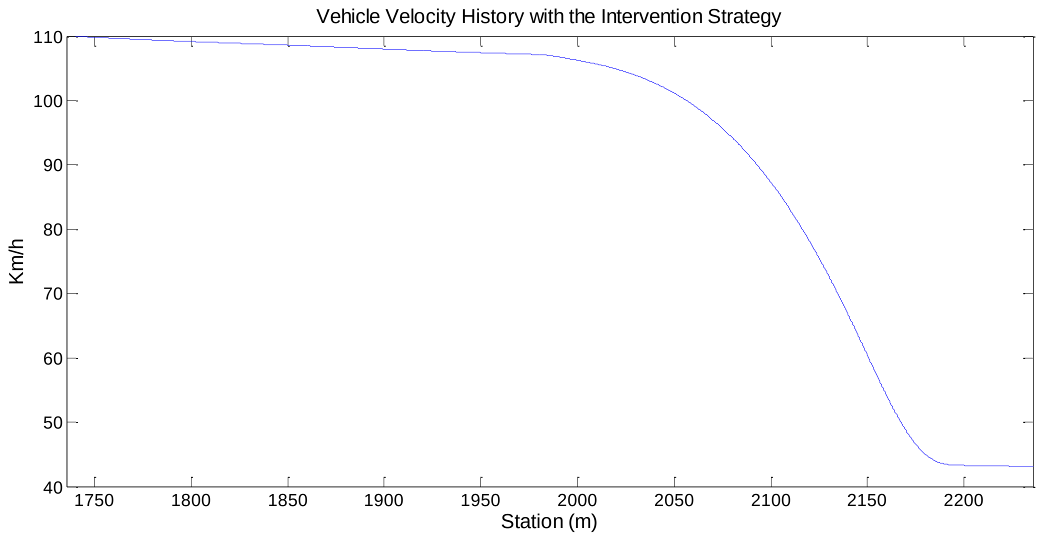

Figure A.21. The Velocity before Entering the 4th Corner

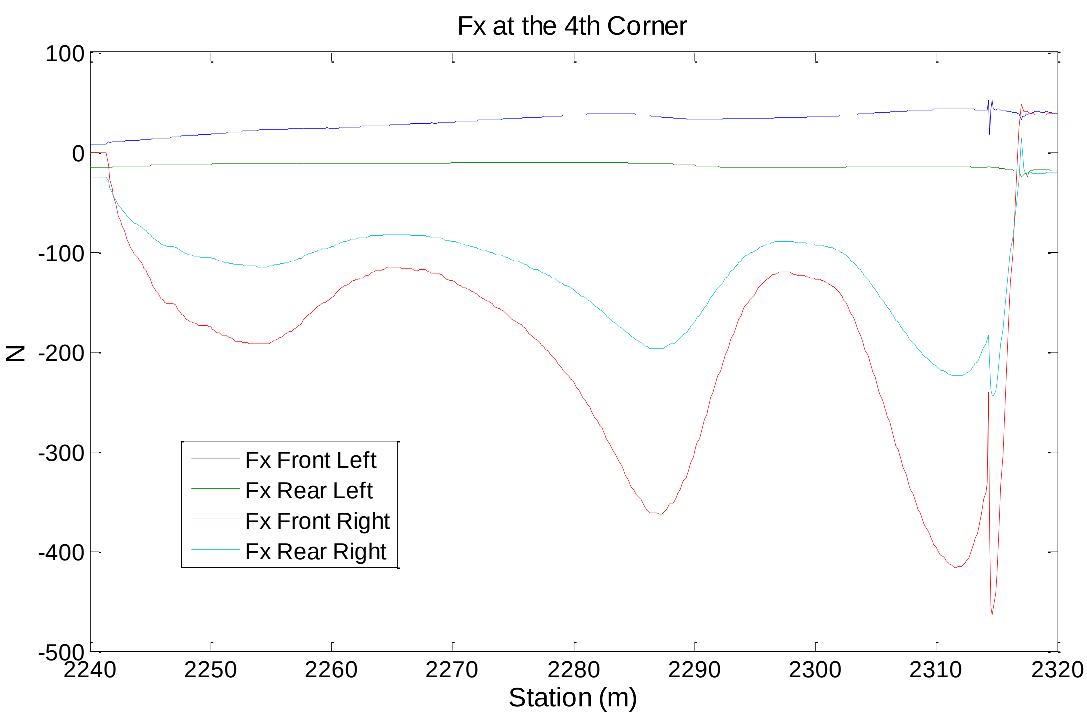

Figure A.22. The Change in Fx during cornering for the 4th Corner

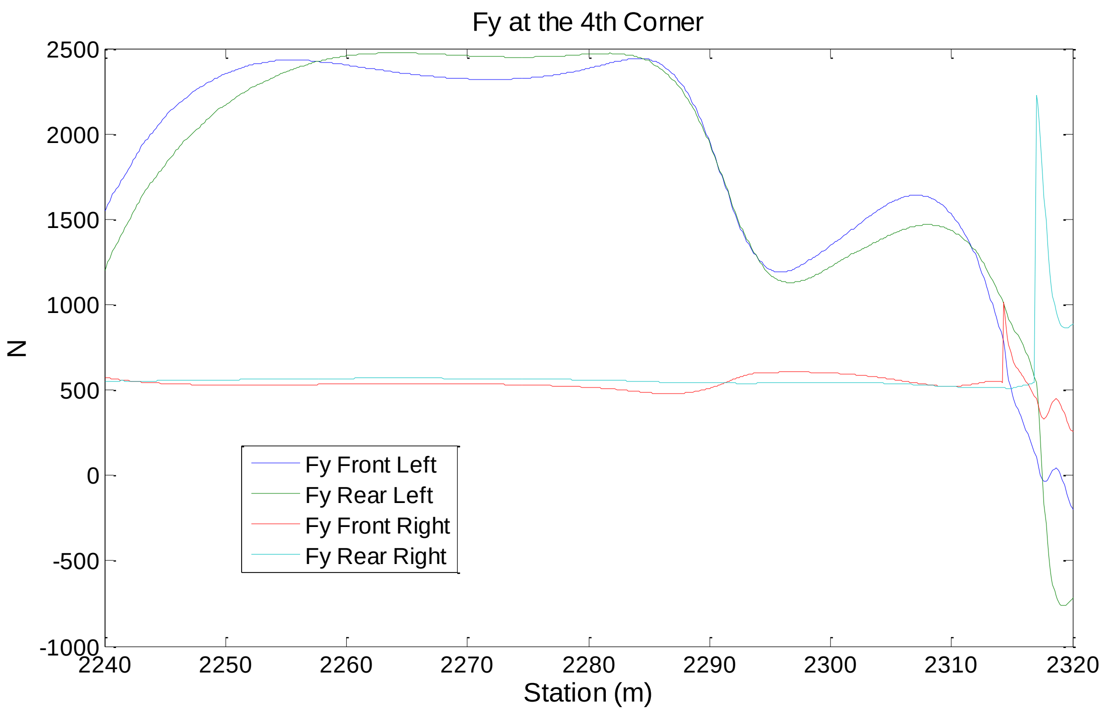

Figure A.23. The Change in Fy during cornering for the 4th Corner

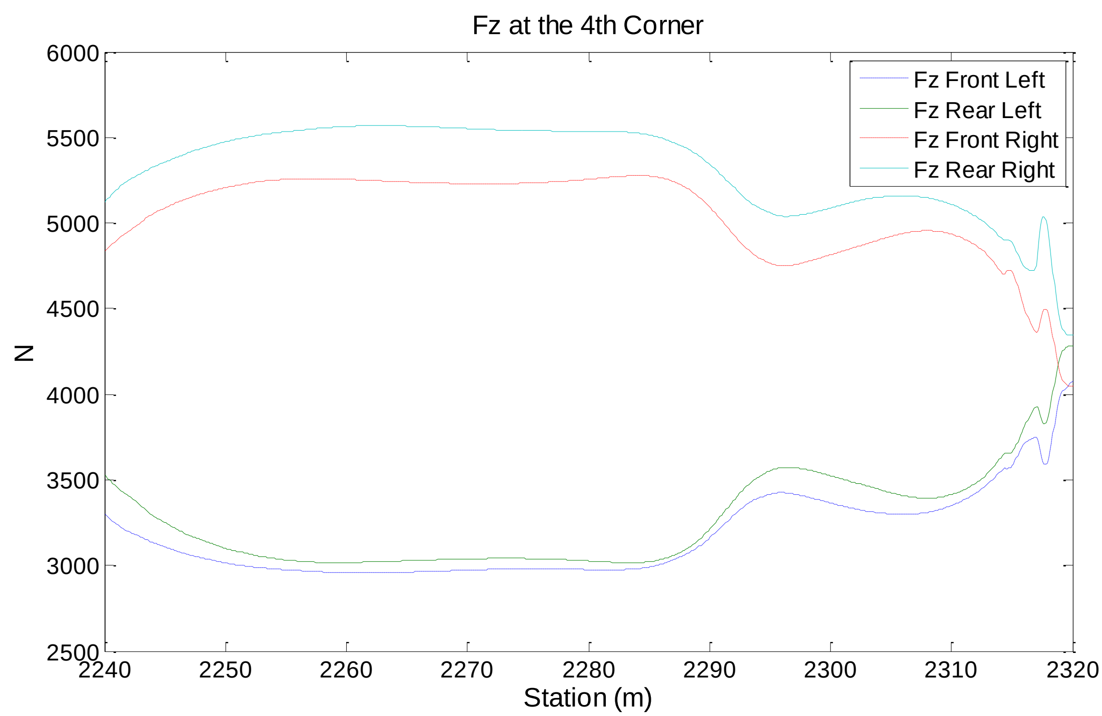

Figure A.24. The Change in Fz during cornering for the 4th Corner

References

1. National Highway Traffic Safety Administration, “Estimating Lives Saved by Electronic Stability Contro, 2008-2010”, Traffic Safety Facts Research Note, November 2012

2. Matthews, C. C., Cho, S., Ferris, J. B., Schlinkheider, J., et al., "Using Performance Margin and Dynamic Simulation for Location Aware Adaptation of Vehicle Dynamics," SAE International Journal of Passenger Cars-Mechanical Systems 6(1):225-30, 2013, doi:10.4271/2013-01-0703.

3. N.Amann., D.H.Owens., E.Rogers., “Iterative Learning Control for Discrete-Time Systems with Exponential Rate of Convergence,” IEE Proc.-Control Theory Appl., Vol. 143, No. 2, March 1996

4. Bandy, R. A., Cho, S., Matthews, C., Celli, J., et al, “Location-Aware Adaptive Vehicle Dynamics System: Concept Development,” SAE International Journal of Passenger Cars-Mechanical Systems.

5. Ford, “Ford Showcasing vehicle-to-vehicle communication for crash avoidance: Potential for Leveraging WiFi and Smartphones to extend quickly the number of participating Vehicles”, Green Car Congress, June 2011

6. Shnae McGlaun, “Volvo Vehicle-to-Vehicle Communication Services Promise Improved Safety”, Daily Tech, Oct 2012

7. BMW Official Website, “Car-to-Car Communication”, BMW Technology Guide

8. Wikipedia, “Collision Avoidance System”, http://en.wikipedia.org/wiki/Collision_avoidance_system

9. Wikipedia, “Lane Departure Warning System”, http://en.wikipedia.org/wiki/Lane_departure_warning_system

10. Wikipedia, “Driver Monitoring System”, http://en.wikipedia.org/wiki/Driver_Monitoring_System

11. SAE International Surface Vehicle Recommended Practice, “Vehicle Dynamics Terminology,” SAE Standard J670, Rev. Jan. 2008.

12. Yoon, P., Park, S., and Sunwoo, M., “A Nonlinear Dynamic Model of SI Engines for Designing Controller,” World Automotive Congress F2000A177, 2000.

13. Kang, S., Yoon, M., and Sunwoo, M., “Traction Control Using a Throttle Valve based on Sliding Mode Control and Load Torque Estimation,” Proceedings of the Institution of Mechanical Engineers, Part D: Journal of Automotive Engineering, 219(5):645-53, 2005, doi:10.1243/095440705X11059.

14. Y. Chamaillard, P. Higelin, A. Charlet, “A simple method for robust control design, application on a non-linear and delayed system: engine torque control,” Control Engineering Practice, Volume 12, Issue 4, April 2004, Pages 417-429, ISSN 0967-0661, http://dx.doi.org/10.1016/S0967-0661 (03)0113-8

15. Vermillion, C., Butts, K., and Reidy, K., “Model Predictive Engine Torque Control with Real-Time Driver-in-the-Loop Simulation Results,” presented at American Control Conference, USA, June 30 – July 2, 2010.

16. Ioannou, P. and Xu, Z., “Throttle and Brake Control Systems for Automatic Vehicle Following,” Journal of Intelligent Transportation Systems, 1(4):345-77, 1994, doi:10.1080/10248079408903805.

17. Gerdes, J.C., and Hedrick, J.K., “Vehicle Speed and Spacing Control Via Coordinated Throttle and Brake Actuation,” Control Engineering Practice, 5(11): 1607-14, 1997, doi:10.1016/S096706619

18. Yi, K. and Chung, J., "Nonlinear brake control for vehicle CW/CA systems," IEEE/ASME Transactions on Mechantronics 6(1):17-25, 2001, doi:10.1109/3516.914387.

19. Liang, H., Chong, K., No, T., and Yi, S., “Vehicle longitudinal brake control using variable parameter sliding control,” Control Engineering Practice 11(4):403-11, doi:10.1016/S0967-0661(02)00176-4.

20. Trachtler, A. “Integrated Vehicle Dynamics Control Using Active Brake, Steering and Suspension Systems,” International Journal of Vehicle Design 36(1), 2004, doi:10.1504/IJVD.2004.005316.

21. Ackermann, J., D. Odenthal, and T. Bünte. "Advantages of active steering for vehicle dynamics control." In Proceedings of 32nd ISATA, Automotive Mechatronics Design and Engineering, pp. 263-270. 1999.

22. Bing Zheng; Oh, P.; Lenart, B., "Active steering control with front wheel steering," American Control Conference, 2004. Proceedings of the 2004 , vol.2, no., pp.1475,1480 vol.2, June 30 2004-July 2 2004

23. Baslamisli, S.C.; Polat, I.; Kose, I.E., "Gain Scheduled Active Steering Control Based on a Parametric Bicycle Model," Intelligent Vehicles Symposium, 2007 IEEE , vol., no., pp.1168,1173, 13-15 June 2007 doi: 10.1109/IVS.2007.4290276

24. Falcone, P.; Borrelli, F.; Asgari, J.; Tseng, H.E.; Hrovat, D., "Predictive Active Steering Control for Autonomous Vehicle Systems," Control Systems Technology, IEEE Transactions on , vol.15, no.3, pp.566,580, May 2007 doi: 10.1109/TCST.2007.894653

25. Keviczky, T.; Falcone, P.; Borrelli, F.; Asgari, J.; Hrovat, D., "Predictive control approach to autonomous vehicle steering," American Control Conference, 2006 , vol., no., pp.6 pp.,, 14-16 June 2006

26. Yi, Kyongsu, Taeyoung Chung, Jeontae Kim, and Seungjong Yi. "An investigation into differential braking strategies for vehicle stability control." Proceedings of the Institution of Mechanical Engineers, Part D: Journal of Automobile Engineering 217, no. 12 (2003): 1081-1093.

27. Chenming Zhao; Weidong Xiang; Richardson, P., "Vehicle Lateral Control and Yaw Stability Control through Differential Braking," Industrial Electronics, 2006 IEEE International Symposium on , vol.1, no., pp.384,389, 9-13 July 2006, doi: 10.1109/ISIE.2006.295624

28. Wanki Cho , Jangyeol Yoon , Jeongtae Kim , Jaewoong Hur & Kyongsu Yi, “An investigation into unified chassis control scheme for optimised vehicle stability and manoeuvrability”, Vehicle System Dynamics: International Journal of Vehicle Mechanics and Mobility, 46:S1, 87-105, DOI: 10.1080/00423110701882330

29. Siqi Zhang; Tianxia Zhang; Shuwen Zhou, "Vehicle Stability Control Strategy Based on Active Torque Distribution and Differential Braking," Measuring Technology and Mechatronics Automation, 2009. ICMTMA '09. International Conference on , vol.1, no., pp.922,925, 11-12 April 2009, doi: 10.1109/ICMTMA.2009.380

30. S. Arimoto., “Mathematical Theory of Learning with Applications to Robot Control,” In Proceedings of 4th Yale Workshop on Applications of Adaptive Systems, Pages 379-388, New Haven, Connecticut, May 1985

31. Y.C.Huang and R.W.Longman., “The Source of the Often Observed Property of Initial Convergence Followed by Divergence in Learning and Repetitive Control. Advances in the Astronautical Sciences, 90:555-572,1996

32. L.M.Hideg., “Stability and Convergence Issues in Iterative Learning Control,” In Proceedings Intelligent Engineering Systems Through Artificial Neural Networks in Engineering Conference, Volume 4, pages 211-216, St. Louis, MO, November 1994.

33. K.L.Moore., “Design Techniques for Transient Response Control,” PhD thesis, Texas A&M University, College Station, Texas, 1989.

34. G.Heinzinger, D.Fenwick, B.Paden, and F.Miyazaki, “Stability of Learning Control with Disturbances and Uncertain Initial Conditions,” IEEE Transactions on Automatic Control, 37(1), January 1992.

35. S.S.Saab. “A Discrete-Time Learning Control Algorithm for a Class of Linear Time-Variant Systems,” IEEE Transactions on Automatic Control, 40(6), June 1995.

36. G.Li, H.Li, and J.Xu, “The Study and Design of the Longitudinal Learning Control System of the Automobile. In Proceedings of the 2nd Asian Control Conference, Seoul, Korea, July 1997.

37. K.P. Venugopal, A.S.Pandya, and R.Sudhakar, “A Recurrent Neural Network Controller and Learning Algorithm for the On-Line Learning Control of Autonomous Underwater Vehicles,” Neural Networks, 7(5):833-846, 1994.

38. Beiker, S., Gaubatz, K. H., Gerdes, J. C., and Rock, K. L., "GPS Augmented Vehicle Dynamics Control," SAE Technical Paper 2006-01-1275, 2006, doi:10.4271/2006-01-1275.

39. Ahn, C. S., "Robust estimation of road friction coefficient for vehicle active safety systems." Ph.D. dissertation, Department of Mechanical Engineering, The University of Michigan, 2011.

40. Lee, C., Hedrick, K., and Yi, K., “Real-Time Slip-Based Estimation of Maximum Tire-Road Friction Coeffcient,” IEEE/ASME Transcations on Mechatronics, 9(2):454-8, 2004, doi:10.1109/TMECH.2004.828622.

41. Pasterkamp, W. R., and Pacejka, H. B., "The tyre as a sensor to estimate friction," Vehicle System Dynamics 27(5):409-22, 1997.

42. Erdogan, G. "New Sensors and Estimation Systems for the Measurement of Tire-Road Friction Coefficient and Tire Slip Variables," Ph.D. dissertation, Department of Mechanical Engineering, University of Minnesota, 2009.

43. Hsu, Y.-H. J., Laws, S. M., and Gerdes, J. C., "Estimation of tire slip angle and friction limits using steering torque." IEEE Transactions on Control Systems Technology 18(4):896-907, 2010.

44. Yoon, P., Park, S., and Sunwoo, M., “A Nonlinear Dynamic Model of SI Engines for Designing Controller,” World Automotive Congress F2000A177, 2000.

45. Kang, S., Yoon, M., and Sunwoo, M., “Traction Control Using a Throttle Valve based on Sliding Mode Control and Load Torque Estimation,” Proceedings of the Institution of Mechanical Engineers, Part D: Journal of Automotive Engineering, 219(5):645-53, 2005, doi:10.1243/095440705X11059.

46. Vermillion, C., Butts, K., and Reidy, K., “Model Predictive Engine Torque Control with Real-Time Driver-in-the-Loop Simulation Results,” presented at American Control Conference, USA, June 30 – July 2, 2010.

47. Ioannou, P. and Xu, Z., “Throttle and Brake Control Systems for Automatic Vehicle Following,” Journal of Intelligent Transportation Systems, 1(4):345-77, 1994, doi:10.1080/10248079408903805.

48. Gerdes, J.C., and Hedrick, J.K., “Vehicle Speed and Spacing Control Via Coordinated Throttle and Brake Actuation,” Control Engineering Practice, 5(11): 1607-14, 1997, doi:10.1016/S096706619

49. Cho, S., Bandy, R. A., Ferris, J. B., Schlinkheider, J., et al., “Location-Aware Adaptive Vehicle Dynamics System: Throttle Modulation,” submitted to: SAE World Congress 2014.

50. Yi, K. and Chung, J., "Nonlinear brake control for vehicle CW/CA systems," IEEE/ASME Transactions on Mechantronics 6(1):17-25, 2001, doi:10.1109/3516.914387.

51. Liang, H., Chong, K., No, T., and Yi, S., “Vehicle longitudinal brake control using variable parameter sliding control,” Control Engineering Practice 11(4):403-11, doi:10.1016/S0967-0661(02)00176-4.

52. Trachtler, A. “Integrated Vehicle Dynamics Control Using Active Brake, Steering and Suspension Systems,” International Journal of Vehicle Design 36(1), 2004, doi:10.1504/IJVD.2004.005316.

53. Cho, S., Bandy, R. A., Ferris, J. B., Schlinkheider, J., et al., “Location-Aware Adaptive Vehicle Dynamics System: Brake Modulation,” submitted to: SAE World Congress 2014.

54. Bandy, R., “Location-Aware Adaptive Vehicle Dynamics System: Linear Chassis Predictions”, Master Thesis, Department of Mechanical Engineering, Virginia Tech, 2014.

55. Ferris, J. B. "Factors affecting perceptions of ride quality in automobiles." In *Proceedings of ASME Dynamic Systems and Control Division (DSC)*, vol. 67, pp. 649-654. 1999.

56. Cho, S. “Method for Judging the Driving in Self-Lane for a Vehicle, in which the Time Counter is Applied, In or Out of Preceding Cars is Decided in the Driving Path, and the Distance of the Car are Controlled.”, Granted Korea Patent 1011140430000

57. Sol, David, and Shunso F. Watanabe. "Vehicle inertia and center of gravity estimator." U.S. Patent 5,136,513, issued August 4, 1992.

58. Rajamani, Rajesh. *Vehicle dynamics and control*. Springer Science & Business Media, 2011.